

4

THE KINETICS
OF THE REDUCTION OF URANIUM TETRAFLUORIDE
BY MAGNESIUM

A thesis presented for the degree of
Doctor of Philosophy
in the
University of London

by

José T. H. Domingues

London,

May, 1964

ABSTRACT

The kinetics of the reduction of sintered UF_4 pellets by Mg vapour was investigated at 620° and 690°C, using a transportation technique and highly purified argon as the carrier gas. The products of the reaction were identified by microscopic observation of cross sections and by X-ray powder diffraction, electron probe and chemical analyses. Two coherent product layers (UF_3 and MgF_2) are formed on the UF_4 , the uranium metal being interspersed in the outer layer (MgF_2) as fine globules or thin lamellae. Marker experiments showed that the MgF_2 layer grows by inward migration of Mg^{2+} ions and the UF_3 layer grows inwards probably by outward migration of fluorine ions. The rate of both reactions follows a parabolic rate law, after an initial period for which a different law applies, probably a direct logarithmic relationship. A discussion is given of the possible mechanisms in the two cases. From reduction experiments with UF_3 pellets it was demonstrated that migration through the MgF_2 layer is the rate determining step of the overall reaction. The parabolic rate constants for the overall reaction are 1.8×10^{-11} and $4.75 \times 10^{-10} \text{ g}^2 \text{ cm}^{-4} \text{ min}^{-1}$ at 620° and 690°C respectively. The parabolic rate constants for the partial reaction yielding UF_3 are 6.7×10^{-13} and $1.1 \times 10^{-10} \text{ g}^2 \text{ cm}^{-4} \text{ min}^{-1}$.

The industrial process of bomb production of uranium was reviewed and discussed, and suggestions are made for the interpretation of the mechanism of ignition of the reaction by a simple theory of self heating.

A preliminary thermodynamic study on a new process of producing uranium metal by the reduction of UF_6 by Na is also reported.

TABLE OF CONTENTS

	Page
CHAPTER I Introduction	
1.1 General	2
1.2 The Production of Uranium Metal	3
1.3 The Reduction of UF_4 by Mg	5
1.3.1 The Thermal Characteristics of the Process	6
1.3.2 The Effect of the Process Variables on the Yield of Uranium	10
1.3.3 The Mechanism of Ignition	16
1.3.4 The Reaction and Post- Reaction Period	19
1.3.5 Summary	22
1.4 Gas-solid Reactions	23
1.4.1 General	23
1.4.2 Wagner's Theory of the Rate of Growth of Protective Layers	26
1.4.3 Lattice Defects	31
1.4.4 Inert Markers	36
1.5 Objects of the Present Work	39
1.6 Previous Research	40
CHAPTER II Experimental Methods	
2.1 Materials	43
2.1.1 Argon	43
2.1.2 Hydrogen	43
2.1.3 Uranium	44
2.1.4 Uranium Tetrafluoride	44
2.1.5 Uranium Trifluoride	45
2.1.6 Magnesium	52
2.2 Apparatus for Kinetic Studies	54
2.2.1 Flowmeter	54
2.2.2 Purification Train	54

	Page
2.2.3 Reaction Tube Arrangement and Furnace	58
2.2.4 Temperature Control	61
2.2.5 Evacuation of the Reaction Zone and Measurement of Pressure	61
2.3 Experimental Techniques	61
2.3.1 Production of UF_4 and UF_3 Compacts	61
2.3.2 Sintering of UF_4 and UF_3 Pellets	67
2.3.3 Analysis for F and U in Aqueous Solutions	70
2.3.4 Sectioning and Polishing of Reacted Pellets	71
2.3.5 Photomicrography	72
2.3.6 Analyses with the Microscan X-ray Analyser	73
2.3.7 X-ray Powder Diffraction Analysis	73
2.3.8 Gold Marker Technique	73
2.4 The Development of Technique for Kinetic Studies	74
2.5 Experimental Procedure	82

CHAPTER III Experimental Results

3.1 Preliminary Experiments	89
3.2 Kinetics of the Overall Reaction	102
3.2.1 Reproducibility	109
3.2.2 Errors	109
3.3 Kinetics of the U and UF_3 producing Reactions	111
3.3.1 Chemical Analysis for Uranium	
3.3.2 Determination of Uranium by Oxidation in Air	112
3.3.3 Kinetics	117
3.4 X-ray Powder Analysis of the Reaction Products	120

	Page
3.4.1 Errors in X-ray Diffraction Studies	125
3.5 Microscan X-ray Analyser	126
3.6 Identification of the Product Layers	132
3.7 Appearance	133
3.7.1 Final Experiments	133
3.7.2 Preliminary Experiments	138
3.8 Marker Experiments	141
 CHAPTER IV Discussion	
4.1 Kinetics	148
4.4.1 The Parabolic Rate Period	148
4.1.2 The Initial Period of Reaction	152
4.2 Mechanism of the Reaction	157
4.2.1 Marker Experiments	157
4.2.2 Mechanism of Migration through the MgF ₂ Layer	159
4.2.3 Migration Mechanism through the UF ₃ Layer	166
4.2.4 Mechanism of formation of Uranium Metal	168
4.2.5 Wagner's Theory	170
4.2.6 Mechanism of the Reaction in the Initial Period	175
4.2.7 Activation Energy	179
4.3 Preliminary Experiments	180
4.3.1 Single Time Experiments	180
4.3.2 Consecutive Time Experiments	182
4.3.3 Balloon Formation	185
4.4 Powder Experiments	186
4.5 Discussion of the Technological Process	189
4.6 Suggestions for Further Work	197
APPENDIX I Contribution to the Study of the Reduction of UF ₆ by Na	199
APPENDIX II Analysis for Uranium and Fluorine in in Aqueous Solutions	217
REFERENCES	222
ACKNOWLEDGEMENTS	

1.1 General

Although at the present time, most metal extraction and refining processes remain empirical, much research has been carried out, during the last twenty five years, in an attempt to improve these processes and develop new ones. Broadly speaking these investigations have been mainly concerned with two different types of questions: the determination of the conditions of equilibrium for any given system, and the study of the variables influencing the rate at which this equilibrium is attained. Investigations of the first type deal with the physical, chemical and thermodynamic properties of elements, compounds and systems of metallurgical interest, and represent the major part of recent research in extractive metallurgy. The second type of investigation deals mainly with the kinetics of the chemical and physical changes and though a number of studies have been reported they are still of a fragmentary nature.

It is a well known fact that processes of mass transfer and heat and fluid flow, rather than chemical reactions, are the controlling steps in most metallurgical operations. As a consequence, a great deal of work in the field of kinetics has been dedicated to those processes. However, in the case of the production of uranium metal by reduction of UF_4 with Mg, which is the

concern of the present work, evidence has been found that the kinetics of the reaction plays an important role in the reduction process. For some years investigations were carried out in the Nuffield Research Group[‡] on molten salt systems of interest for the process. These investigations resulted from difficulties encountered at one time (1956), at the Springfields Uranium Production Plant^{‡‡}, in obtaining good slag-metal separation and in avoiding the loss of uranium metal as inclusions in the slag. As a result of these and many other investigations the efficiency of the process has been greatly improved and the knowledge of the factors affecting the reaction has been increased. However, little is still known of the kinetics and mechanism of the reaction. It is an aim of the present work to achieve a greater understanding of the factors involved, by dealing with this neglected aspect of the process.

1.2 The Production of Uranium Metal

There are at the present time many possible methods of producing and refining uranium metal, the choice depending upon the requirements of the individual cases. The methods already developed include:

‡ Royal School of Mines, Imperial College, London.

‡‡ Operated by United Kingdom Atomic Energy Authority.

- (i) Reduction of uranium halides with metals
- (ii) Reduction of uranium oxides with metals or carbon
- (iii) Electrolyte reductions in fused salt
- (iv) Disproportionation of uranium halides.

By far the method most widely used for the large scale production of uranium is the reduction of uranium tetrafluoride with magnesium or calcium, where a solid regulus of metal is obtained under a cover of slag. All the other methods yield uranium shot in a high-melting slag or uranium powder. Since the demand is mainly for massive uranium, these last methods are only used for special purposes.

Although all these methods are well established and work reasonably well, much work has been dedicated to develop new and more economical ones. Recent developments in the magnesium reduction of sodium uranium fluoride appear to make this method attractive for commercial use.⁽¹⁾ Also, the direct reduction of uranium dioxide to massive uranium, by the use of a flux, has been carried out on a laboratory scale and further development of the method may represent a significant advance, since it would eliminate the need for halogenating the uranium oxide⁽¹⁾. The direct reduction of uranium hexafluoride by sodium is yet another promising process and preliminary studies on this reaction are presented in Appendix I of this Thesis.

In the next section, the process for the reduction of UF_4 by Mg will be discussed in detail as it is an aim of the present work to shed some light on some fundamental aspects of the reduction process.

1.3 The Reduction of UF_4 by Mg

An indispensable characteristic of a method intended to produce massive uranium is that the ultimate temperature reached by the reaction be sufficient to ensure melting of the uranium, and to bring the slag to a condition of sufficient fluidity. In this respect the calcium reduction of the UF_4 is more favourable since it is more exothermic than the magnesium reduction and the heat evolved, when the reaction is started at room temperature, is enough to bring about the fusion of the products. (2, 3, 4) On the other hand, the magnesium reduction requires the supply of heat necessary to bring the charge and container to a temperature around $650^{\circ}C$ before the reaction is carried out. At present, the magnesium reduction is preferred because magnesium is less expensive, only 63% as much by weight is required, and magnesium is less apt to pick up and introduce impurities (calcium reacts easily with nitrogen and moisture in the atmosphere and therefore requires special storage facilities).

The usual practice consists of charging a refractory lined, steel vessel with a compacted mixture of UF_4 and Mg. The vessel is then sealed, and heated until the reactants ignite (at about $650^\circ C$); the reaction goes rapidly (a few minutes) to completion. Once the reaction has subsided the vessel is allowed to cool to room temperature. The resultant metal "biscuit" or "derby" is removed and, if necessary, chipped free of slag. Reaction vessels up to 13 in. inner diameter and 45 in. long have been used for making derbies and much larger vessels for making direct reduction ingots (dingot process). Details of the technique may be found in the original paper by Wilhelm⁽⁵⁾ or in more recent reviews.^(1, 6)

Although a great amount of work has been done to establish the effect of the process variables on the quality and yield of uranium, very little is known of the mechanism of the reaction, and of the conditions prevailing during the process, as will be shown in the following sections.

1.3.1 The Thermal Characteristics of the Process

The thermochemistry of the reaction plays an important role in obtaining good yields and a good quality regulus. Beatty and Magoteaux⁽⁷⁾ have derived an equation for estimating the minimum temperature of the reactants that

can possibly result in the production of molten slag (1264°C). With 4% excess of magnesium they found a value of 228°C as compared with about 180°C when no excess of magnesium is used. Therefore, the reactants must be heated before the reaction is "triggered" by a booster or spontaneously initiated. Since preheating is necessary, many side reactions may occur in the bomb, as the charge is being heated, which affect the final yield of uranium.

Experimental evidence has been found that the reaction ignites spontaneously when some parts of the charge reach a temperature in the range 600 - 650°C. (1, 11) Though this temperature is well above the minimum value calculated by Beatty and Magoteaux, the presence of temperature gradients in the charge and heat losses during the reaction may result in only partial fusion of the slag. This emphasises the importance of the thermal conductivity characteristics of the liner and charge and the heating rate, i.e., the temperature of the external furnace. Also, the thermal losses may be important, particularly for small vessels where the surface/volume ratio is greater than in larger vessels. Use of thermal boosters to supplement the external heating is therefore quite common in vessels with internal diameter less than 10 in.

Many materials are used as liners. In the Ames Laboratory[‡] a liner of tamped, electrically fused dolomitic lime is used.⁽⁵⁾ A coated graphite crucible is employed in the laboratory exercises of the International Institute of Nuclear Science and Engineering^{‡‡(8)} and recycled magnesium fluoride slag is commonly used in the commercial production of uranium.⁽⁹⁾ The thickness of the liner must be sufficient to prevent initiation of the reaction before enough heat has entered the major part of the charge, and to prevent weakening of the bomb while pressure is high. Also, on cooling, the use of liners which are too thin results in bad insulation, which may prevent the molten metal from collecting before it freezes.

As for the charge, better results are obtained with high packing density, since this means a greater amount of heat generated per unit area of wall and better thermal conductivity within the charge, with the consequent greater thermal penetration before the surface reaches ignition temperature. For the packed densities normally achieved in practice the thermal diffusivities, α , of the dolomite, MgF_2 and $UF_4 + Mg$ charge are not very different.⁽¹⁰⁾ With this assumption and that of a long cylindrical furnace pot, Beatty and Magoteaux⁽⁷⁾ have calculated

‡ Iowa State College, U.S.A.

‡‡ Argonne National Laboratory, The University of Chicago, U.S.A.

the time θ , for preheating at a given external temperature t_1 , to bring the charge and the liner up from an initial temperature t_i to a mean temperature t_m , by using the equations for variable state transmission of heat. The plot of $t_m = \frac{t_m - t_i}{t_1 - t_i}$ versus $\alpha \cdot \theta / r_1^2$ with r_c / r_1 as a parameter (where r_c and r_1 are the radius of the charge and the outer radius of the liner, respectively) shows, that increasing the liner thickness increases the time to reach a determined mean temperature and that the degree of sensitivity of the mean temperature to changes in liner thickness decreases somewhat with increasing lengths of heating time. A second effect of increasing the liner thickness is to decrease the ratio between the maximum temperature in the charge and its average temperature.

If a graphite liner is used, however, a new factor is introduced, i.e., its high thermal conductivity as compared with that of the charge. This requires either the use of lower furnace temperatures so that the charge is heated more gradually and/or higher packing densities of the charge. (1)

From the above considerations and from the standpoint of reaction temperature it would appear that the most desirable preheating conditions would be those which bring the reactants to a fairly uniform elevated

temperature by the time the reaction initiates. This can be achieved, however, for maximum compacting densities, only at a cost of increased pre-heating times, and other factors have to be taken into consideration, namely the effects of the side reactions taking place during preheating.

1.3.2 The Effect of the Process Variables on the Yield of Uranium

As a result of numerous investigations, the conditions affecting the yield of massive uranium are, at present, reasonably well established. Losses of uranium, however, have a twofold origin and are due to the occurrence of both small particles of uranium metal and uranium compounds, mainly UO_2 , in the slag. Since it is practically impossible to determine quantitatively the relative importance of the two contributions, interpretation of the results is not always easy.

The variables found to have a most profound effect on the yield are: packing density of the charge, excess of magnesium, impurities in the charge, and length of the preheating period.

a. Packing Density of the Charge

There is evidence that the packing density of the charge affects the losses of uranium, at least as far as the trapped particles of metal are concerned.

Harper and Williams⁽¹¹⁾ noted that a decrease in charge density from 2.3 to 1.3 g/cc resulted in a decrease of the yield from 92% to 70%. The grey colour of the slag from the lower density charge indicated that considerable quantities of metal were trapped in the slag. Tests made at the Argonne Laboratory⁽¹²⁾ with charges hand-tamped to a density up to 3.49 g/cc and with charges compacted to a density of 3.64 g/cc by double pressing, gave highest yields of 93.7% and 97.2%, respectively. In both cases a 6% excess of magnesium was used and the furnace temperatures were 700°C and 600°C, respectively. The ignition temperatures were 600 ± 5°C in the first case and 600 ± 10°C in the second. The occurrence of uranium metal in the fast freezing, $\frac{1}{8}$ in. thick slag layer next to the graphite liner was found to be less with compacted charges than with hand-tamped charges.

b. Excess of Magnesium

The effect of the excess of magnesium on the yield was studied by Magoteaux and Smitherman⁽¹³⁾ who found that an increase of 2 to 6% increased the yield from 93.0 to 94.3%. In the Ames Laboratory⁽⁵⁾ an initial excess of magnesium effected a sharp increase in recovery which increased with the excess up to a maximum. Further increases did not benefit the recovery and caused difficulties due to skull formation and pyrophoric

coatings. The optimum excess of magnesium decreased with increasing size of the reaction vessel. Bombs may require 20 - 30% excess, whereas 10 in. vessels require as little as 5% excess of magnesium in the charge.

c. Impurities in the System

The impurities in the system may have different origins:

- (i) The green salt (commercial UF_4) whose impurities are mainly UO_2 , UO_2F_2 and water. A typical analysis given by Baker et al.⁽¹⁴⁾ for these impurities is 0.29, 2.08 and 0.04%, respectively.
- (ii) The magnesium which may be coated with a thin film of oxide.
- (iii) The liner material, which usually has gases absorbed, mainly moisture.
- (iv) The atmosphere in the vessel (argon or hydrogen) whose main impurities are usually moisture and oxygen.

Apart from these main impurities, there are others present in the liner and charge, mainly elements, in concentrations varying from a few ppm, to 500 ppm. Since these impurities are eventually picked up by the metal, the materials used in the process have to satisfy standard specifications of purity, but they do not affect

otherwise the efficiency of the process.

The purity of the UF_4 was found to have the most profound effect on the yield⁽¹³⁾, an increase in purity from 92.9% to 97.7% increased the recovery from 78% to 93%. Although the effort devoted to increasing the purity of the fluoride cannot be carried too far, due to economic considerations, green salt is today available commercially with a purity of around 99.6%⁽¹²⁾.

The effect on the recovery of the oxide film coatings on the magnesium is difficult to determine since they are difficult to reproduce. Superior results were reported by the Ames Laboratory⁽⁵⁾ with magnesium produced by the ferrosilicon reduction process, (rather than the electrolytic or carbothermic) although all these grades meet normal purity requirements. Although the magnesium from the various sources differs in the micro forms of the crystals and in the shapes of the fine particles, the major effect is believed to be the temperature at which the magnesium is first exposed to air in a retort or to the leakage of air in vacuum systems, which would affect the nature of the oxide film.

Apart from the original oxide films, filming of the magnesium may occur during the preheating period due to reaction with UF_4 , UO_2F_2 , water and HF, or with film forming additives, such as $NaHF_2$, KHF_2 and HF, and they

may have some effect on the subsequent reduction reaction. The nature of these films was studied by Schwartz and Vaughan⁽¹⁵⁾ who showed the presence of MgO and Mg(OH)₂ on the extreme outer surface of the coating while the MgF₂ was below. In the case of UF₄ in the presence of HF only MgF₂ was detected. The formation of HF, in the charge, during the preheating period is usually assumed to occur due to side reactions. One reaction producing HF is thought to be a cyclic reaction of the type⁽¹⁶⁾:



Such a reaction is very likely to occur when the reduction is carried out in a hydrogen atmosphere, but might also occur in other atmospheres since H₂ is formed by reaction between residual moisture and magnesium, in the early stages of heating⁽¹⁷⁾. Another possible source of HF in the bomb atmosphere is the reaction of residual moisture with UF₄. Evidence of this reaction is found in the form of thin layers of UO₂, at the liner charge interface, in bombs which are heated short of ignition and then cooled. In the case of CaO liners UO₂ may even be produced due to reaction of HF with the liner, producing CaF₂ and more water, which hydrolyses more UF₄. A corrective measure is to add some fine Ca or Mg to the refractory powder before packing.

Filming of the magnesium can also be carried out before blending with the green salt. Reaction with HF-air mixtures and SO_3 proved to form rather tough films, while reaction with sulphur vapour gives a weak film⁽¹⁸⁾. A strong anhydrous film of magnesium fluoride is formed in contact with anhydrous HF at elevated temperatures⁽¹⁹⁾. The thickness of the magnesium fluoride film increases with increasing filming temperature until at about 475°C an abrupt decrease occurs.

The effect of filming on the ignition of the charge is exemplified by the experiments of Leifield and Newmann⁽¹⁶⁾, who found that with increased thickness of the film, the pre-ignition time is increased, other variables being kept constant. These authors also found evidence of the cyclic reaction (Equations 1.1) already mentioned. Increased additions of UO_2F_2 to the green salt resulted in increased pre-ignition times.

d. The Length of the Pre-ignition Period

In bomb reductions, a significant decrease in the yield occurred whenever the reactants were held at temperatures between 400°C and the ignition temperature for more than 30 minutes⁽¹¹⁾. The resultant slag in one case had a uranium content ranging from about 18% near the slag-metal interface to about 2% at the top of the slag.

An increase in the length of the pre-ignition period is reported by Harrington and Ruehle⁽⁶⁾ with decreasing specific area of the magnesium and increasing furnace temperature.

1.3.3 The Mechanism of Ignition

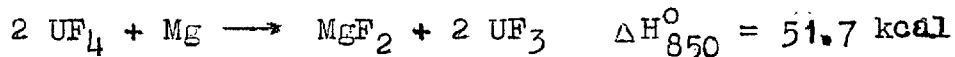
Conflicting theories are advanced for the mechanism of ignition.

Since variables such as thickness of MgF_2 film, specific area of Mg and heating rate, introduce conditions tending to vary the pressure of the magnesium vapour in the charge and seem to affect the pre-ignition time in a predictable way, they were advanced by Harrington and Ruehle⁽⁶⁾ as partial evidence that the bomb reaction starts as a magnesium vapour - UF_4 solid reaction. Other evidence is given by these authors. Examination of mixtures of UF_4 and magnesium which have been heated to just short of firing, reveal darkened areas in the green salt surrounding particles of magnesium. These areas contain UF_3 and MgF_2 . With an experimental arrangement such that only magnesium vapour could reach the UF_4 , the reaction proceeded through an intermediate UF_3 stage, then to metal⁽²⁰⁾. Furthermore, mixtures with a two-to-one mole ratio of UF_4 to magnesium yielded UF_3 , MgF_2 and little uranium when fired in a bomb.

There is no doubt that pre-ignition reaction occurs between the magnesium vapour and the UF_4 , but whether it is this reaction or the direct contact of the uranium fluoride with molten magnesium bursting through the MgF_2 film, which "triggers" the ignition, remains to be proved. In this respect it is more conclusive to determine the dependence of the ignition temperature, rather than pre-ignition time on the different variables, since longer ignition times may be due in part to lower thermal conductivity of the charge caused by the presence of films on the Mg.

More interesting evidence of pre-ignition reactions is reported by Wilkinson^(1, 12). Sections of charges which had been heated for two hours at pre-ignition temperatures, showed no change in the green colour at $320^\circ C$, but a core of brownish coloration was found near the crucible bottom at 350° . Increases in the temperature increased the size and darkness of the brown coloration. At $580^\circ C$ the whole mass looked fused. This change in colour occurred only when magnesium was present. For charges heated to the range $570 - 630^\circ C$ the magnesium appears to segregate in the lower part of the charge. Since this temperature range is below the melting point of the magnesium and X-ray patterns show the presence of substantial amounts of UF_3 the fusion of the magnesium

must be due to the heat evolved in the reaction:



Heating curves on charges that had been outgassed for 12 hours were obtained for two locations of the thermocouples, 1 in. above the bottom, one at the center of the charge and the other at the liner-charge interface. The curves generally intersected between 375 and 475°C indicating that localized exothermic reaction occurred at a lower temperature. This reaction is not directly connected with ignition, which is marked by the upward inflection of the curves that is observed above 600°C. This evidence of a localized exothermic reaction could be detected only for small charges.

It is doubtful whether the change in colour of the charge, reported by Wilhelm to occur at such low temperatures as 350°C, is due to Mg vapour-UF₄ reaction. Paine et.al.⁽²⁰⁾ reported 540°C as the minimum temperature at which the reaction is detectable. Also, the brownish colour reported is more typical of UO₂ than UF₃ which is usually darker in appearance.

The fact that change in colour only occurs in presence of Mg may be due to side reactions of the type discussed before.

Evidence of pre-ignition reaction was also found by Harper and Williams⁽¹¹⁾ who noted, on heating a pellet of Mg + UF₄, evolution of heat at about 560°C. Ignition of the pellet, detected by a rapid rise in the temperature, took place only between 600 - 650°C.

Since the temperature at which the reactants ignite seems to correspond closely to the melting point of the magnesium (651°C) it has been suggested⁽¹¹⁾ that the liquid magnesium and uranium fluoride mixture would provide the intimate contact required for the rapid propagation of the reaction. This is supported by the results obtained by Harper and Williams⁽¹¹⁾ when a Mg-Pb alloy (m.p. 460°C) was used in place of pure Mg. An exothermic reaction was noted just above the melting point of the alloy at 470°C.

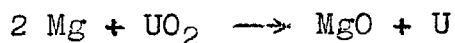
1.3.4 The Reaction and Post-Reaction Period

The furnaces employed to fire the reduction bombs are generally designed to heat the bottom of the bomb faster than the top. This starts the reaction at the bottom of the charge and once ignited the burning front moves up through the charge with a rate of propagation of the order of 0.2 in. per second⁽⁶⁾. As the temperature increases the products and reactants encounter numerous phase changes, e.g. Mg, UF₄, U and MgF₂ liquify, in that order, at 650°C, 1036°C and 1260°C respectively, and Mg

boils at 1104°C . The fluidity of the slag is a function of the ultimate temperature attained by the reaction and has, as mentioned before, great influence on the yield of uranium. In the case of a graphite liner, uranium particles are primarily trapped in a fast freezing $\frac{1}{8}$ in. thick slag layer next to the graphite wall, but they are also encountered just above the uranium regulus⁽¹⁾. It is difficult to know whether this concentration gradient pattern is also found when a liner with lower thermal conductivity is used. At least, in the case of reductions carried out in unfavourable conditions, such as some of Harper and Williams' experiments⁽¹¹⁾, where a substantial amount of UO_2 is also present in the slag, the concentration gradient trend seemed to be inverse, i.e., higher concentration of uranium at the metal-slag interface. It was suggested that, in such cases, the UO_2 prevented the agglomeration of the uranium by the formation of a viscous high density bridge at the slag-metal interface. An alternative suggestion was that the UO_2 prevented the agglomeration of the metal by adhering to the surface of the globules by a surface tension effect. Phase equilibrium studies involving UO_2 , UF_4 and MgF_2 were carried out in this laboratory by Bell⁽²¹⁾ and Welch⁽²²⁾. In none of the three binary systems was evidence found of solid solution, and the solubility of UO_2 in molten slag was shown to be very small.

Bell suggested that, in view of its low solubility in MgF_2 and high density, the UO_2 , even if taken into solution at the maximum temperature of the reaction (ca. $1700^\circ C$), would be precipitated as the slag cooled and would settle rapidly to form a layer at the slag-metal interface. Droplets of metal encountering this layer would find difficulty in penetrating to the regulus. The microscopic observation of a polished section of slag, from the top portion of a typical bomb reduction, did not show any apparent association between the droplets and the UO_2 ⁽²¹⁾.

The presence of UO_2 in the products is not very easily explained from a thermodynamic point of view. The free energy of the reaction:



is less than - 10 kcal up to $1130^\circ C$ and only becomes positive around $1300^\circ C$. It was suggested⁽⁷⁾ that UO_2 is reduced below $1130^\circ C$ and formed again when the temperature rises above this temperature and that on cooling when the equilibrium favours again the reduction of UO_2 , either because the amount of free magnesium is no longer sufficient or because the reaction is too slow, no effective reaction takes place.

1.3.5 Summary

To summarize, the losses of uranium are due firstly to minute particles of metal trapped in the slag, which can be reduced at least to some extent by improved thermal characteristics of the charge and/or by a suitable programmed heating. A second source of loss in yield is the occurrence of uranium compounds, mainly UO_2 , whose origin may be traced to the presence of impurities in the system and to various side reactions taking place during preheating.

The mechanism by which the reactants ignite is not known, evidence having been advanced either for a vapour-solid or for a liquid-solid reaction.

One of the great difficulties in interpreting the results of the numerous investigations is the practical impossibility of determining quantitatively the relative importance of the two contributions to the losses of uranium.

The other difficulty resides in the fact that, because of the great number of process variables, the results of different investigations are not easily comparable.

The foregoing review shows the lack of data on the mechanism and kinetics of the reactions taking place either in the pre-ignition period or in the short period

where the reaction is rapid and selfpropagating. Some work has been done on the kinetics of the reaction of UF_4 powder with Mg vapour⁽²⁰⁾, H_2O ⁽²³⁾ and O_2 ^(24,25) and the reaction of UO_2F_2 with H_2 ⁽²⁶⁾. These investigations, however, were carried out on powders and the results have only a qualitative value. They did not shed a great deal of light on the more fundamental aspects such as the mechanism of the reactions and their relative rates under the conditions prevailing in the bomb.

1.4 Gas Solid Reactions

1.4.1. General

Because of their practical interest, gas solid reactions have been the object of a wide number of investigations, especially in the field of oxidation of metals and alloys.

When the clean surface of a solid is exposed to the attack of a gas, unless the reaction product is volatile, an intermediate product layer is initially formed that separates the gas from the metal. Further progress of the reaction is only possible by transport of matter through this layer. The mechanism of transport will depend on the nature of the product layer, mainly on whether it is compact or interspersed with cracks and pores. In the first case some sort of diffusion mechanism through the layer has to be assumed. In the second case simple

passage of the gas molecules through the cracks or pores can explain the progress of the reaction. The formation of compact layers is theoretically the most interesting case and since it is relevant to this work will be discussed in more detail.

The first question which arises is the nature of the diffusing species. Electrical and electrochemical investigations and diffusion experiments on oxides, sulphides and halides carried out in particular by Tubandt, Reinhold, Jost, Braune, Von Hevesy, Seith and associates have shown that in these phases cations, anions and electrons are mobile but that the mobility of the various particles may differ widely. In view of these facts Wagner⁽²⁷⁾ suggested the hypothesis that simultaneous ionic and electronic conduction in oxides, sulphides and halides accounts for the rate of formation of tarnish layers on metals exposed to oxygen, sulphur or halogens at high temperatures, whereas migration of electrically neutral atoms or molecules may be neglected. Likewise the reduction of oxides and sulphides and the photographic processes may involve simultaneous migration of ions and electrons⁽²⁸⁾.

The second question that needs to be dealt with refers to the different time laws encountered for the growth of the product layers.

As a limiting case one can assume that diffusion

through the layer of oxide or other product is the rate determining step. If a quasi-stationary state is established, i.e. the activities of the reactants at the boundaries of the product layer are independent of time and thermodynamic equilibrium is practically established at the interfaces, it follows from Fick's law that the rate of increase of the layer will be inversely proportional to the thickness of the layer x :

$$\frac{dx}{dt} = k/x \quad (1.1)$$

where k is a constant proportional to the diffusion coefficient. Integration of equation (1.1) yields:

$$x^2 = 2kt$$

if $x = 0$ when $t = 0$, or

$$x = (2kt)^{\frac{1}{2}}$$

This "parabolic rate law" was first derived by Tammann (29) in 1920 and has often been confirmed experimentally. However, other rate laws may govern the growth of product layers in gas-solid reactions. If for instance the phase boundary reactions are slow enough to be comparable to the diffusion rate of the ions, one obtains the "mixed parabolic law" developed by Evans (30), Fischbeck (31), Jost (32) and Noltige (33):

$$\frac{dx}{dt} = \frac{kl}{k+lx}$$

where k and l are constants.

In the limiting case of a very thick product layer the phase boundary reaction may become time determining and the "mixed parabolic law" turns into the "linear law".

$$\frac{dx}{dt} = l$$

Other phenomena may also play a determinant role as; pointed (34) by Mott in the case of very thin layers. In this case electric double layers at the boundaries of the film may establish an extremely high electrical field strength which makes the reaction rate decrease more rapidly with increasing thickness of the layer than would be predicted from the parabolic law. This is an interpretation for the logarithmic rate law first established empirically by Tammann and Koster (35) in 1922. A full account of these and other growth rate laws (as for instance the cubic and inverse logarithmic rate laws) can be found in recent books (36) by Kubaschewski and Hopkins and (37) Evans. For a given reaction more than one rate law may be observed, the change over from one to another depending on the product layer thickness. For thin films logarithmic and cubic, for normal layers parabolic and linear rate laws predominate. Since it is relevant for the present work, the parabolic law will be discussed here in more detail.

1.4.2. Wagner's Theory of the Rate of Growth of Protective Layers

In what follows we consider an ionic compound of metal Me and non metal X in which cations, anions and electrons

designated as constituents $i = 1, 2$ and 3 respectively, may migrate.

The basic assumption made by Wagner is that of independent migration of each type of particle and therefore the theory is only valid for small concentration of lattice defects and small deviations from ideal stoichiometric ratio.

Under the action of both local electrical potential and its chemical potential μ_i (in erg/mole), the particle will move in the x-direction with an average drift velocity u_i in cm/sec given by:

$$u_i = - B_i \left[\frac{1}{N} \frac{d\mu_i}{dx} + z_i e \frac{d\phi}{dx} \right]$$

where N is Avogadro's number, z_i is the electrical valence of a particle of type i (positive for cations, negative for anions), e is the electronic charge and B_i is the mobility of particles of species i , i.e. the steady state velocity under unit force per particle, corresponding to a change in the chemical potential per particle by unit energy (1 erg) for a displacement of unit length (1 cm).

Hence the number of moles of constituent i migrating per unit cross section (1 cm^2) per unit time (1 sec) will be

$$\frac{dn_i}{dt} \cdot \frac{1}{S} = c_i u_i = - B_i c_i \left[\frac{1}{N} \frac{d\mu_i}{dx} + z_i e \frac{d\phi}{dx} \right]$$

where S is the cross section in cm^2 , c_i is the concentration of i in moles per cm^3 .

The mobility B_i may be derived (i) from electrical data, such as electrical conductivity and the transference number t_i of particle i , or (ii) from self diffusion measurements involving isotopes and upon use of Einstein's equation:

$$D_i^{\#} = B_i kT$$

where k is the Boltzmann constant, T the absolute temperature and $D_i^{\#}$ the self-diffusion coefficient of particle i . As pointed out by Wagner⁽³⁸⁾, the validity of this equation is restricted to the case where self diffusion is accomplished essentially by random motion of particles in interstitial positions or random motion of vacancies, but not by direct exchange of two particles of the same type in equivalent lattice positions.

Using the mobilities of ions and electrons derived from electrical data, introducing the condition of electrical neutrality and considering the relationships for the chemical potentials, Wagner⁽²⁷⁾ derived the following equation for the rate of formation of a coherent layer of an oxide, halide or sulphide

$$\frac{dn}{dt} \cdot \frac{1}{S} = \left\{ \frac{300}{96500Ne} \int_{\mu_y}^{\mu_x} \frac{1}{|z|} (t_1 + t_2) t_3 \sigma \, d\mu_x \right\} \frac{1}{\Delta x} \quad (1.2)$$

$$= \left\{ \frac{300}{96500Ne} \int_{\mu_{Me}''}^{\mu_{Me}'} \frac{1}{z_1} (t_1 + t_2) t_3 \sigma d\mu_{Me} \right\} \frac{1}{\Delta x}$$

$$= \frac{k_r}{\Delta x}$$

where $\frac{dn}{dt} \frac{1}{S}$ is the rate of both outward migrating cations and inward migrating anions in terms of equivalents per cm^2 per second, Δx is the instantaneous thickness of the reaction product in cm, e is the electronic charge in absolute electrostatic units, σ is the electrical conductivity in $ohm^{-1} cm^{-1}$, μ_X and μ_{Me} are the chemical potentials of non-metal and metal respectively, in erg per gram atom, and μ_X' and μ_X'' are the chemical potentials of non-metal at the inner and outer interfaces respectively.

The expression in brackets has been named by Wagner the "rational rate constant" k_r , indicating the rate in equivalents per square centimeter per second for a layer of the reaction product which is 1 cm thick.

An equivalent form of equation (1.2) was derived by Wagner in a later paper (39):

$$k_r = c_e \int_{a_X''}^{a_X'} \left(\frac{z_1}{|z_2|} D_1^{\#} + D_2^{\#} \right) d \ln a_X \quad (1.3)$$

$$= c_e q \int_{a_{Me}''}^{a_{Me}'} \left(D_1^{\#} + \frac{|z_2|}{z_1} D_2^{\#} \right) d \ln a_{Me} \quad (1.3a)$$

if $t_3 \cong 1$

where $c_{eq} = z_1 e_1 = z_2 e_2$ is the concentration of cations or anions in equivalents per cubic centimeter and a_{Me} and a_X are the thermodynamic activities of metal and non-metal respectively. Equations (1.3) are derived on the assumption that $t_3 \cong 1$ and t_1 and t_2 are small (e.g. $< 10^{-4}$), which is a very usual case in practice. Thus equations (1.3) provide an alternative possibility of calculating k_p under conditions where use of equation (1.2) would be impractical due to the experimental difficulties in determining ^{such} ~~so~~ small transference numbers.

Equations (1.2) and (1.3) have been derived in order to check the underlying assumptions set forth by Wagner, particularly that of independent migration of ions and electrons and not to replace the direct determination of the rate constants. Wagner⁽³⁹⁾ has compared the calculated (from equation 1.2) and experimental rate constants for a few cases and found satisfactory agreement between the two sets of values. Equation (1.3) has been proved correct at least in one case, by Carter and Richardson⁽⁴⁰⁾ who measured the oxidation rate of cobalt and the diffusion coefficient of Co^{60} in CoO as a function of oxygen pressure. Since marker experiments have shown that oxidation of cobalt occurs mainly by cation diffusion, equation (1.3) is simplified by putting $D_2 \cong 0$; a_X is equal to the oxygen pressure at all points in the oxide, $z_2 = 2$ and

$z_1 = (O/Co) \times z_2 \cong 2$. Equation (1.3) thus becomes:

$$k_r = c_{Oq} \sqrt{\frac{a_X^{\ddagger}}{a_X^{\ddagger}}} D_1^{\ddagger} d \ln p_{O_2}$$

Integration of D_1^{\ddagger} vs. $\log p_{O_2}$ -curves allowed the comparison of the rational constants thus calculated with the experimental ones obtained from the parabolic plots. The agreement between the two values was well within the limits of the experimental error.

1.4.3 Lattice Defects

From the discussion above, it is apparent that the rate of growth of a coherent layer is directly related to its electrical conductivity and the transference numbers of ions and electrons, but no reference was then made to the nature of the conduction mechanism. Since a mutual interchange of two ions each carrying the same electrical charge can never result in transport of electricity⁽³⁸⁾, one may conclude that ionic conduction is due to lattice defects. Moreover, where measurements of both electrolytic conduction (and transference numbers) and diffusion have been possible, there is sufficient agreement between the mobilities derived from either set of observation to conclude that diffusion processes in ionic crystals are also due to lattice defects.

Disregarding complex cases there are three basic types of misarrangement within the crystalline lattice: substitutional, interstitial ions and vacancies. In general, substitutional disorder is not important for crystals with predominantly ionic bonding because of the mismatch in atomic size and charge. In a stoichiometric ionic crystal and in order to maintain electrical neutrality there are at least two different ways in which these interstitial ions and vacant lattice sites may arise. They are called "Frenkel defects" and "Schottky defects". The four possible cases are: (i) the Frenkel disorder type involving equal concentration of interstitial cations and vacant cations sites, (ii) the antiFrenkel disorder type consisting of equal concentration of anion interstitials and vacancies, (iii) the Schottky disorder type involving cation and anion vacancies in the same ratio as the stoichiometric, (iv) the anti-Schottky disorder type consisting of cation and anion interstitials. The concentration of these defects are determined by an internal thermodynamic equilibrium which depends, of course, on temperature. The predominance of one type of disorder is determined by the energy required to form the different types of lattice defects, the lower energy being, of course, the more favourable. Only if the energy for two different types of disorder is very similar, there will be coexistence.

The mechanism of migration obviously depends on the type of disorder. In the case of a "Schottky disorder" which is typical of the alkali halides, one ion in a normal lattice site may jump to an adjacent vacancy of the same type of ion and hereby create a vacancy at the initially occupied site. This is the vacancy mechanism of migration, the net result being a migration of the ions in the opposite direction. In such a lattice we may, therefore, expect both ions to be mobile and their relative mobility will depend on the height of the potential barriers they have to overcome on jumping. The influence of the distance between adjacent ions will decrease with the thermal expansion of the crystal

In the case of a "Frenkel disorder" (or "anti-Frenkel disorder") cations (or anions) are mobile as the anion (or cation) sublattice is complete. Thus, their mobility will be due to the vacancy mechanism and/or the motion of interstitial cations (or anions). An interstitial ion can move either by jumping directly to another interstitial site (interstitial mechanism) or by pushing one of its nearest neighbouring ions into an interstitial position and taking its place (interstitialcy mechanism).

In the case of a growing product layer, small deviations from the ideal stoichiometric composition must be assumed, since whenever there is a diffusion process, there must be a concentration gradient. There is ample evidence that such deviations from stoichiometry actually occur and in a few cases within wide limits (e.g., wustite). According to Wagner, Schottky, Stroock, Laves and others¹, there are the following basic types of disorder for compounds involving deviations from the ideal stoichiometric composition: (i) compounds with excess of metal, consisting either of cations in interstitial positions and excess free electrons, or anion vacancies and quasi-free electrons (in which case the compound is said to have a deficit of non-metal), (ii) compounds with deficit of metal (equivalent to an excess of non-metal) in which there are either cation vacancies and electron holes or anions in interstitial positions and electron holes. The term electron hole means that somewhere in the lattice an electron is missing as compared to the state of the ideal lattice. For instance, a trivalent nickel ion in nickel oxide represents an electron hole. Quasi-free electrons are, of course, mobile and the same is true for electron holes since electrons may be exchanged between ions of the same type but of different

¹ See references quoted by Wagner. (39)

valence, e.g., Ni^{3+} and Ni^{2+} . Compounds, such as most of metal oxides, sulphides and nitrides where deviations from the ideal stoichiometric composition occur, exhibit therefore electronic conductivity (apart from the ionic conductivity which is characteristic of pure ionic compounds), and are generally classified as semiconductors. A recent book by Mandlecorn⁽⁴¹⁾ contains much detailed information on non-stoichiometric compounds.

One can, therefore, expect a change in the electrical properties of a compound due to deviations from the ideal integral stoichiometric composition. Pohl, Stasiw, Smakula, Hilsch, Mollowo and their associates⁽⁴²⁾ have shown in fact that, though alkali halides of ideal stoichiometric composition are ionic conductors, electronic conduction in addition to ionic conduction occurs when either an excess of metal or an excess of halogen is present. Baedeker^(43, 44) observed that with rising partial pressure of iodine there was a very marked increase in the conductivity of CuI . The "pure" CuI is a poor conductor at low temperatures, the conduction being at least partially electrolytic, and above 300°C exhibits strong electrolytic conductivity. Wagner⁽⁴⁵⁾ measured the conductivity of AgBr at 200°C without bromine and in presence of 0.23 atm. of bromine vapour. In the later case the conductivity was increased by 12% above that obtained in pure nitrogen.

1.4.5 Inert Markers

Pfeil^(46, 47) was the first to use inert markers to show that anions and cations could diffuse at very different rates in oxides. He found that when iron painted with chromic oxide was oxidised, the markers were found close to the metal surface but in the "FeO" layer. This result did not conclusively prove that the oxide layer grew only by the outward migration of iron ions but it has shown a significant difference in mobility of the oxygen and iron ions. The method was later applied to the interdiffusion of alloys and it is now in general use to determine the diffusion mechanism of growing product layers. Using a more refined technique¹ than Pfeil; Davies, Simnad and Birchenal⁽⁴⁸⁾ have shown that when iron is marked and oxidised in O₂ to give a scale of "FeO", Fe₃O₄ and Fe₂O₃, the markers are found precisely at the Fe/"FeO" interface, indicating that outward migration of iron ions is mainly responsible for the growth of the "FeO" layer. When "FeO" was marked and completely oxidised to Fe₃O₄ the markers were found to enclose 80% of the Fe₃O₄. This was later interpreted by these authors⁽⁴⁹⁾ as due to the outward migration of iron ions forming Fe₃O₄ outside the markers the removal of which from the FeO lattice also causes Fe₃O₄ to be produced within the FeO. A block of

¹ Davies et al. marked the surface of the blocks to be oxidised by applying to the surface a silk thread wetted in radioactive AgNO₃ solution.

Fe_3O_4 was also marked and partially oxidised to Fe_2O_3 in O_2 . The markers could not be found and were thus assumed to have remained on the surface and volatilised off during the long oxidation period. This indicates that Fe_2O_3 grows by the inward migration of oxygen ions, a result supported with measurements by Himmel⁽⁵⁰⁾ who found that the diffusion rate of iron ions in Fe_2O_3 is negligible. Radioactive platinum was used by Carter and Richardson⁽⁴⁰⁾, to determine the mechanism of oxidation of cobalt. The markers were found at the metal-oxide interface, thus indicating that the oxide layer grows by outward migration of cobalt ions. Hocking⁽⁵¹⁾ used gold markers to study the growth of sulphate layers on blocks of cobaltous and cuprous oxides. For the CoO blocks the markers were found at the CoO/CoSO_4 interface, thus showing that the sulphate grows by outward migration of cobaltous ions. For the Cu_2O blocks at 688°C , two sulphate layers (CuSO_4 and $\text{CuO}\cdot\text{CuSO}_4$) and an oxide layer beneath these two were formed. The markers were found at the $\text{CuO}\cdot\text{CuSO}_4/\text{CuSO}_4$ interface. Hocking suggested that the outer CuSO_4 layer and the underlying CuO layer were produced by the outward migration of copper ions and that the inward growing $\text{CuO}\cdot\text{CuSO}_4$ layer must grow by the inward migration of a sulphating aggregate which attacks the CuO layer to form $\text{CuO}\cdot\text{CuSO}_4$.

Marker experiments (those mentioned above are only a few examples) are not without ambiguity and very often conflicting reports are found in the literature. One obvious condition for the successful use of this technique is that the markers should be inert, but other precautions must also be taken. If the markers are too large they may act as barriers protecting the material beneath, which is consumed only by lateral diffusion; thus the marker may be found embedded in, for instance, an oxide scale at some distance from the metal interface even if the oxide grows entirely by cation diffusion. On the contrary, very thin markers may be held to the metal interface by surface tension even when the oxide grows by inward migration of oxygen ions. Sachs' (52) experiments give a good example of such phenomena. Nickel and copper markers in ^{the} form of electrodeposits and wires of various thicknesses were placed on the surface of mild steel specimens which were subsequently oxidised at 900°C. It was found that, during oxidation, thick wires (0.12 - 0.2 cm diameter) moved outwards, very thin electrodeposits moved inwards and intermediate sizes (0.02 cm diam. wires) occupied intermediate positions. Sachs explained that the movement of the large markers was due to interference with normal diffusion. They are not easily covered with oxide and are pushed outward by lateral diffusion beneath

the markers. Kubaschewski and Evans⁽⁵²⁾ found less acceptable Sachs' explanation for the movement of the very thin markers, according to which the markers would dissolve in the oxide and migrate towards the metal oxide interface where they are precipitated in the form of flashes. Such^a mechanism, argue Kubaschewski and Evans, is very unlikely since it would involve diffusion against a concentration gradient of cations and either the very thin markers are held to the metal surface by surface tension, or their movement represents the true behaviour, the thin wires being also moved by some mechanical effect.

1.5 Objects of the Present Work

In selecting the programme for the present work, attention was primarily focussed on the kinetics and mechanism of the Mg vapour - UF_4 solid reaction, as a first step for a better understanding of the fundamental aspects of the industrial process of production of uranium metal. This study would be an extension of the preliminary studies carried out by Paine et al⁽²⁰⁾ and was thought to be of great theoretical interest for elucidating the mechanism of reaction between reducing metal vapours and solid uranium fluorides. Many studies of high temperature gas/solid reactions, such as the oxidation of metals, by oxygen, sulphur and halogens, the reduction of sulphides by hydrogen and more complex reactions have been reported

in the literature. No reference, however, was found to kinetic studies of gas/solid reactions involving a metal vapour with the exception of the one mentioned above. One purpose of this investigation was to find out whether product layers are formed on the UF_4 and if so, whether diffusion across the layers is the rate controlling step and in this case what is the nature of the diffusing species.

Before the kinetic studies were initiated, it was suggested by one of the sponsors of this work (UKAEA) that a theoretical study should be made of the possibility of using the reduction of UF_6 by sodium as a continuous process of producing massive uranium. After a literature survey and some preliminary thermodynamic calculations on the reaction, the chemical feasibility of the process was established, and only an engineering development would be necessary before its economic potentialities could be evaluated. The project was consequently not developed further and this preliminary work and conclusions are presented in Appendix I of this thesis.

1.6 Previous Research

Only one reference has been found in the literature on the reduction of UF_4 by Mg vapour. Paine, Ruehle and Lewis⁽²⁰⁾, using UF_4 powder, studied the reaction in the temperature range $540^\circ - 820^\circ C$ and found that the reduction

proceeds through the formation of an intermediate fluoride, UF_3 . The rate of reaction at each temperature was assumed to be roughly proportional to the time and the rate constant, at different temperatures, expressed as percentage of conversion to uranium per hour, was found to give roughly a linear curve of slope 1.5 when plotted in a logarithmic scale versus the logarithm of the vapour pressure of magnesium, expressed in mm of Hg. No theoretical interpretation was given for this relationship. A more detailed analysis of these experiments will be given later in the Discussion.

CHAPTER II

EXPERIMENTAL METHODS

2.1 Materials

2.1.1 Argon

Two grades of argon were used, both supplied by British Oxygen Co., Ltd. The makers analyses were as follows:

	Normal grade (99.95%)	High purity grade (99.995%)
Nitrogen	500 v.p.m.	30 v.p.m.
Oxygen	10 v.p.m.	6 v.p.m.
Hydrogen	10 v.p.m.	1 v.p.m.
CO ₂ and carbonaceous compounds as CO ₂	5 v.p.m.	5 v.p.m.
Water Vapour	Usually below 0.01g/m ³ , gradu- ally rising as the cylinder empties, to about 0.5 g/m ³	Identical, 0.01 and 0.5g/m ³ , respectively

2.1.2 Hydrogen, high purity grade, (99.99%)

This gas was also obtained from British Oxygen Co., Ltd., with the following analysis:

Oxygen	10 v.p.m.
Carbon monoxide	10 v.p.m.
Carbon dioxide	10 v.p.m.
Carbonaceous compounds as CO ₂	5 v.p.m.
Nitrogen	0.01%
Water vapour	Usually below 0.15 g/m ³ , gradually rising as the cylinder empties to about 1.0 g/m ³

2.1.3 Uranium

Uranium swarf was supplied by the Springfields Works of the United Kingdom Atomic Energy Authority. When cleaned with acid its purity was better than 99.94%.

2.1.4 Uranium tetrafluoride

The uranium tetrafluoride was supplied by the Springfields Works of the U.K.A.E.A. The impurity content was given as:

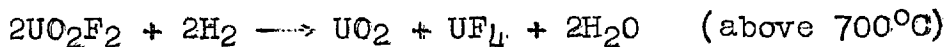
UO₂ - 0.09 wt %

UO₂F₂ - 0.40 wt %

H₂O - 0.15 wt %

Further purification was thought desirable and the technique developed by Bell⁽²¹⁾ was adopted. Full details of this technique may be found in his thesis. Only a general outline of the method and some alterations introduced during this work will be given here.

The tetrafluoride is dried in vacuo at ca. 450°C for several hours and then heated in hydrogen to ca. 800°C for two hours to reduce the UO₂F₂ according to the equation:



Since no reaction takes place between UO₂ and UF₄ the latter can be separated from the former by sublimation in vacuum (less than 10⁻³ mm). The UF₄ was contained in a pure nickel crucible which could be heated by high

frequency induction, and the sublimate was condensed in a cylinder of the same material sitting on the top of the crucible.

Instead of the one-piece condenser used by Bell, a two-sections one was used. This permitted the collection of two fractions of sublimed UF_4 ; the lower one, condensed at higher temperatures, was rejected and used in the next purification. The sublimation apparatus is shown in Figure 2.1. The need for such alteration arose when it was observed that after sublimation some UO_2 was present on the walls of the crucible and that therefore contamination of the UF_4 condensed on the bottom of the condenser was likely to occur, since in this region the temperature was only slightly lower than that of the crucible. Steeper gradients of temperatures on the condenser were also achieved by this arrangement. Another alteration found useful was to melt the UF_4 charge under argon prior to sublimation. In this way the slow process of degassing the UF_4 powder was avoided and a vacuum of better than 10^{-3} mm Hg could be easily maintained on heating up and during the sublimation.

After the sublimation was terminated the apparatus was allowed to cool down in an argon atmosphere and then quickly transferred into a dry box and taken apart. Care was taken to keep the assembly upright during all this procedure.

The upper fraction was easily removed by tapping with a hammer and was stored either in the dry box or in an evacuated desiccator. The lower fraction could not usually be completely removed by tapping and the tetrafluoride was dissolved in a boiling solution of equal parts of ammonium hydroxide (7N) and hydrogen peroxide (100 volumes).

2.1.5 Uranium Trifluoride

a. Methods of Preparation

Uranium trifluoride is not available commercially and had to be prepared.

Preparation of UF_3 by both wet and dry methods is reported in the literature. The wet methods are very recent (53, 54) and consist essentially in reducing solutions of uranium compounds with zinc amalgam and then precipitating uranium trifluoride by the addition of a fluoride solution. The product thus obtained is somewhat impure and the dry methods were preferred.

Three successful dry preparations of UF_3 have been reported. Spencer-Palmer (55), prepared the trifluoride by reduction of the tetrafluoride with hydrogen at 1000°C



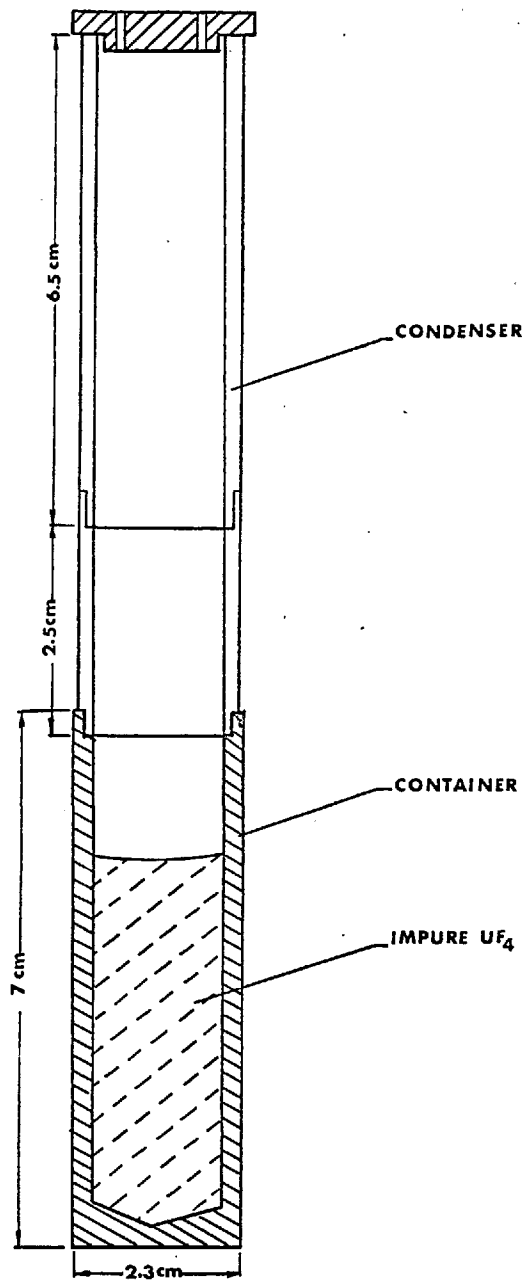


Fig.2.1: Container and Condenser for Subliming Uranium Tetrafluoride

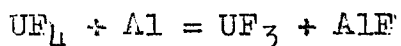
The purity of the trifluoride is contingent upon the exclusion of all traces of moisture or oxygen. Since hydrogen fluoride is also produced, the reaction must be carried out in a suitable all-metal apparatus or alternatively its glass or silica parts must be protected by ceresin wax in the cooler regions and by a stainless steel liner in the hot zone.

A second method of preparation was developed by American workers⁽⁵⁶⁾ in which UF_3 is obtained by reduction of UF_4 with uranium metal, at $1050^\circ C$



The control of temperature is important since the reaction is reversible and above $1050^\circ C$ the equilibrium is displaced to the left. The reaction may be carried out in a nickel vessel by mixing the stoichiometric amounts of UF_4 and uranium turnings. An intimate mixture of the reactants is achieved by converting the uranium to hydride at $250^\circ C$, in hydrogen, followed by its decomposition at $400^\circ C$.

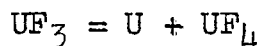
The third and more recent method of preparation of UF_3 by dry methods was reported by Runnalls⁽⁵⁷⁾ and consists essentially in heating, in vacuo, to $900^\circ C$, a mixture of "super-pure" aluminium filings and uranium tetrafluoride:



The product uranium trifluoride contains less than 2% of uranium dioxide.

b. Apparatus and Adopted Procedure

A determining factor in the choice of the method of preparation was the fact that uranium trifluoride cannot be purified by sublimation since it disproportionates in vacuo at all temperatures from 750°C upwards:



as reported by Spencer-Palmer⁽⁵⁵⁾ and Gilpatrick et al.⁽⁵⁸⁾

The method thought to be most likely to give a high purity product with a minimum of experimental trouble was the reduction of UF_4 by uranium metal.

The apparatus used in this preparation is shown in Figure 2.2. It consisted essentially of a pyrex glass envelope (GE), 6 cm in diameter and 17 cm long, which could be evacuated to a vacuum better than 10^{-4} mm Hg. Provision was made for the measurement of pressure (pirani head) and temperature (thermocouple). The reaction container (RC), 2.3 cm diameter x 7 cm long, was made of pure nickel and suspended by three nickel wires from a pyrex rod (PR) with three hooks on its end. A vacuum seal (VS) allowed the rod to be rotated by hand. High frequency induction heating was used. The system could be filled either with hydrogen or argon gases purified by passing through

Fig.2.2: Apparatus for the Preparation of UF_3

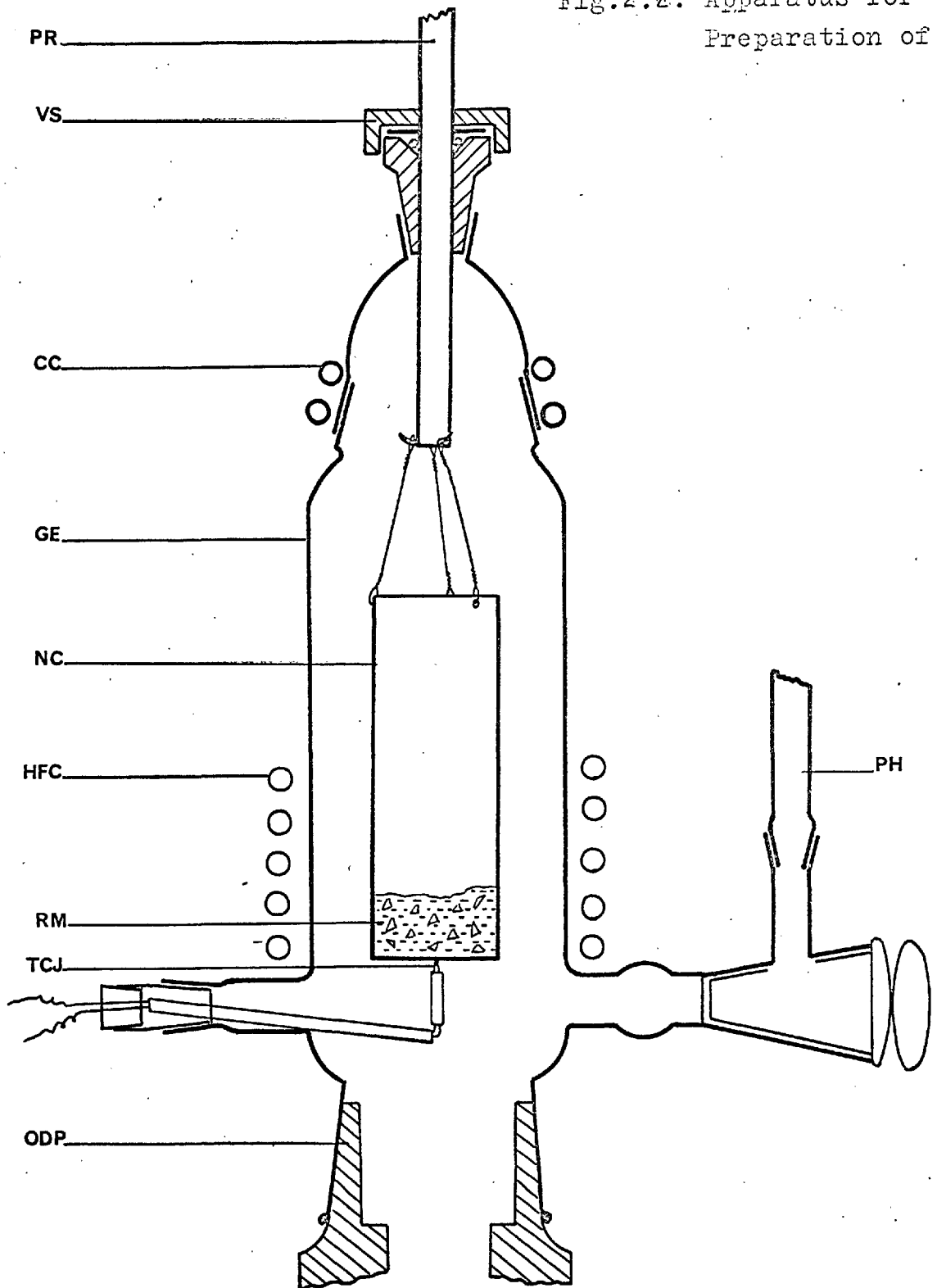


Fig. 2.2 Apparatus for the Preparation of UF_3

PR = pyrex rod

VS = vacuum seal

CC = cooling coil

GE = pyrex glass envelope

NC = nickel crucible

HFC = reactants mixture ($UF_4 + U$)

TCJ = thermocouple junction

ODP = oil diffusion pump

PH = pirani head

silica gel, magnesium perchlorate, phosphorus pentoxide and a uranium furnace held at ca. 800°C. The rate of admission of gases into the system could be finely controlled by means of a needle valve so that the flow rate of gas through the uranium furnace was slow enough to ensure efficient purification.

Prior to the actual preparation the nickel crucible was heated to 900°C, in hydrogen, for some hours. The system was then evacuated and degassed with the crucible temperature kept around 900°C. The system was refilled with argon and after cooling the crucible was rapidly transferred into a dry box where it was charged with the stoichiometric amounts of UF_4 and uranium. The uranium turnings cut in small pieces had been previously cleaned with acid and weighed in a stoppered weighing bottle filled with dry argon. Sublimed uranium tetrafluoride powder was used each time and the total charge could weigh up to 15 grams.

The charged crucible was hooked into position with the upright thermocouple junction touching its bottom. The system was degassed at room temperature and then filled with hydrogen. Uranium hydride was formed by heating to ca. 250°C for 2 - 3 hours and was then decomposed by increasing ^{the} temperature very slowly to 400°C.

A reasonably intimate mixture of the reactants was obtained in this way and improved by giving sharp half turns to the glass rod. The system was refilled with argon, the temperature set at about 500°C and kept at this value for 24 hours. Only then was the temperature increased to ca. 1000°C for about 30 minutes to ensure that the reaction was complete. The long treatment at 500°C was intended to ensure that most of the uranium had reacted with the tetrafluoride at low temperature since it was found[¶] that uranium metal reacts extensively with nickel at temperatures above about 600°C.

The final product had a black, coke-like appearance with no visible traces of any greenish (UF_4) or brownish (UO_2) material. For each batch an x-ray powder diffraction pattern was taken and the interplanar spacings (d Å) were calculated. A typical result is given in Table 2.1 alongside the data reported in the literature⁽⁵⁹⁾. The corresponding diffraction pattern is shown in Fig. 3.7.

2.1.6 Magnesium

Matthey specpure magnesium rods were used in all runs. The rods were machined down to a convenient diameter and cut in lengths of about 1 cm.

¶ See Section 2.3.2.

TABLE 2.1 X-Ray Powder Diffraction Data for UF₃

Ref. (59)			This Work			
d Å calculated	d Å observed [⊚]	I/I ₀	d Å observed	I	d Å observed (cont.)	I
3.672	3.67	60	3.67	MS	1.055	M
3.589	3.58	30	3.57	M	1.038	VF
3.225	3.21	100	3.21	VS	1.010	F
2.567	2.56	20	2.56	F	1.004	F
2.0725	2.069	60	2.069	S	0.9992	S
2.0227	2.022	90	2.022	VS	0.9984	M
1.8362	1.834	20	1.833	F	0.9625	VF
1.8049	1.803	60	1.806	S	0.9243	F
1.7948	1.795	15	-		0.9108	F
1.7435	1.741	40	1.743	MS	0.9076	F
1.6348	1.633	15	1.635	F	0.9047	MS
1.6124	1.611	10	1.612	VF	0.8927	F
1.4475	1.447	30	1.447	MS	0.8576	MS
1.3744	1.374	35	1.377	MS	0.8442	MS
1.3596	1.359	35	1.360	MS	0.8405	MS
1.3568	-	-	-		0.8316	MS
1.3342	1.334	40	1.335	S	0.8260	MS
1.2835	1.282	5	1.286	VF	0.8199	MS
1.2727	1.272	10	1.272	VF	0.8072	UF
1.2241	1.224	10	1.225	VF	0.8050	F
1.9666	1.196	20	1.197	F	0.7971	MS
1.1867	1.187	40	1.187	S	0.7919	MS
			1.161	F	0.7843	S
			1.139	S	0.7815	MS
			1.093	VF		

I = intensity VS = very strong F = faint
I/I₀ = relative intensity S = strong VF = very faint
 MS = medium strong
 M = medium

[⊚] Staritzky and Douglass reported that 29 additional indexable lines were observed but the d values are not given. In this work 27 additional lines were found and are listed here.

2.2 Apparatus for Kinetic Studies

A diagram of the apparatus in its final form is shown in Fig. 2.3.

Except for the connection with the gas cylinder no rubber or polythene tubing was used in the entire assembly. It consisted of:

- (i) Flowmeter of the conventional capillary type
- (ii) Purification train for the carrier gas (argon)
- (iii) Reaction tube arrangement and furnace
- (iv) Temperature controlling device
- (v) Arrangements for evacuation of the reaction zone and measurement of pressure.

2.2.1 Flowmeter

The capillary of the flowmeter was calibrated by means of a soap-bubble flowmeter and its readings checked from time to time whenever any alteration of the resistance through the gas path was anticipated. The argon from the cylinder was fed into the flowmeter at constant pressure by means of a blow-off. All blow-offs attached to the apparatus and the manometer of the flowmeter contained n-dibutyl phthalate.

2.2.2 Purification Train

The purification train was altered several times during the development of the technique. In the earlier

experiments argon was purified by passing through sofnolite, silica gel, magnesium perchlorate and a phosphorus pentoxide dryer, followed by a furnace containing titanium granules held at 900°C. After some runs (see Section 2.4) it was apparent that the purification thus achieved was not enough to prevent hydrolysis of the uranium tetrafluoride pellets by traces of moisture. Extra precautions were taken by using high purity argon, eliminating all rubber tubing connections and furthermore, by placing cleaned uranium swarf just before the reaction chamber. In a later stage a permanent uranium furnace was introduced into the gas path after the titanium furnace and held at ca. 800°C. As an extra guarantee for the purity of the argon the uranium turnings just before the reaction chamber were maintained in all experiments. In the final experiments the efficiency of the purification method was demonstrated by the fact that after each run the pieces of uranium nearer to the reaction chamber were only slightly oxidised and the interior surface of the stainless steel reaction tube remained bright. The use of uranium metal as a getter has been reported previously⁽⁶⁰⁾ and it was then found that it removed practically all traces of oxygen (at temperatures above 300°C), nitrogen (above 600°C), carbon dioxide and carbon monoxide (above 750°C) and water (above 600°C).



UF₄ pellet held upright in SMB

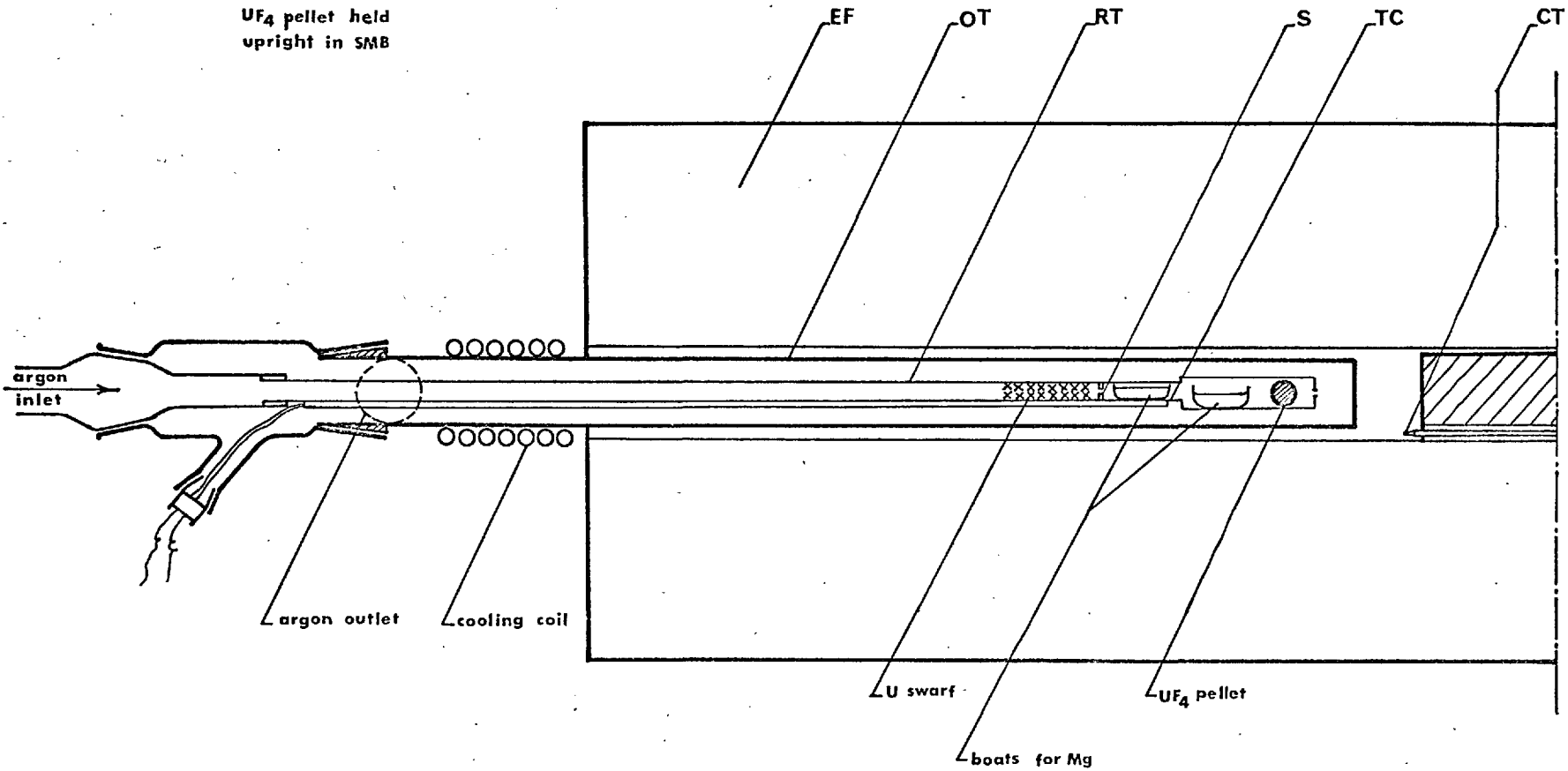


Fig.2.3: Diagram of Apparatus for Kinetic Studies

Fig. 2.5 Apparatus for Kinetic Studies- Reaction
Tube and Furnace

EF = electrical furnace

OT = outer tube

CT = controller thermocouple

RT = reaction tube

RC = reaction chamber

S = septum

SMB = special molybdenum boat

TC = thermocouple

2.2.3 Reaction Tube Arrangement and Furnace

A horizontal kanthal-wound electric furnace (EF) could be slid on rails over the outer tube (OT) to the heating position or completely withdrawn leaving the tube clear. The arrangement is shown diagrammatically in Fig.2.3. The far end of the furnace tube was closed with a refractory cylinder through a slit in which the controlling thermocouple (CT) was firmly held. The furnace had an alumina winding tube 45 cm long and 3.8 cm internal diameter enclosed in a sindanyo case filled with alumina powder. Eight electrical leads were connected to the winding at regular intervals along the furnace tube and firmly secured with bolts to one of the side panels of the furnace. This arrangement made the introduction of external resistances in parallel with selected sections of the winding possible. By trial, a set of external resistances was selected so that a convenient temperature gradient was established along the reaction chamber.

The reaction tube (RT) consisted of a stainless steel tube (6 mm i.d., 9 mm o.d. and 43 cm long) joined to a B19-B14 cone-socket by means of Araldite adhesive. It was positioned inside the outer tube (OT) as shown in Fig. 2.3. One end was connected with the carrier gas source. The reaction chamber (RC), 8 mm i.d., 14 mm o.d. and 3.8 cm long, was screwed on the other end. The

reaction chamber space was delimited inside the reaction tube by a circular septum (S) with a 1 mm diameter orifice drilled in the center. The septum was stopped against a shoulder positioned at 2 cm from the end of the reaction tube. The uranium turnings for the final purification stage of the argon (see Section 2.2.2) were tightly packed against this septum for a length of 3 - 4 cm. Inside the reaction chamber two molybdenum boats were placed side by side containing magnesium sticks followed by a specially designed molybdenum boat (SMB) in which the UF_4 pellet was held vertically.

The outer tube (OT) made of stainless steel (15 mm i.d., 18 mm o.d., and 25.7 cm long) was at one end closed by welding and at the other end brazed to a brass tube 22 cm long with a machined B29 cone on the extremity. The outlet for the carrier gas was provided by a lateral brass tube brazed adjacent to the B29 cone and joined to a glass tube by means of Araldite adhesive.

The temperature at the tip of the reaction tube was measured by a Pt/Pt-Rh (13%) thermocouple (TC), fastened with platinum wire to the tube. The two thermocouple wires were led out of the system through a rubber bung sealed with picein wax. To protect the thermocouple junction from contamination alumina cement was sintered

around the tip and covered with a platinum foil sheath about 10 cm long. Contamination of the thermocouple was indicated by a change in its reading for a given temperature controller setting. Whenever a new thermocouple was used the temperature gradient was rechecked and the thermocouple calibrated against another thermocouple which was kept as a standard. The temperature gradient along the reaction chamber allowed the pellet to be kept at temperatures two or three degrees centigrade higher than the nearest magnesium stick. In this way condensation of magnesium metal on the pellet was avoided.

The temperature survey was carried out always with the same thermocouple that was inserted along the reaction tube inside a silica sheath. The conditions in which the survey was made were identical to an actual run with the exception of the septum (S), which had to be removed, and the magnesium and UF_4 boats, which were absent. Also, rubber connections had to be used to keep the argon flowing during the survey.

The results of two typical surveys for controller settings of $630^{\circ}C$ and $700^{\circ}C$ are shown in Fig. 2.4. The temperature at the site of the pellet was in this way related to the readings of the thermocouple (TC).

2.2.4 Temperature Control

The temperature control was provided by a Smiths Mk V proportional controller (PC) which maintained the temperature of the reaction zone within $\pm 1^\circ\text{C}$. A Sorensen voltage regulator (220 - 240 volts output) was included in the electrical circuit to compensate for changes in the line voltage during long duration runs.

2.2.5 Evacuation of the Reaction Zone and Measurements of Pressure

The reaction zone could be evacuated to less than 10^{-4} mm by means of a 1 inch oil diffusion pump (Edwards type 102) backed by a two stage rotary pump. The evacuated zone was delimited by high vacuum stopcocks and the vacuum measured with a Phillips gauge. A Pirani gauge mounted on the backing line was also provided for leak testing.

2.3 Experimental Techniques

2.3.1 Production of UF_4 and UF_3 Compacts

a. Development of the Technique

Since for the quantitative study of the kinetics of the reactions between a gas and a solid, the area of the solid must be known, the problem was to fabricate UF_4 compacts of a simple geometrical shape the surface of which could be easily measured.

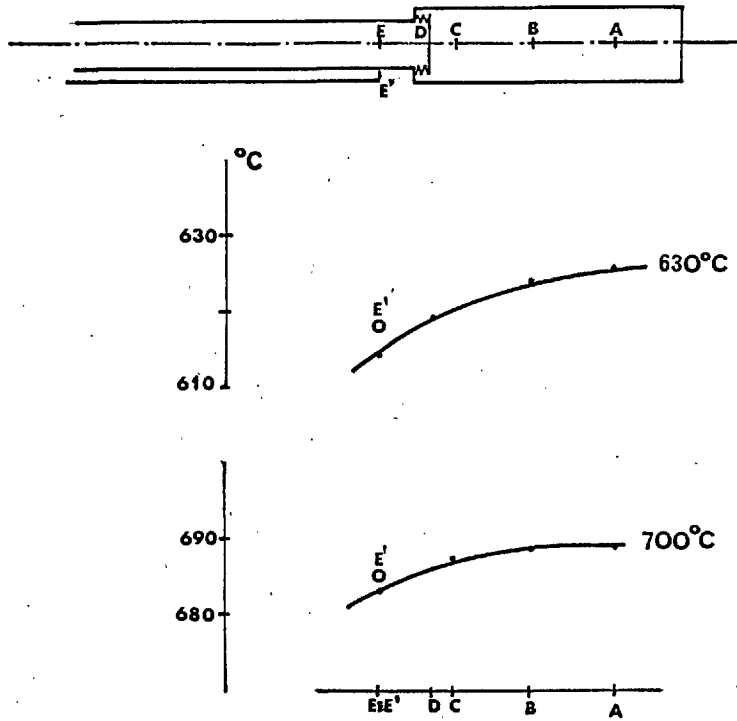


Fig.2.4: Temperature Gradient along the Reaction Chamber for two different Controller Settings

Attempts were first made to produce "beads" of UF_4 in a "shot tower". A small nickel crucible with a funnel shaped bottom and filled with UF_4 powder was placed on the top of a glass tube about 5 cm in diameter and 3 metres high. The crucible was heated inside a small vertical silica tube furnace and, when the melting point of the tetrafluoride was reached, small "beads" of molten UF_4 would fall down the tube and be collected in a beaker half full with mercury. To avoid contamination of the tetrafluoride an upward flow of helium was maintained during the procedure. After some trials this method was abandoned since most of the "beads" either shattered or were badly deformed on impact with the mercury. Moreover, a thin film of a brownish product (probably UO_2) was formed each time on the surface of the UF_4 due to contamination by impurities (probably H_2O and O_2) in the atmosphere.

Other attempts were made to cast UF_4 discs by melting the powder in small flat-bottomed nickel crucibles. The melting was done by induction heating under a purified argon atmosphere. It was found, however, that it was very difficult to remove the UF_4 blocks from the crucibles without breaking them, and thus in every case the crucible had to be destroyed.

The only method that was at all reliable was the compacting of powder by pressing, followed by sintering, though a special technique had to be developed for this. The earlier trials to press pellets in a $\frac{1}{4}$ " steel die failed completely due to the tendency of the pellet to break or laminate on ejection. A new isostatic method of compacting powder, proposed by Penrice⁽⁶¹⁾ was then used. In this method, direct contact between the powder and the steel die is avoided by the use of certain reversible gels as moulds, which are subjected to pressure from the die plunger. The gel shows substantially the same resistance to compression as a liquid and exerts uniform pressure on all the faces of the mould cavity containing the powder. The gel used in this work was the product Vinamold[†] HMC. 1028 (red) which consists of a highly plasticised and gelled polyvinyl chloride. The pellets pressed in this way, though showing a reasonable regular shape, had a tendency to stick to the vinamold and removal of the adherent gel could only be achieved by dissolution in ethyl ketone. To avoid the possible contamination of the pellet with organic products a new technique was devised in which the powder was contained in P.V.C. bags with the shape of the mould cavity.

[†] Supplied by Vinatex Ltd., Carshalton, Surrey.

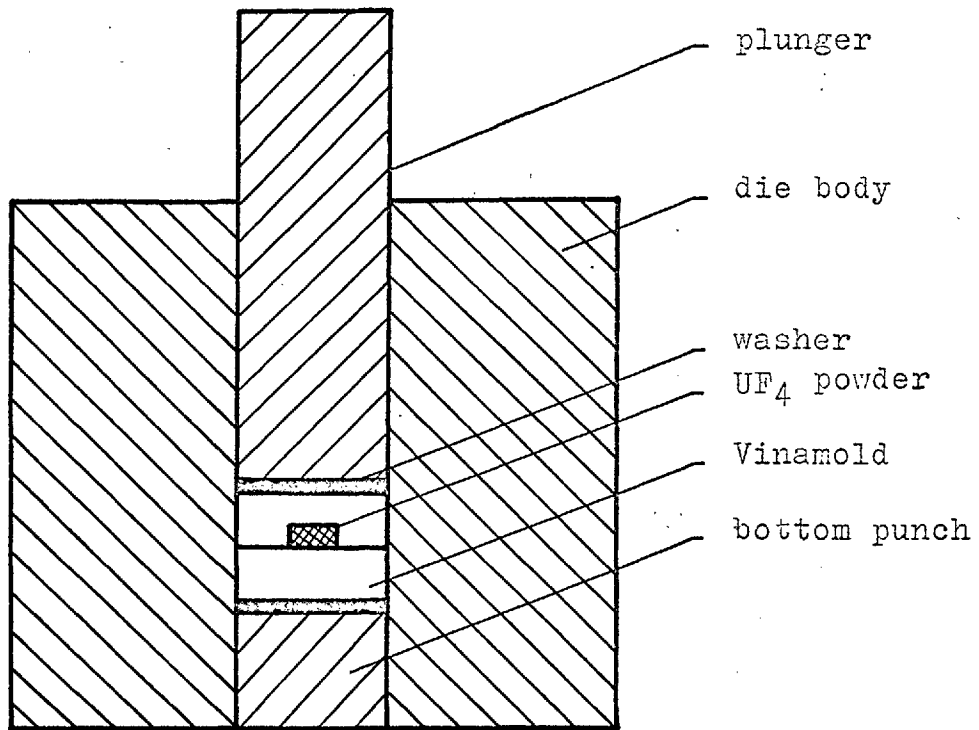
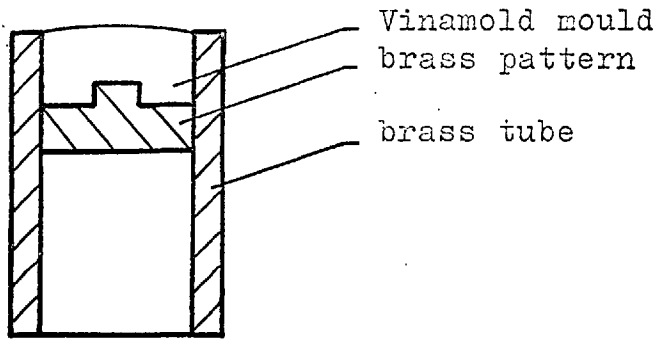


Fig.2.5: Vinamold Die for Pressing
UF₄ and UF₃ Pellets

Regular shaped pellets about 6 mm in diameter and 2 -3 mm thick were obtained in this way.

b. Adopted Procedure

A brass pattern of the pellet to be produced (see Fig. 2.5) was placed in a brass tube with the same internal diameter (1") as the steel die body and molten vinamold was poured into the brass tube for a depth of about 2 cm. Once the cast vinamold had cooled down, the brass block could be easily removed leaving an exactly corresponding die cavity. A mould lid was fabricated in the same way this time using the flat bottom of the brass block.

The P.V.C. bags were fabricated in the following way. A solution was made adding 1 volume of sodium polyacrylate (I.C.I. Wulcastab T), diluted 1:9 in water, to 3 volumes of Geon 652 P.V.C. latex. Several coatings of this solution were given to a brass pattern similar to that used for the Vinamold but with its linear dimensions reduced by about 0.4 mm. After each coating the solution was dried for about 5 minutes in an oven held at 120°C, and allowed to cool. Five or six coatings were usually sufficient to produce a bag with a wall thickness of 0.3 - 0.4 mm. A P.V.C. lid was made in a similar way.

Before pressing, the coarse UF_4 was crushed in an agate mortar to about 500 mesh powder. The mould fitted

with the P.V.C. bag was placed inside the steel die and filled evenly with the powder. The P.V.C. and mould lids were placed in position and pressure applied by means of a plunger and a bottom punch actuated from the hydraulic ram on a Tangye press (150 tons). A pressure of 7.6 tons/cm² was applied each time. The mould could be used a dozen times but the P.V.C. bags would deteriorate after two or three pressings.

UF₃ pellets of the same size were produced in a similar way.

2.3.2 Sintering of UF₄ and UF₃ pellets

The sintering of the UF₄ and UF₃ pellets was carried out in the apparatus shown diagrammatically in Fig. 2.6.

A nickel tube (2 cm diameter, 80 cm long), welded closed at one end, was inserted into a horizontal platinum wound furnace. The gap between the furnace tube and the nickel tube was closed with silastomer at both ends of the furnace. An outlet and inlet to the chamber thus formed was provided by two copper tubes piercing through the silastomer at both ends. Argon was kept flowing into this chamber during the sintering in order to prevent oxidation of the nickel tube and contamination of the pellets by diffusion through the nickel walls.

Provision was made for the evacuation of the nickel tube by a two stage rotary pump. The nickel tube could then be filled with argon purified by passing through silica gel, magnesium perchlorate-phosphorus pentoxide drier and titanium granules held at 900°C. A Pt/Pt-Rh (13%) thermocouple situated in the hot zone between the furnace and the nickel tubes allowed the temperature to be controlled by means of a Kelvin-Hughes Mk III proportional controller. The pellets to be sintered were placed inside a molybdenum boat (4 x 0.6 x 0.6 cm) and covered with a lid of the same material. This boat was fitted inside a longer (18 cm long) nickel boat containing some uranium metal turnings previously cleaned with acid. The uranium was intended to act as a final getter for traces of impurities in the argon and was found indispensable for preventing contamination of the pellets. In early sinterings it was observed that the uranium reacted extensively with the nickel boat in the temperature regions estimated to be above 600°C. This was avoided by lining the nickel boat with molybdenum foil. After sintering the pellets showed no sign of contamination.

The sintering of the UF_4 pellets was carried out for 72 hours at 800°C. This long sintering period was intended to reduce any further grain growth during the actual runs. Densities ranging from 5.9 to 6.2 g/cm³

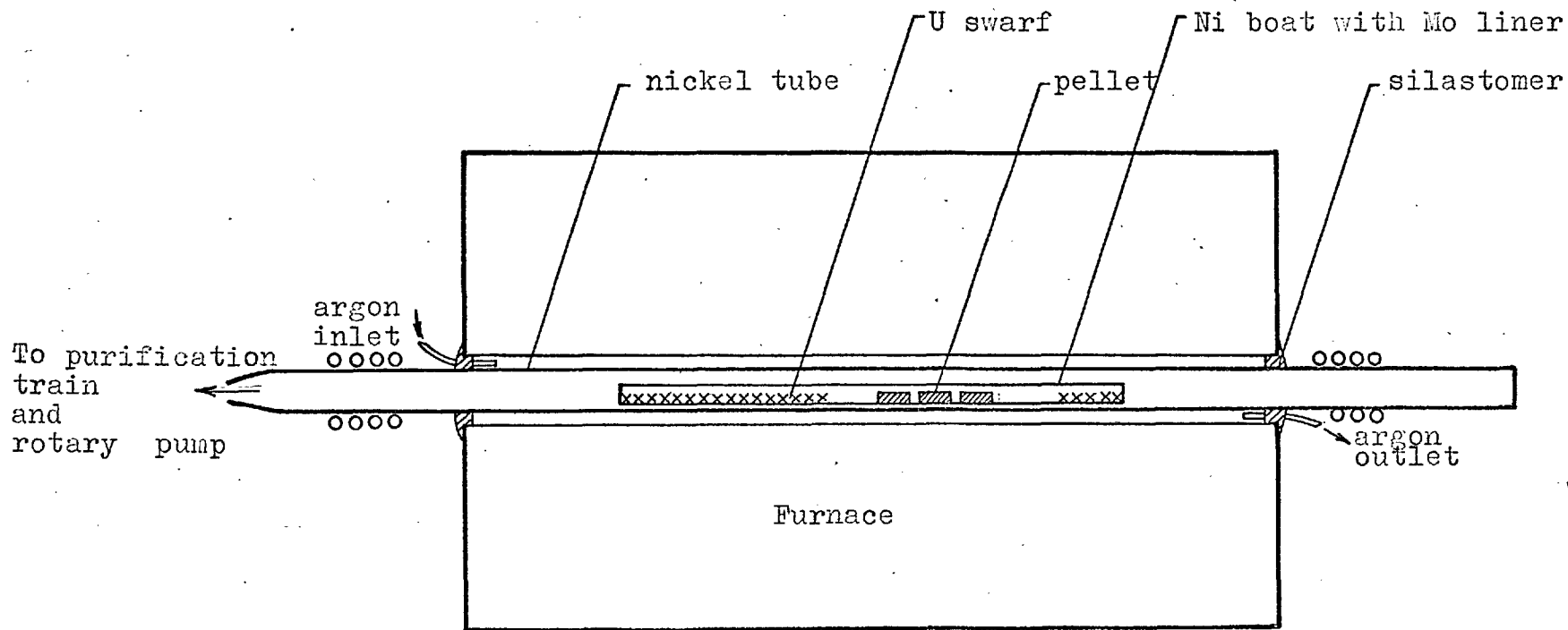


Fig.2.6: Argon Sintering Furnace

were usually obtained, i.e. about 90% of the theoretical density (6.7 ± 0.1) calculated from x-ray data. These results are identical with those obtained by Bell and Proudfoot⁽⁶²⁾ in their study of the sintering characteristics of uranium tetrafluoride.

During the development of the sintering technique similar difficulties to those reported by Bell and Proudfoot were encountered in the prevention of hydrolysis of the tetrafluoride. Only the use of both uranium getter and the argon blanket succeeded in preventing contamination. Attempts to sinter in vacuum had to be abandoned due to serious contamination of the UF_4 . Other attempts to sinter in an atmosphere of argon, hydrogen fluoride and ammonia succeeded in preventing the hydrolysis of the UF_4 , but most of the pellets were entirely disintegrated after some hours at $800^\circ C$.

The UF_3 pellets were sintered at $600^\circ C$ for 72 hours. Attempts to sinter at higher temperatures resulted in shattered pellets, probably because of dissociation into UF_4 and U. The sintered pellets had a density around 7.2 g/cc, i.e. about 80% of the theoretical density: 8.95 g/cm.

2.3.3 Analysis for Fluorine and Uranium in aqueous solutions

At one stage of the work it was necessary to estimate

the amount of uranium metal produced during the reduction of the UF_4 and a method was required to find the amount of fluorine and uranium in solutions containing 1 - 15 μ /ml F and 3 - 16 mg μ /ml U. The method for the determination of fluorine is based essentially on the procedure proposed by Kortüm-Seiler⁽⁶³⁾. For the analysis of uranium the method proposed by Davenport and Thomason⁽⁶⁴⁾ was followed. Details of the procedure are given in Appendix II of this thesis.

2.3.4 Sectioning and Polishing of Reacted Pellets

Most of the reacted pellets were sectioned in order to be observed in the microscope and eventually to be analysed with the Cambridge microscan x-ray analyser. To avoid damage to the product layers, the pellets were first mounted vertically in cold setting resins (Ceemar and Araldite) and then grounded and polished.

Experience in this case has shown that, though in some ways inconvenient, Araldite was better than Ceemar. When Ceemar was used, its greater hardness could cause the outside film of magnesium fluoride to be torn off during polishing, resulting in a gap on the site of the layer. In any case, it was always difficult to polish successfully since the uranium tetrafluoride, though very hard, is also very friable and granules of UF_4 , ripped off on polishing, caused scratches on the softer layers of uranium trifluoride and magnesium fluoride.

The following procedure was eventually used in most cases and yielded the best results:

The specimen was first ground on a copper plate using FFF corborundum and water until a perfectly flat surface was obtained. The grinding was continued with 500 mesh silicon carbide and finally with 850 mesh silicon carbide. The polishing consisted of the following stages:

- (i) Polishing on a lap covered with linen, rotating at 500 r.p.m. using 850-mesh alumina and water.
- (ii) Polishing on a lap covered with "Met" cloth using 1.5 micron Diadust and a few drops of thin oil
- (iii) Final polishing using nylon sueded simplex cloth with $0\frac{1}{2}$ micron Diadust and a few drops of thin oil.

The specimen was washed with liquid detergent after each stage in which Dia-dust and oil lubricant was used and dried with Kleenex tissue.

2.3.5 Photomicrography

Colour photomicrographs were taken with a Reichart projection microscope on Ektachrome type B (high speed) film. Dark ground illumination was used in most cases to bring out the natural colour of the materials.

2.3.6 Analysis with the Micro-scan x-ray analyser

In order to determine the localisation and concentration gradients of the different products of the reaction, several analyses were carried out with a Cambridge micro-scan x-ray analyser. These analyses were made in collaboration with the Geology Department.

2.3.7 X-ray powder diffraction analysis

X-ray powder diffraction analysis was used to check the purity of the UF_3 and to identify the products of the reaction.

In the identification studies, the product layers were scratched with a small spatula into a small agate mortar and finely powdered. The sample was then placed in a thin walled capillary of Lindemann glass (0.3 mm wall thickness). Two cameras were used: a 19 cm Debye-Scherrer type camera and later on, when it was available, a 11.54 cm Philips camera. $Cu K\alpha$ radiation was used with both cameras. The line spacings on the film were measured to ± 0.04 mm which gives negligible error in the d values for high angle reflections.

2.3.8 Gold marker technique

In order to discover the direction of growth of the product layer a gold film was condensed onto the surface of some pellets. The apparatus used is similar to that

described by Hocking⁽⁵¹⁾ and full details of the apparatus and technique can be found in his thesis. A strip of gold film about 2 mm across and with a thickness estimated to vary between 10 - 15 Å⁰ was deposited in each case by vaporizing in vacuum (10^{-3} m/m Hg) a speepure gold wire 0.003 inches thick and about 3 cm long.

2.4 The development of technique for kinetic studies

The earlier apparatus differed essentially from the one described in section 2.2 in that: (i) uranium was not used to purify the argon, (ii) polythene tubing was used for some connections, (iii) the outer tube consisted of a closed end mullite tube, (iv) the evacuation of the system was achieved by a two-stage rotary pump.

The reduction of UF₄ by Mg vapour proceeds, according to Paine et al.⁽²⁰⁾, in a detectable way at temperatures above 540°C. A temperature around 580°C was, therefore, chosen for the preliminary experiments. Since, at this stage, the technique of pressing and sintering the UF₄ pellets had not been fully developed, (see Section 2.3.1) irregularly shaped pieces of UF₄, obtained by melting in small nickel crucibles, were used. These pieces were dry polished on Oakey emery paper down to grade 4/0 in order to give them smooth surfaces. Due to the irregularity in shape no attempt was made to measure their

surface area. After polishing, the UF_4 piece was scrubbed in redistilled acetone, weighed and placed in a small molybdenum boat. The boat and a stick of magnesium were slid, in this order, into the reaction chamber held horizontally in a vice. The reaction tube was screwed onto the chamber and the ensemble fitted to the apparatus. The system was evacuated and then filled with argon which was kept flowing for 3 - 4 hours before the heating was started. A flow rate of about 60 ml/min. was used for the runs. This value for the flow rate was expected to achieve saturation with Mg vapour and was selected by comparison with the flow rates used by Hooper⁽⁶⁵⁾ for the determination of the vapour pressure of silver by a transportation method. The furnace was slid slowly over the outer tube until the temperature in the reaction chamber reached $450^\circ C$ (it took usually 30 minutes) and then quickly moved to its final position. The equilibrium temperature was reached in about 20 minutes. At the end of the run the argon flow was reversed and the furnace completely withdrawn (by stages) in about ten minutes. The UF_4 piece was carefully handled with tweezers and weighed after reaction.

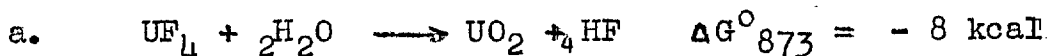
Table 2.2 gives the results of preliminary experiments. The duration of the run was taken as the length of time during which the temperature was above $540^\circ C$.

TABLE 2.2 RESULTS OF PRELIMINARY EXPERIMENTS

Run	Temperature	Flow rate cc/min	Weight g before, W_1	Weight g after, W_2	$(W_2 - W_1) \times 10^6$
A-1	587	62	.217602	.217212	390
A-2	575	58	.376970	.376322	648
A-3	580	60 [*]	.058580	.058310	270
A-6	589	208	.116530	.100362	16168
A-7	585	189	.038510	.33098	5412

* Reverse flow of argon

In all these runs a decrease in weight after the reaction was recorded and the microscopic examination of a cross section showed a continuous layer of a brownish product surrounding the green core of UF_4 . This is shown in Plate 2.1. The thickness of the layers in runs A-1 and A-2 was approximately 30 and 40 μ respectively. The fact that run A-3, conducted with reverse flow of argon, i.e. with little chance of any magnesium vapour reaching the UF_4 piece, showed a similar weight decrease and product film, led to the suspicion that contamination rather than reduction was actually taking place. In fact, an X-ray powder analysis of the product layer showed only the characteristic lines of UO_2 . Thermodynamically, the only feasible reaction leading to the production of UO_2 is the hydrolysis of the UF_4 :



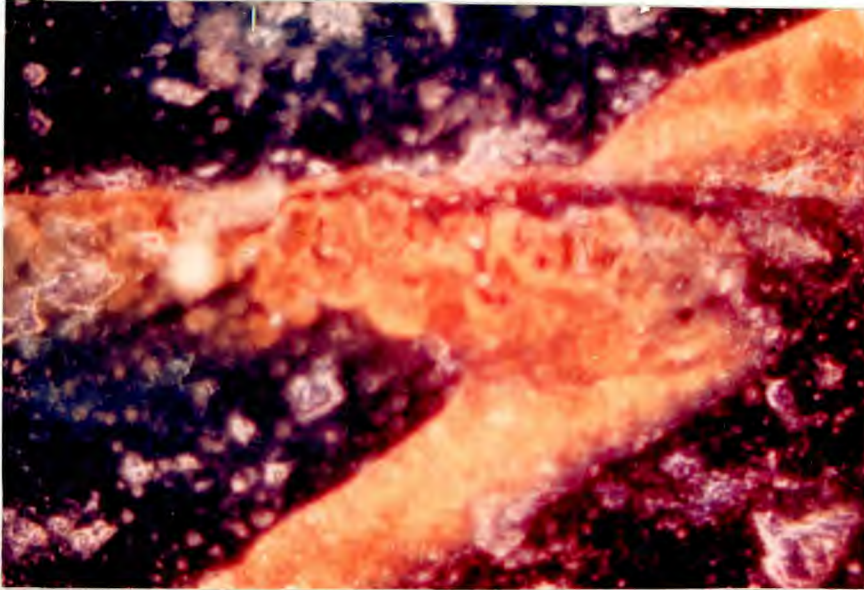


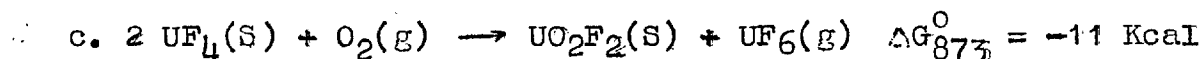
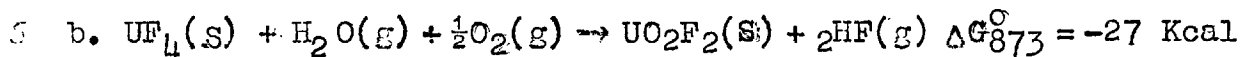
Plate 2.1 - PRODUCT LAYER IN RUN A.1

Region where there was a crack
in the original pellet. The
reaction product filled almost
completely the crack.

(650x)

There are very few quantitative data on the kinetics of this reaction. Qualitative observations indicate, however, that it proceeds fairly rapidly at 600°C⁽⁶⁶⁾.

Other thermodynamically favourable reactions are:



The weight change corresponding to complete reaction is different for the three cases given above. This provides an easy way of checking whether there is any contribution from reactions b and c to the contamination of the pellet. In runs A-6 and A-7, the UF_4 pieces were made to react for a longer time and at a higher flow rate to ensure complete conversion of the UF_4 . The results of the calculation, assuming that the product is entirely uranium dioxide with the stoichiometric composition, are given below:

	Run A-6	Run A-7
No. of initial moles of UF_4	3.7103×10^{-4}	1.2261×10^{-4}
No. of moles assuming all the product to be $UO_{2.0}$	3.7101×10^{-4}	1.2255×10^{-4}

The agreement is very good and rules out any detectable contribution from reactions b and c.

The partial pressure of water present in the argon can be estimated from the data in Table 2.2, assuming that

all the moisture carried by the argon reacts with the UF_4 . The values obtained in this way range from around 0.03 mm Hg for runs A-1 and A-3 to 0.009 mm Hg for run A-2. These are minimum values, the actual ones being probably higher. The residual moisture that should be attained theoretically by drying with silica gel alone is 0.002 mm Hg. One of the main sources of contamination was thought to be the polythene tubing and it was replaced by glass tubing. In the following B-runs two sticks of magnesium instead of one were placed in the reaction chamber so that impurities had more chance of being removed by reaction with the first stick. The results obtained are given in Table 2.3.

The moisture content of the argon revealed from the weight change in these runs is still higher than that expected for the type of purification train used. In runs up to B-4 it was noticed that the stick of magnesium nearer to the UF_4 showed dark spots while the other stick was only slightly or not contaminated at all. This suggested back diffusion of some sort of impurities, which was confirmed in run B-5 where the UF_4 piece was placed between the two sticks of magnesium. The stick at the far end of the chamber showed extensive signs of attack in the region adjacent to the outlet orifice and at the same time the hydrolysis was significantly reduced.

A possible explanation for the origin of this back diffusing impurity is the attack of the silica in the mullite tube by the HF, formed initially during hydrolysis by traces of moisture, yielding SiF_4 and more water.

TABLE 2.3 RESULTS AFTER SUCCESSIVE MODIFICATIONS IN THE APPARATUS OR IN THE EXPERIMENTAL PROCEDURE

Run	Temp. °C	Flow rate cc/min	Duration min	Weight, g		
				before, W_1	after W_2	$(W_2 - W_1) \times 10^6$
B-2	580	60	145	0.027820	0.027730	- 90
B-4	580	60	980	0.133605	0.133430	-175
B-5	583	60	150	0.109125	0.109085	- 40
C-1	200	vacuum	30	0.092730	0.092728	- 2
D-1	200	vacuum (10^{-5} mm)	240	0.008515	0.008512	- 3
D-2	200-580	vacuum (10^{-5} mm)	30	0.008512	0.008510	- 2
D-8	580	10	150	0.040105	0.04015	0
D-9	630	10	420	0.093550	0.093610	+ 60
D-10	630	10	840	0.035060	0.035150	+90
D-11	630	10	90	0.059520	0.059500	- 20
E-1	up to 530°C	10	90	0.032873	0.032870	- 3
E-2	630	10	90	0.53360	0.053630	+270
E-3	630	10	150	0.371545	0.372012	+647
E-4	630	10	20	0.03051	0.030590	+ 80

The next step was to replace the mullite tube by an alumina one. An oil diffusion pump and a Phillips gauge were also mounted so that the system could be degassed at higher vacuum. In run C-1 the UF_4 was heated in vacuum (ca. 10^{-3} mm Hg) for 30 minutes and showed no signs of hydrolysis. The weight change observed is within the limits of experimental error. After some time the alumina tube ceased to be vacuum tight and was replaced by a stainless steel tube. Some more degassing experiments were carried out (runs D-1 and D-2) showing that no contamination occurred after four hours at $200^\circ C$ and on heating up to $580^\circ C$ at least for short periods. The vacuum was kept below 10^{-4} mm Hg in all cases and mostly remained below 10^{-5} mm.

For the reduction runs magnesium turnings were packed inside the reaction tube against the septum (S), see fig. 2.3, and a magnesium stick in a molybdenum boat was placed into the reaction chamber. The system was evacuated and degassed at $200^\circ C$ for 2 - 4 hours. The result of some experiments are shown in Table 2.3 (runs D-8 to D-11). For the first time a weight increase was recorded in some cases. However, the results suggested that some contamination, at least in the initial stages of the reaction, was still occurring. In the following runs cleaned uranium swarf was packed inside the reaction

tube for a length of about 4 cm so that the argon was cleaned of any impurities just before entering the reaction chamber. On cooling the flow of argon was not reversed to avoid any contamination of the pellet. The results in Table 2.3 (runs E-1 to E-4) show that in this way hydrolysis was completely eliminated. This arrangement provided also a very easy way of checking the purity of the argon entering the reaction chamber. After reaction the pieces of uranium immediately adjacent to the reaction chamber would show no signs of oxidation while the remaining pieces were more or less oxidized according to their relative position. A permanent uranium furnace made of a silica tube and held at 800°C was later on introduced into the gas train, but the uranium swarf in the reaction tube was still used in all subsequent runs.

2.5 Experimental procedure

The following series of procedures was carried out in the quantitative final experiments:

A. Preparation of the Pellet

- (i) Freshly sublimed UF_4 or recently prepared UF_3 powder was pressed and sintered in argon.
- (ii) The pellet was dry polished and given a regular cylindrical shape on Oakey emery paper down to grade 4/0.

- (iii) The area of the pellet was calculated after measurement of its diameter with a microscope and its thickness with a micrometer.
- (iv) The pellet was scrubbed in acetone with a fine bristle brush and washed with redistilled acetone.
- (v) The pellet was weighed always in the ~~same~~ microbalance, placed inside the molybdenum boat and weighed again. The boat had been cleaned with nitric acid, washed in water and acetone and weighed.

B. Preparation of the Reaction Tube

Whenever a new thermocouple was fitted the following procedure was used:

- (vi) The tube was cleaned with hydrochloric acid (2N), washed in water and dipped in acetone.
- (vii) The tube was held horizontally in a vice and the thermocouple fastened into position with platinum wire. Care was taken not to touch either of them with bare hands.

C. Preliminaries to the Run

- (viii) The septum (S), Fig 2.3, was slid into position and pressed against the shoulder by means of a glass rod sitting on the top of the laboratory bench while the tube was held upright.

- (ix) Cleaned uranium turnings were packed against the septum by means of a cleaned brass rod.
- (x) The reaction tube was restored to the horizontal position and a molybdenum boat containing a cleaned magnesium stick was inserted in the chamber delimited by the septum at the end of the tube.
- (xi) The reaction chamber, cleaned with acid and washed in water and acetone, was held horizontally in a vice.
- (xii) The boat containing the pellet and a molybdenum boat containing another stick of magnesium were slid, in this order, inside the reaction chamber.
- (xiii) The reaction tube was screwed onto the reaction chamber and, after releasing the chamber from the vice, the whole assembly held horizontally was carefully transferred and fitted to the apparatus.

D. The Carrying Out of the Run

- (xiv) The system was evacuated for some minutes, filled with argon and evacuated again. The diffusion pump was switched on and the system kept under vacuum overnight when a pressure of around 10^{-5} mm Hg was attained.
- (xv) The system was slowly heated up to 200°C maintaining the vacuum below 10^{-4} mm Hg and held at this temperature for about 2 hours.

- (xvi) Argon was let in and kept flowing at a rate of 3 - 6 mL/min while the furnace which was at a temperature about 20°C higher than the set temperature for the run was slowly slid over the outer tube. When the temperature in the reaction zone reached 510°C for runs at 620°C and 530°C for runs at 690°C, the furnace was quickly moved into its final position and the time recorded. The whole operation would take usually 30 minutes.
- (xvii) The temperature of the reaction chamber was then recorded every minute. When a value 10°C lower than the intended run temperature was reached, the controller setting was slowly returned to the predetermined run setting. This procedure was intended to reduce the heating period to a minimum. The temperature during the run was checked periodically.
- (xviii) At the end of the run the flow of argon was stopped and the furnace slowly withdrawn at a rate typified in the graphs of Fig 2.7. During the first five minutes of cooling 0.5 ml of argon were sent through every minute in reverse direction. At a temperature around 500°C the direct flow of argon was resumed (see Section 3.1).
- (xix) Once the system reached room temperature the reaction tube was withdrawn, unscrewed and the boat

with the pellet transferred in a small desiccator to the balance room.

(xx) The pellet and boat were weighed and the pellet was examined under the microscope.

(xxi) The pellet was placed in a small glass boat. covered with a watch-glass and heated for 24 hours at 180°C by means of an infra-red lamp in order to determine the amount of uranium metal by oxidation to U_3O_8 (see Section 3.3.2). The pellet and boat were weighed before and after this treatment.

(xxii) Procedure (xxi) was repeated.

(xxiii) Either before or after procedure (xxi) the pellet was mounted in Araldite, ground and polished and examined under the microscope. Pellets not submitted to treatment (xxi) were eventually examined with the microscan X-ray analyser.

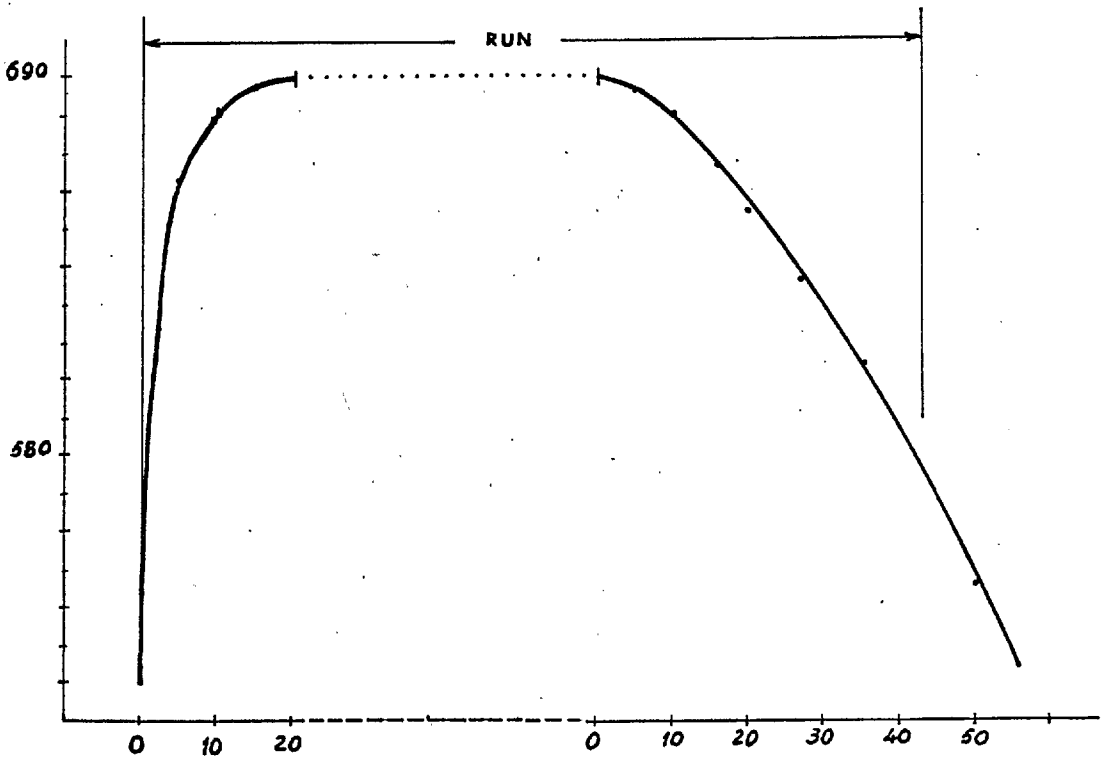
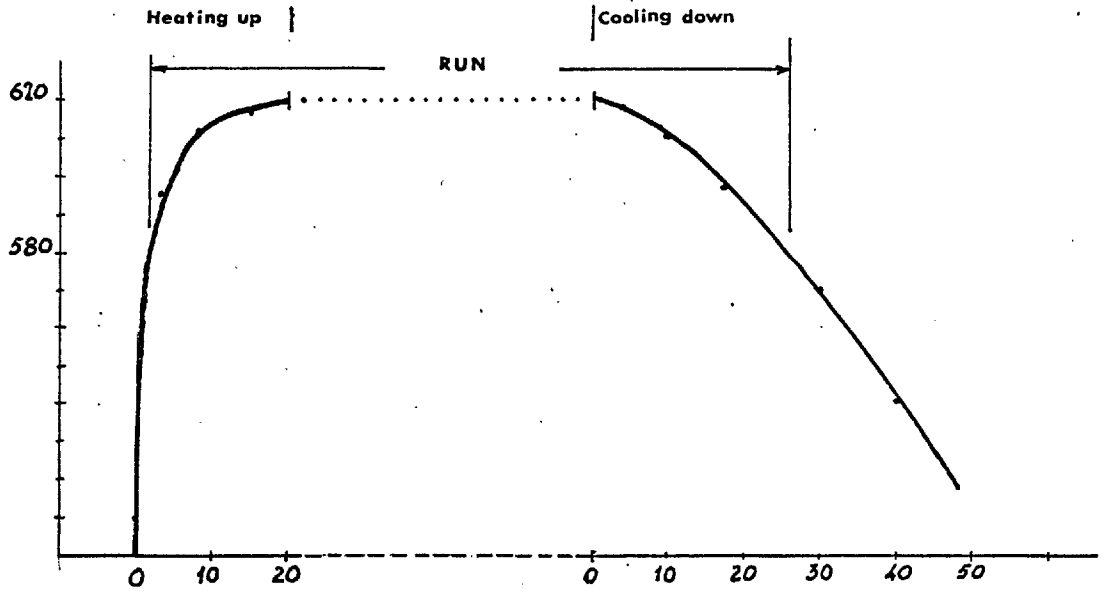


Fig.2.7: Heating and Cooling Rates for the Final Experiments

CHAPTER III

Experimental Results

3.1 Preliminary Experiments

After the development of the technique described in Section 2.4, where the main concern was to prevent the hydrolysis of the uranium tetrafluoride, two sets of preliminary experiments were carried out to test the reliability of the adopted experimental procedure. In one case, the weight gain of each UF_4 pellet was determined after a single reaction period (single time experiments), and in the other case, after each one of a succession of reaction periods (consecutive time experiments).

The experimental procedure was essentially the same as described in Section 2.5 except for the cooling period. On cooling, and in order to ensure that all the argon reaching the pellet had passed over the uranium getter, the argon flow was not reversed, but reduced to about 3 cc./min. The complete withdrawal of the furnace took about 15 minutes. It was expected that due to the lower thermal conductivity of the pellet as compared with that of the metallic reaction chamber and boat, and due to the steep temperature gradient established on cooling, the condensation of magnesium on the pellet would be negligible. The uranium getter was cleaned just before each run and kept in the apparatus under argon, while the pellet was being weighed between two consecutive reaction periods.

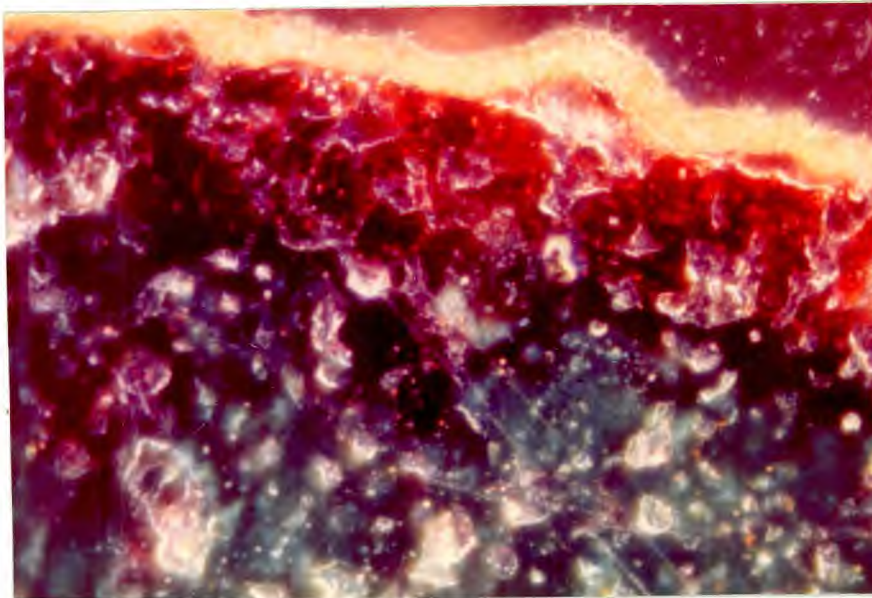


Plate 3.1 - PRODUCT LAYERS FOR A CONSECUTIVE
TIME EXPERIMENT

Cross section showing the layers
produced on UF_4 for a consecutive
time experiment (run F.14). Note
the convoluted nature of the outer
layer and its uniform yellow-brown-
ish colour.

($\times 1000$)

The results of these preliminary experiments are given in Table 3.1. In the single time experiments up to run F.6 the weight increase per unit area showed considerable scatter. Microscopic observation of the surface of the reacted pellets revealed a very thin polycrystalline surface layer generally white in colour, but smeared with irregular yellow-brownish patches which in some cases spread all over the surface of the pellet. A number (varying roughly from 10 to 30 for each face of the pellet) of lustrous metallic crystals were also found on the top of the layer. These crystals were identified as magnesium since they did not form coloured oxides after some hours exposure to the room atmosphere and reacted easily with a drop of dilute acid. Microscopic observation of cross sections of the pellets showed the presence of an irregular inner layer of a product which was red-violet in colour. (see Plate 3.1). Both the outer and inner layers appeared to be coherent without any visible cracks or pores. X-ray powder analysis of the product layers, which could be removed by scraping, showed the presence of UF_3 and some unidentified lines (see Section 3.4). Uranium and magnesium were detected in the outer layer with the microscan x-ray analyser (see Section 3.5). The product layers were tentatively identified as UF_3 in the interior and MgF_2 , possibly with some UF_3 in solid solution, in the outer layer. The identification and

TABLE 3.1 - RESULTS OF THE PRELIMINARY EXPERIMENTS

Run	Temp. °C	Duration t min	Flow rate cc/min	Pellet						$\frac{\Delta W}{S} \times 10^6$ g/cm ²	t _a (min)
				D cm	T cm	S cm ²	Weight g				
							Before	After	Increase W x 10 ⁶		
F.1	629	1240	6	-	.080	(.85)	.158601	.158817	216	250	35.2
F.2	630	1250	6	-	.110	(.69)	.162150	.162368	218	315	35.3
F.3	628	1238	6	-	.070	(.43)	.067500	.067608	108	265	35.2
F.4	630	1245	6	-	.068	(.63)	.139000	.139120	120	200	35.2
F.5	629	640	6	.595	.118	.78	.209390	.209470	80	105	25.3
F.6	629	643	6	.580	.109	.73	.190328	.190413	85	115	25.3
F.7	631	70	6	.585	.130	.78	.192945	.193030	85	110	8.3
	631	70+190	6	"	"	"	.193030	.193172	85+142	290	16.1
	631	260+314	6	"	"	"	.193172	.193344	227+172	510	23.9
	631	574+430	6	"	"	"	.193344	.193500	399+156	710	31.7
	631	1004+553	6	"	"	"	.193500	.193752	555+250	1030	39.4
	631	1557+670	6	"	"	"	.193532	.194572	805+1040	(2350)	47.2
F.8	631	430	6	.628	.120	.86	.234920	.234990	70	80	20.7
	631	430+553	6	"	"	"	.234990	.235172	70+182	295	31.3
	631	983+670	6	"	"	"	.235172	.235530	252+358	710	40.7
F.9	631	630	6	.635	.100	.83	.186771	.186981	210	255	25.1
F.10*	631	75	6	.440	.050	.37	.062123	.062163	40	110	10.3

D = Diameter

T = Thickness

S = Surface area

Values in brackets were estimated

TABLE 3.1 - RESULTS OF THE PRELIMINARY EXPERIMENTS (cont)

Run	Temp.	Duration t min	Flow rate cc/min	Pellet						$\frac{\Delta W}{S} \times 10^6$ g/cm ²	$t^{\frac{1}{2}}$ (min) ^{$\frac{1}{2}$}
				D cm	T cm	S cm ²	Weight g				
							Before	After	Increase W x 10 ⁶		
F. 12	621	274	6	.550	.100	.65	.152280	.152375	95	154	16.5
	621	274+334	6	"	"	"	.152375	.152465	95+90	285	24.6
	621	608+442	6	"	"	"	.152465	.152560	185+95	430	32.4
	621	1050+556	6	"	"	"	.152560	.152630	280+70	540	40
	621	1606+682	6	"	"	"	.152630	.152690	350+60	630	47.8
	621	2288+794	6	"	"	"	.152690	.152760	410+70	740	55.8
	621	3082+916	6	"	"	"	.152760	.152815	480+55	825	63.2
	621	3998+1047	6	"	"	"	.152815	.152875	535+60	915	71.0
	622	5045+1159	6	"	"	"	.152875	.152935	595+60	1010	78.8
	622	6204+1276	6	"	"	"	.152935	.153090	655+155	1250	86.5
	622	7480+1399	6	"	"	"	.153090	.153268	810+178	1520	94.2
622	8879+1516	6	"	"	"	.153268	.153638	988+370	2090	101.9	
F. 13	622	79	6	.615	.119	.82	.230750	.230927	177	215	8.9
F. 14	622	79	6	.610	.130	.83	.232700	.232882	182	220	8.9
	622	79+200	6	"	"	"	.232882	.232959	182+77	310	16.7
	622	279+1276	6	"	"	"	.232959	.233116	259+157	500	39.4
	622	1555+1399	6	"	"	"	.233116	.233240	416+124	650	54.4
	622	2954+1516	6	"	"	"	.233240	.233410	540+170	855	66.9
	622	4470+1637	6	"	"	"	.233410	.233552	710+142	1030	78.1
	622	6107+1511	6	"	"	"	.233552	.233681	852+129	1180	87.3
F. 15	622	1511	6	.520	.155	.68	.205220	.205325	105	155	38.9
F. 17	to 613	20	6	-	-	-	.091790	.091780	-10	-	-
F. 18	622	40	6	.585	.115	.75	.194171	.194225	54	72	6.3
⊠ F. 19	622	7200	6	.597	.120	.79	.199930	.200262	332	420	84.9

⊠ Gold marker experiments

morphology of the product layers is fully discussed in Sections 3.6 and 3.7.

At this stage, it was assumed that the scatter of the results was mainly due to the condensation of magnesium during the cooling period. A different cooling procedure was therefore tried, in which the flow rate of argon was increased to about 100 cc./min. so that on cooling the concentration of Mg vapour was kept well below the saturation point. In run F.7 (consecutive time experiment) and all subsequent ones, no condensation of magnesium was observed on the pellets. The weight gains per unit area for the first four reaction periods of run F.7^{lie} on a straight line when plotted against the square root of the time (Fig. 3.1, curve 1). In the 5th and 6th reaction periods a sudden increase in weight was recorded and a rim of a black powder was observed on the edges of the pellet. When handling the pellet, some powder was lost and thus the figures given for the weight gains in the two last reaction periods are only approximate. Microscopic observation showed that the powder was an agglomerate of small green to black crystals, which were also found, but in greater sizes (up to 30μ), all over the surface of the pellet. The colour of the pellet itself changed from the whitish appearance found in the single time experiments to a deep brown in the last reaction periods. Since the results of this run suggested a parabolic time

Law, at least in the first stages of the reaction, all the preliminary results were plotted as weight gain per unit area vs. $\text{time}^{\frac{1}{2}}$ in Fig. 3.1.

During the last three reaction periods of run F.7 a second pellet was introduced in the reaction chamber (run F.8). The results were lower, but the line defined by the first two points has a slope very near to that of run F.7 (curve 2, Fig. 3.1). A sudden increase in weight was also observed after the 3rd reaction period.

In the consecutive time experiments F.12 and F.14, carried out at a lower temperature, two straight lines were obtained for each run (Fig. 3.1, curves 3 and 4 respectively). Break away from the parabolic behaviour was observed in run F.12 after around 104 hours of reaction, but not in run F.14. The three last reaction periods of run F.12 were carried out at the same time as the 4th, 5th and 6th of run F.14, respectively.

To summarize, the main features of the preliminary runs, up to run F.15 were:

- i. Non-uniformity of the yellow-brownish colour of the outer layer for the single time experiments as compared with the deep brown colour presented by the pellet after two or three reaction periods in the consecutive time experiments.

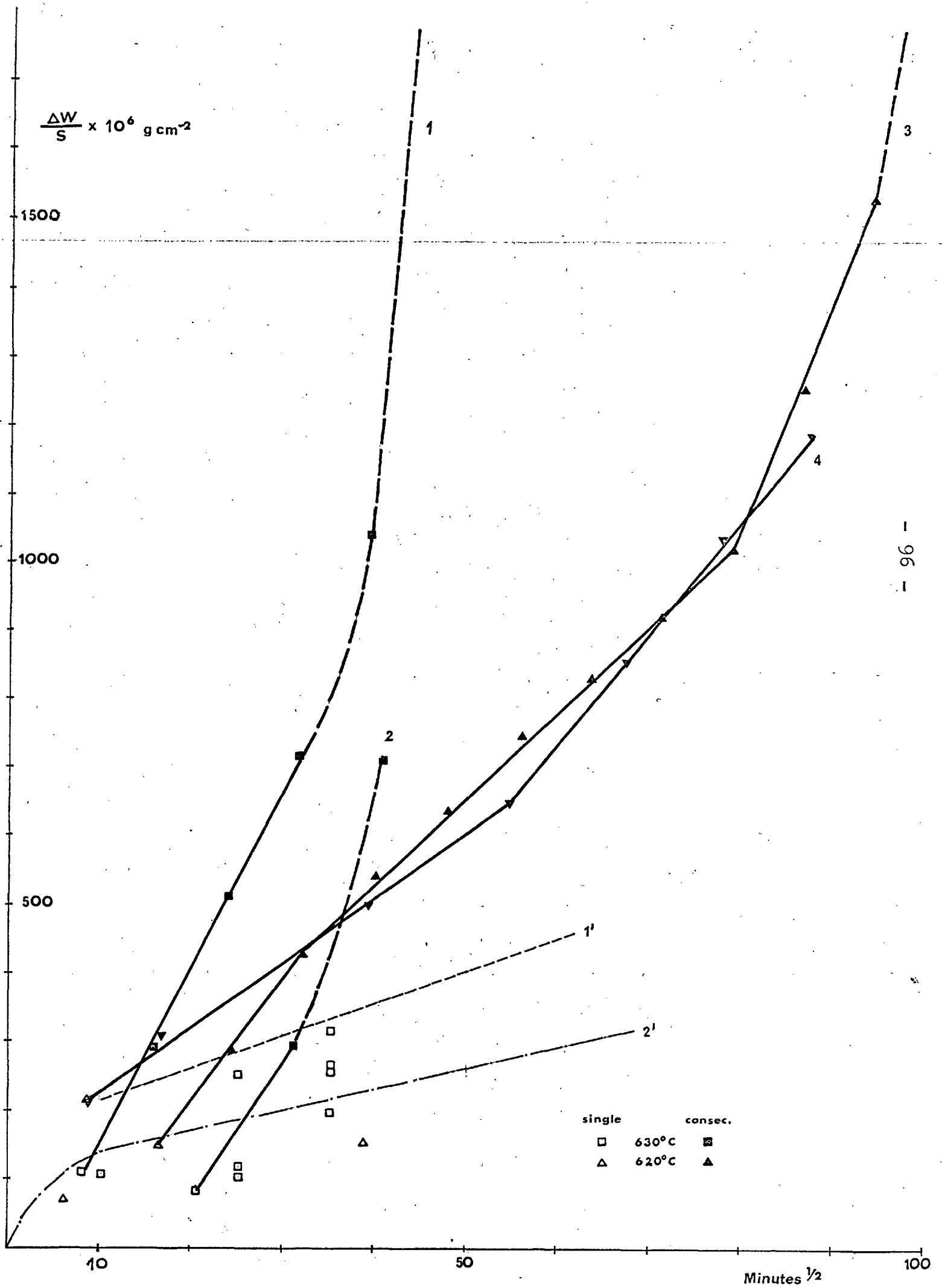


Fig.3.1: Results of the Preliminary Experiments

- ii. Scatter of the results and lower weight gains in all single time experiments.
- iii. Discontinuities in the slope of the parabolic plots for runs F.12 and F.14
- iv. Break away from parabolic behaviour for all consecutive time experiments except run F.14 with no apparent relation to the total reaction time or the thickness of the layers.
- v. The extrapolation to zero reaction time of the parabolic plots did not pass through the origin and revealed an initial reaction rate which was lower than the parabolic in runs F.7 and F.8, and higher in runs F.12 and F.14.

As was stated before, it was assumed at this stage that the yellow-brownish colour of the MgF_2 layer was due to UF_3 taken up into solid solution. The non-uniformity of the colour for the relatively short single time experiments could then be explained by incomplete saturation of the UF_3 in MgF_2 . Also, the higher reaction rates observed for the consecutive time experiments might have been due to the cracking of the magnesium fluoride layer on heating the pellet at the beginning of each reaction period. Due to the small weight gains involved and the discontinuous way in which they were determined, the overall curves, which otherwise would appear as a succession of discontinuous parabolic curves, appeared

relatively smooth and continuous for longer periods of time. However, the scatter of the results and the break away from parabolic behaviour for the consecutive time experiments still had to be explained. A full discussion of these results will be given in Section 4.3 taking into account the results of later experiments. At this point only the scatter of the results will be discussed, since it is necessary for the understanding of the modifications introduced in the experimental procedure.

Condensation of magnesium on the pellet had been ruled out as a possible cause of scatter from run F.7 onwards. Results, such as those for the first reaction periods of runs F.7 and F.8, strongly suggested a delaying action at the beginning of the reaction which might have been caused by slight hydrolysis of the uranium tetrafluoride on heating up, when the temperature and the vapour pressure of magnesium were too low to initiate the reduction. Hydrolysis of the tetrafluoride had been prevented in the development technique by the use of fresh cleaned uranium swarf. In the present preliminary experiments, however, the same uranium swarf was used for the consecutive runs after cleaning with acid. Fresh uranium would be added only from time to time to make up for the losses. It was then observed that after cleaning the old swarf presented a dull grey appearance as compared with the shining surface of the new swarf. No great significance was given

to this phenomenon up to run F.15. At this point, however, it was felt necessary to investigate whether this change in appearance corresponded to a decrease in the reactivity of the uranium caused, for instance, by alloying with the stainless steel tube. Some cleaned uranium swarf, old and new, was exposed to air for some hours. The old uranium showed only slight signs of oxidation, while the fresh uranium was completely covered with a brown oxide, probably UO_2 . To test the possibility of hydrolysis of the UF_4 in the initial stage of the reaction, run F.17 was carried out by heating up to $613^\circ C$ and immediately cooling down to room temperature. Patches of a brownish product were observed on the green surface of the pellet and a small decrease in weight (10 μg) was recorded.

In the subsequent runs fresh uranium was used every time and the consecutive time experiments were discontinued.

The reacted pellet in run F.18 showed a thin white surface layer which under the microscope appeared darker due to the presence of UF_3 underneath.

Runs F.20 to F.23 (see Table 3.2) were carried out at $690^\circ C$ for the same length of time using different flow rates of argon. The results agreed within 5% of the average value and the flow rate of argon did not seem to affect the results in any predictable way. Due to its greater thickness and to the rapid cooling to which it

was subjected, the magnesium fluoride layer tended to crack. In one case, run F.21, the layer flaked off so badly that the experiment had to be rejected.

To avoid cracking of the outer layer, it was decided to adopt a lower cooling rate in the subsequent longer runs though still increasing the direct flow of argon up to 100 cc/minute. The furnace was completely with-drawn only one hour after cooling was initiated. Once more, random yellow-brownish patches were observed on the magnesium fluoride layer and the results were considerably scattered. Since the only alteration introduced in the procedure had been the extension of the cooling period, this accounted for the results obtained. Due to the high flow rates used, the efficiency of the purification of the argon was considerably reduced, particularly at low temperatures and the longer exposure of the pellet to the impure argon caused partial oxidation of uranium metal produced during the reaction. The presence of uranium metal had not been suspected before and it was assumed that it would start to be formed only when all the tetrafluoride had been reduced to trifluoride. Paine et al.⁽²⁰⁾ had reported the production of uranium metal together with uranium trifluoride at these temperatures, but since their experiments had been carried out on UF_4 powder, they did not contradict that hypothesis.

In an attempt to detect the presence of uranium metal, the pellets were dipped into a few millilitres of dilute hydrochloric acid and the solution analysed for uranium and fluorine by colourimetric methods. This method, though it proved to be unreliable for quantitative purposes, confirmed the presence of uranium metal in the reacted pellets (see Section 3.5). In later runs the pellets were oxidised in air at about 180°C to determine quantitatively the amount of uranium produced in the reaction. These results unequivocally confirmed the presence of U metal. X-ray powder analyses of the product layers also showed most of the lines for UF_3 and the strongest characteristic lines of MgF_2 and uranium metal (see Section 3.4).

The cooling procedure had, once more, to be modified and the final procedure described in Section 2.5 was devised to ensure that:

- i. No condensation of magnesium occurred on cooling; for this purpose the flow of argon was reversed at the beginning of the cooling down period using an extremely low flow rate (about 0.5 cc/min.).
- ii. The cooling rate was not so rapid as to cause cracking of the outer layer.
- iii. The purity of the argon in the reaction chamber was always kept at a high level by

resuming the direct flow of argon (3 cc/min) when the danger of condensation of magnesium on the pellet had been greatly reduced.

Moreover, a uranium furnace held at 800°C was introduced in the gas train to reduce the impurity content of the argon before reaching the uranium getter in the reaction tube.

From run F.30 onwards neither condensation of magnesium nor oxidation of uranium was observed. The only exception was run F.33 where the pellet was kept inadvertently at 160°C for some hours with no argon flowing. The pellet showed a uniform deep brown colour similar to that obtained for the consecutive time experiments.

3.2 Kinetics of the Overall Reaction

At 620° and 690°C, the overall weight gain per unit area of the UF₄ pellets was found to follow a parabolic rate law:

$$m^2 - m_1^2 = k (t - t_1)$$

where

t_1 is the time in minutes, counted from the beginning of the reaction, at which parabolic behaviour starts to be followed

m_1 is the weight gain per unit area corresponding to the time t_1 expressed in $g^2 cm^{-4}$

k is the parabolic rate constant expressed in $g^2 cm^{-4} min^{-1}$.

The results are given in Tables 3.2 and 3.3 and plotted in the graphs of the Figures 3.2 and 3.3, except for the runs marked with an asterisk in Table 3.2 which will be discussed in Section 4.3.1. The reaction times were arbitrarily taken as the length of time during which the thermocouple temperature was above $580^\circ C$.

The overall parabolic rate constants and the threshold values t_1 and m_1 taken from the graphs are:

<u>at $620^\circ C$</u>	$k = 1.8 \times 10^{-11} \text{ g}^2 \text{ cm}^{-4} \text{ min}^{-1}$
	$m_1 = 2.9 \times 10^{-8} \text{ g}^2 \text{ cm}^{-4}$
	$t_1 = 380 \text{ min}$
<u>at $690^\circ C$</u>	$k = 4.75 \times 10^{-10} \text{ g}^2 \text{ cm}^{-4} \text{ min}^{-1}$
	$m_1 = 31 \times 10^{-8} \text{ g}^2 \text{ cm}^{-4} \text{ min}^{-1}$
	$t_1 = 280 \text{ min}$

In Table 3.3 the results of experiments carried out at $690^\circ C$ with UF_3 pellets are given, and the values of k , t_1 and m_1 taken from the graph of Fig. 3.4 are:

<u>at $690^\circ C$</u>	$k = 4.5 \times 10^{-10} \text{ g}^2 \text{ cm}^{-4} \text{ min}^{-1}$
	$m_1 = 24 \times 10^{-8} \text{ g}^2 \text{ cm}^{-4}$
	$t_1 = 240 \text{ min}$

TABLE 3.2 - FINAL RESULTS FOR UF_4 PELLETS AT $690^\circ C$

Run	Temp. $^\circ C$	Duration t min	Flow rate cc/min	Pellet						$\frac{\Delta W}{S} \times 10^6$ g/cm ²	$\left(\frac{\Delta W}{S}\right)^2 \times 10^8$ g ² /cm ⁴	$t^{\frac{1}{2}}$ min ^{$\frac{1}{2}$}
				D cm	T cm	S cm ²	Weight g					
							Before	After	Increase $\Delta W \times 10^6$			
F.20	690	82	7	.580	.153	.81	.233853	.234211	358	440	19	9.0
F.22	690	82	5	.580	.126	.76	.195570	.195865	295	390	15	9.0
F.23	690	83	3	.585	.134	.79	.213340	.213660	320	405	17	9.1
\equiv F.24	690	267	3	.550	.162	.76	.232531	.233030	499	655	43	16.3
\equiv F.25	690	283	4	.555	.139	.72	.209147	.209435	288	400	-	16.8
\equiv F.26	690	270	3	.550	.080	.61	.109301	.109711	410	670	-	16.4
\equiv F.27	690	269	3	.600	.169	.88	.279610	.280140	530	600	-	16.4
\equiv F.28	690	271	4	.590	.131	.79	.202760	.203399	639	810	-	16.5
F.30	690	278	4	.570	.156	.79	.233289	.233731	442	560	31	16.7
\equiv F.33	690	1007	3	.580	.141	.79	.225421	.226340	919	1160	-	31.7
F.34	690	2217	3	.600	.143	.83	.245272	.246235	963	1160	135	47.1
F.35	690	2230	4	.590	.165	.85	.280160	.281066	906	1065	113	47.2
F.36	690	2228	3	.590	.091	.72	.149622	.150410	788	1095	120	47.2
\equiv F.37	690	1737	3	.610	.076	.73	.134550	.135278	728	1000	100	41.6
F.38	690	413	3	.605	.108	.78	.183430	.183910	480	615	38	20.3
F.39	690	64	4	.625	.108	.83	.200775	.201090	315	385	15	8.0
F.48	690	1485	4	.543	.084	.61	.115239	.115821	582	955	91	38.5
F.53	690	179	4	.585	.057	.64	.090410	.090730	320	500	25	13.4

\equiv Runs in which oxidation of the uranium metal occurred on cooling

TABLE 3.3 - FINAL RESULTS FOR UF₄ PELLETS AT 620°C

Run	Temp. °C	Duration t min	Flow rate cc/min	Pellet						$\frac{\Delta W}{S} \times 10^6$ g/cm ²	$(\frac{\Delta W}{S})^2 \times 10^8$ g ² /cm ⁴	$t^{\frac{1}{2}}$ min ^{$\frac{1}{2}$}
				D cm	T cm	S cm ²	Weight g					
							Before	After	Increase $\Delta W \times 10^6$			
F.41	620	1547	4	.565	.076	.64	.113923	.114066	143	225	5.1	39.3
F.42	620	1157	4	.570	.101	.69	.156468	.156610	142	205	4.2	34.0
F.43	620	1530	4	.580	.100	.71	.155153	.155293	140	200	4.0	39.1
F.44	620	2907	4	.575	.126	.75	.197588	.197790	202	270	7.3	53.9
F.45	620	88	5	.580	.565	.63	.086572	.086655	83	130	1.7	9.4
F.46	620	382	3	.615	.063	.72	.114555	.114674	119	165	2.7	19.5
F.47	620	32	4	.543	.044	.54	.061141	.061168	27	50	.25	5.7

TABLE 3.4 - RESULTS FOR UF₃ PELLETS AT 690°C

Run	Temp. °C	Duration t min	Flow rate cc/min	Pellet						$\frac{\Delta W}{S} \times 10^6$ g/cm ²	$(\frac{\Delta W}{S})^2 \times 10^8$ g ² /cm ⁴
				D cm	T cm	S cm ²	Weight				
							Before	After	Increase $\Delta W \times 10^6$		
F.49	690	1133	4	.610	.104	.79	.226506	.227103	597	755	57
F.50	690	111	4	.590	.097	.73	.199660	.199950	290	400	16
F.51	690	290	4	.575	.093	.69	.182620	.182993	373	540	29
F.52	690	2547	4	.565	.092	.66	.175212	.175967	755	1145	130

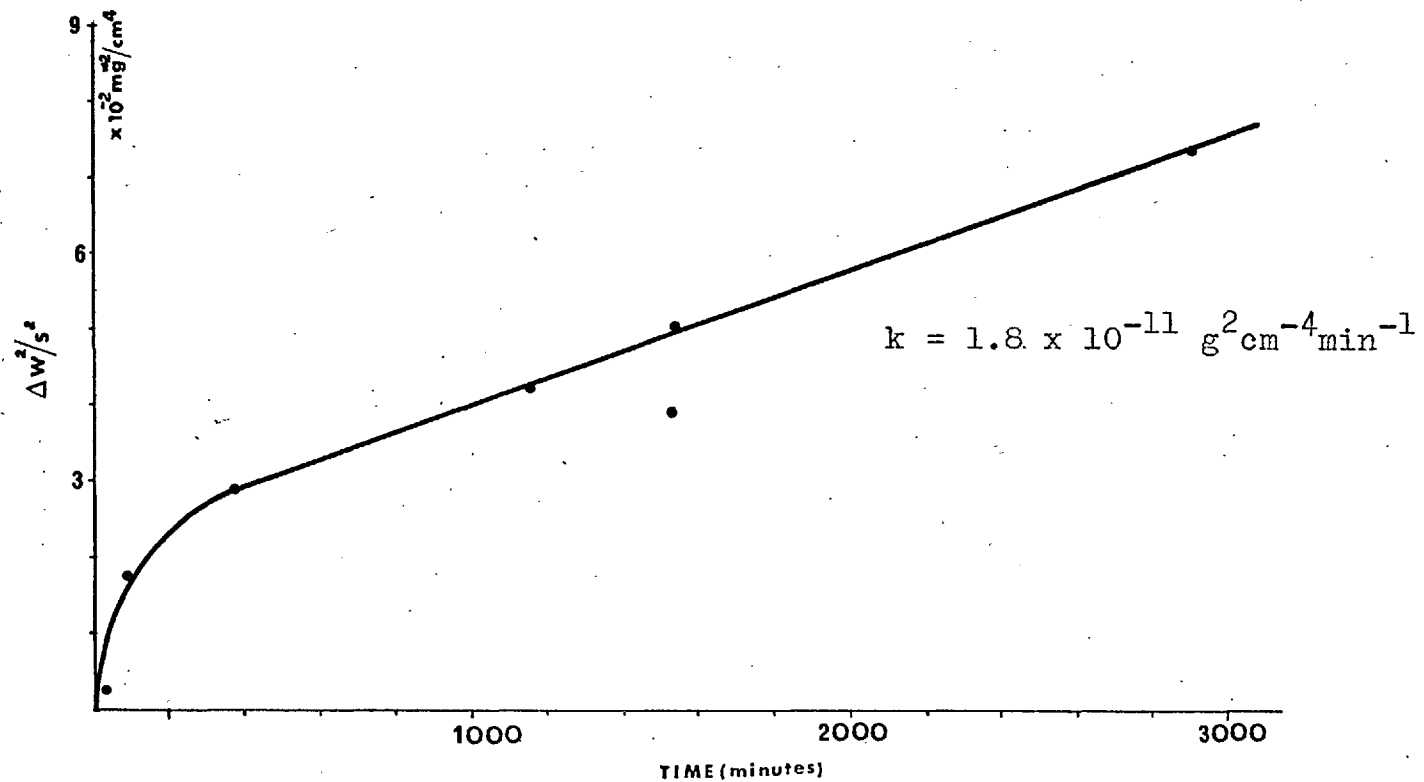


Fig.3.2: Parabolic Plot for the Final Experiments at 620°C

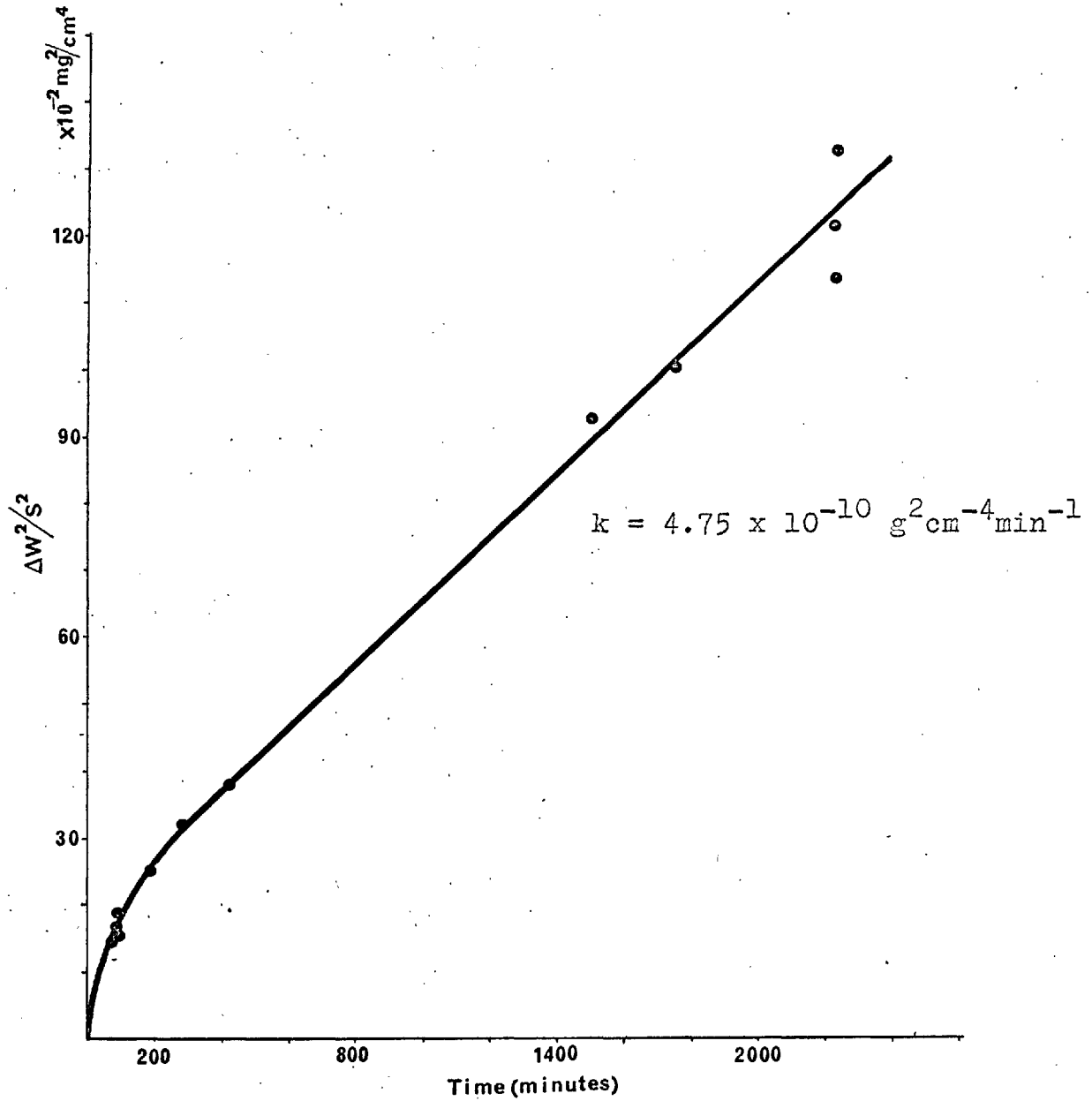


Fig.3.3: Parabolic Plot for the Final Experiments at 690°C

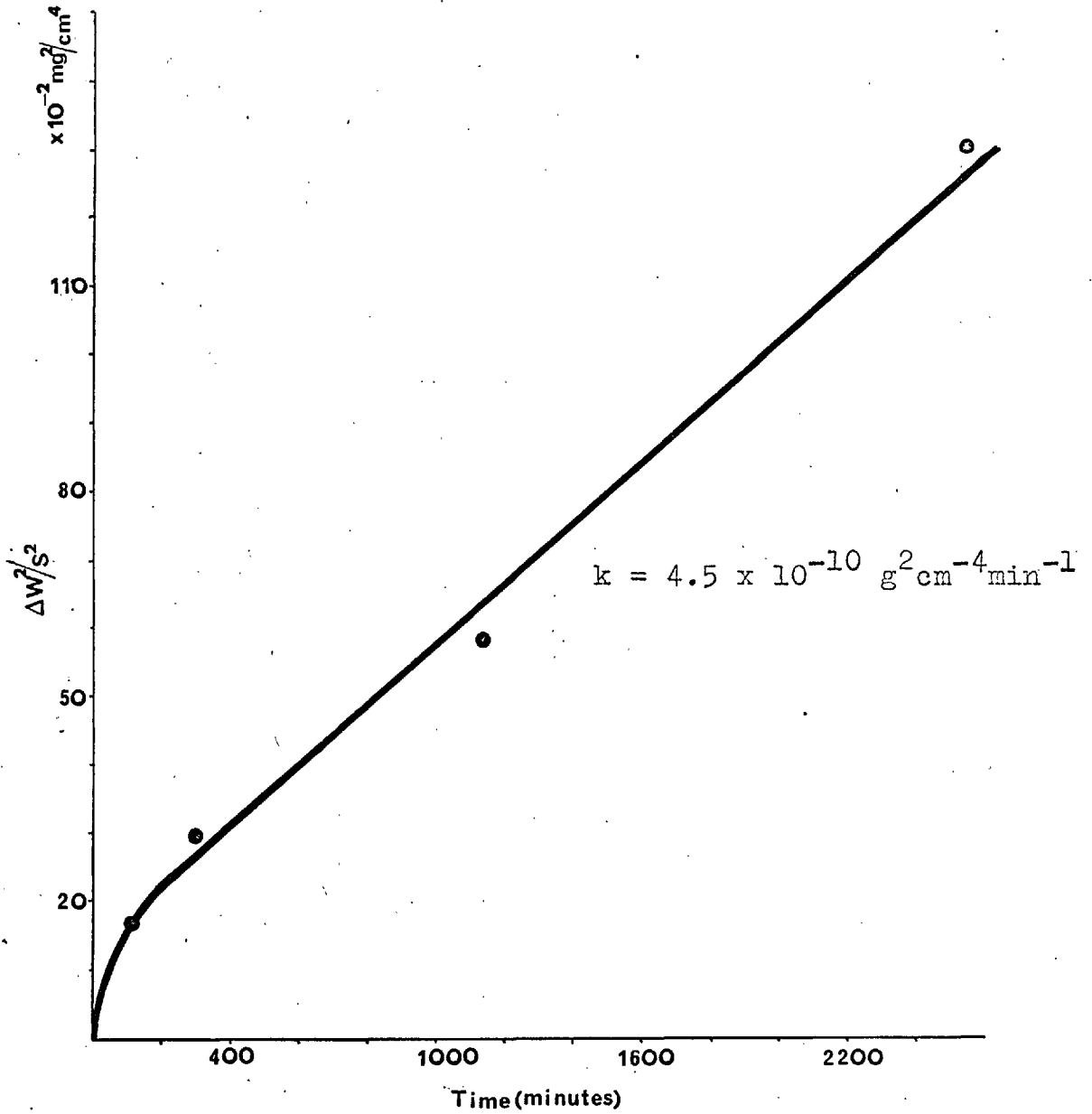


Fig.3.4: Parabolic Plot for UF_3 Pellets at $690^\circ C$

3.2.1 Reproducibility of the Results

Each point on the graphs of Figures 3.1, 3.2 and 3.3 represent a measurement on an individual pellet so that the scatter from the lines gives an idea of the reproducibility of the rate of reaction from pellet to pellet.

From the results of runs F.34, F.35 and F.36 which were carried out for identical periods of time, a relative error of $\pm 7\%$ is obtained, which may be taken as representative of the relative error for the parabolic rate constants. The uncertainty of the t values is the same for all the runs and cancels out when calculating the slope of the curves.

The k values may then be given as:

$$k_{620^{\circ}\text{C}} = (1.80 \pm 0.13) \times 10^{-11} \text{ g}^2 \text{ cm}^{-4} \text{ min}^{-1}$$

$$k_{690^{\circ}\text{C}} = (4.75 \pm 0.34) \times 10^{-10} \text{ g}^2 \text{ cm}^{-4} \text{ min}^{-1}$$

for the UF_4 pellets and

$$k_{690^{\circ}\text{C}} = (4.50 \pm 0.31) \times 10^{-10} \text{ g}^2 \text{ cm}^{-4} \text{ min}^{-1}$$

for the UF_3 pellets.

3.2.2 Errors

The error for the weight gain per unit area is due to the error in weighing and to the error in the area of the pellet.

The weight of the pellet before and after the reaction was determined by direct weighing of the pellet

and by the difference between the weight of the boat alone and the boat and pellet assembly. The two weights, direct and by difference, usually differed up to 30 μg , but the weight gains determined by the two methods agreed in most cases to within 5 μg , and were always less than 15 μg different. The weight gains given in Tables 3.1 to 3.4 are those determined by direct weighing, with the exception of those which differed ^{for} more than 5 μg . In such cases the mean value was adopted as representing the weight gain.

The pellets were carefully shaped and a number of measurements of the thickness (using a micrometer) and of the diameter (using the stage micrometer of a microscope) were made so that the standard error did not exceed 0.02 mm and 0.05 mm, respectively. This gives an error of $\pm 2.5\%$ for the calculated area of an average pellet.

The error for the weight gain per unit area is, therefore, $\pm 5\%$ for a weight gain of 200 μg and $\pm 3\%$ for a weight gain of 1000 μg .

Due to random effects and to the fact that an individual pellet was used for each point the accuracy of the parabolic plots was somewhat better than the estimated errors, in particular at 620°C.

3.3 Kinetics of the U and UF₃ Producing Reactions

The kinetics of the two individual reactions taking place simultaneously cannot be determined from the overall weight gains alone. Either determination of the uranium or of the uranium trifluoride produced in the reaction is also necessary.

Since the analysis of UF₃ in presence of UF₄ is somewhat difficult, the obvious choice was the determination of the uranium metal.

3.3.1 Chemical Analysis for Uranium

As discussed in Section 3.1, the presence of uranium metal was suspected only after the results of runs F.24 to F.28. At first, an attempt was made to determine the amount of uranium metal by washing the pellet for some minutes with a few millilitres of dilute hydrochloric acid and analysing for uranium in the solution. A few seconds after immersion of the pellet in the solution, intense bubbling was observed which subsided after about 10 minutes. The uranium content of the solution was found to be around 360 μg . After second and third washings, when no bubbling occurred, uranium was still found in solution, though in smaller quantity (around 200 μg). The only possible conclusion was that UF₃ was also going into solution and that the fluorine

content of the solution would have to be determined if the amount of free uranium was to be estimated by this method. It was hoped that the dissolution of magnesium fluoride would be negligible, taking into account its extremely low solubility, the small volume of the washing solution and the short time of attack.

The results of the analyses for a few runs are given in Table 3.5. The technique is given in Appendix II of this thesis.

The results of the analyses for the second washings, which were a test of the reliability of the method, varied considerably. The method was subsequently discontinued, but the results did show conclusively the presence of uranium in solution, which could not be accounted for by the dissolution of UF_3 or UF_4 alone.

3.3.2 Determination of Uranium by Oxidation in Air

From run F.37 onwards a new method was used to determine quantitatively the amount of uranium produced in the reaction.

The uranium was oxidised to U_3O_8 by heating the pellet in air, for 24 hours, at ca. $180^\circ C$, using an infra-red lamp. The weight gain of the pellet was then converted into the corresponding stoichiometric amount of uranium.

TABLE 3.5 RESULTS OF THE ANALYSES FOR U AND F IN THE WASHING SOLUTION

Run	1st Washing			2nd Washing		
	U μg	F μg	Free U [#] μg	U μg	F μg	n _F /n _U ^{**}
F.26	488	25	384	942	250	3.33
F.27	508	60	320	825	217	3.30
F.28	390	43.8	207	762	126	2.07
F.30	400	52	183	232	75	4.05
F.36	640	50	431	-	-	-

Assuming the fluorine content of the solution to be due only to the dissolution of UF₃

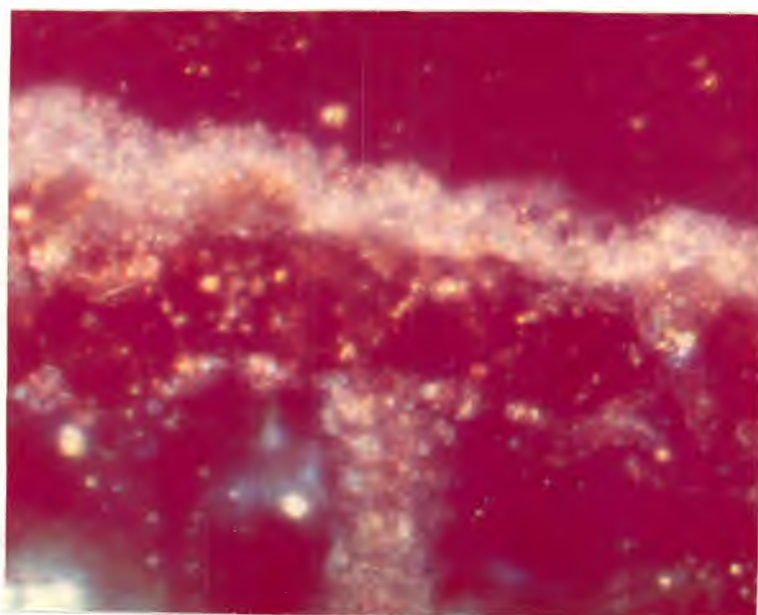
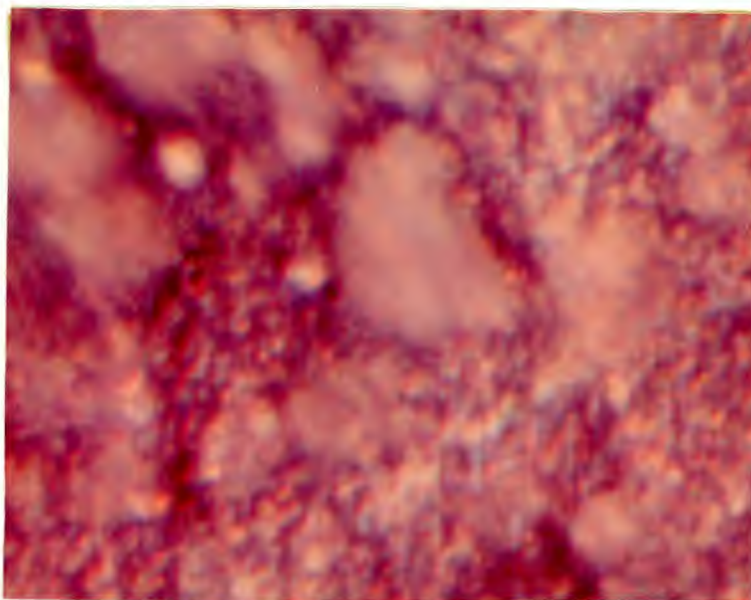
** Ratio of the number of gram atoms of fluorine and uranium in solution

Ignition of uranium precipitates, at 800°C, to the black or greenish black U₃O₈ is a standard method of gravimetric analysis for uranium. In the present case, no such high temperature could be used without the danger of oxidising the uranium fluorides as well. Therefore, a possibility remained that oxidation of the uranium metal, in the pellet, to UO₂ or partial oxidation to U₃O₈ were only achieved by the treatment at 180°C. Alberman and

Anderson⁽⁶⁷⁾ have found, however, that oxidation of UO_2 powder to U_3O_8 is remarkably rapid at 100-175°C. The long treatment at 180°C should, therefore, ensure complete conversion to U_3O_8 . This was confirmed by the fact that after a second similar treatment the weight of the pellets remained constant, within the limits of accuracy of the balance ($\pm 5 \mu g$). Further evidence of the reliability of the method was obtained later from the oxidation of a reacted UF_3 pellet (Run F.50). The weight gain after oxidation was 246 μg as compared with the value of 254 μg calculated from the weight increase of the pellet after reaction with magnesium. The results of all experiments are given in Table 3.6.

After oxidation the pellets became black. Under the microscope the surface of the magnesium fluoride layer appeared blackish on the whole and dotted in some places with small green-olive globules (about 2 μ in diameter). The surface of the layer was highly irregular and in cross sections appeared convoluted (see Plates 3.2 and 3.3) in contrast with its flat and regular appearance in non-oxidized pellets (see Plate 3.4). This alteration of the layer was certainly due to the expansion in volume which accompanies the oxidation of the U metal to U_3O_8 .

The amounts of uranium determined in this way were rather higher than those suggested by colorimetric analyses.



REACTED PELLET TREATED AT 180°C

Plate 3.2 View of the surface of a reacted pellet (run F.38)
(above) oxidised in air at 180°C for 48 hours. The
picture appears out of focus due to the irregu-
larities in the layer produced by the oxidation
of the uranium metal to U₃O₈. Compare with
(1750x) identical view for a pellet not subjected to
treatment at 180°C (e.g. Plate 3.15)

Plate 3.3 Cross section of the product layers for the same
(below) pellet. Note the convolutions of the layer as
(1750x) compared with the regularity found in non-
oxidised pellets (e.g. Plate 3.4)

TABLE 3.6 - RESULTS OF THE OXIDATION OF URANIUM IN AIR

Run	Temp. °C	t min	$t^{\frac{1}{2}}$ min ^{1/2}	S ₂ cm ²	(a) $\frac{\Delta W}{S}$	ΔW_1	$\frac{\Delta W_1}{S}$	$\frac{\Delta W_2}{S}$	(b) $\frac{\Delta W + \Delta W_2}{S}$	(c) $\frac{\Delta W_3}{S}$	(d) $\frac{\Delta W - \Delta W_3}{S}$	(e) $\frac{\Delta^2(W - W_3)}{S^2}$ x 10 ⁻² μg ² cm ⁻⁴
F.37	690	1737	41.6	.73	1000	350	480	360	1360	547	453	2050
F.38	690	413	20.3	.78	615	300	385	289	904	438	177	313
F.39	690	64	8.0	.83	385	250	300	225	610	342	43	19
F.48	690	1485	38.5	.61	955	296	485	364	1319	553	402	1620
F.36	690	2228	47.2	.72	1090	250+ +(77)*	455	341	1431	518	572	3270
F.41	620	1547	39.3	.64	225	104	163	122	347	186	39	15.2
F.42	620	1157	34.0	.69	205	110	160	120	325	182	23	5.3
F.43	620	1530	39.1	.71	200	80	113	85	285	129	71	50.4
F.44	620	2907	53.9	.75	270	150	200	150	420	228	42	17.6
F.45	620	88	9.4	.63	130	67	105	79	209	120	10	1.0
F.50**	690	111	10.5	.73	400	246	337	-	-	384	16	-

* Value obtained from colorimetric analysis (see text)

** UF₃ pellet

ΔW = weight gain after reaction with magnesium (from Tables 3.2 to 3.4) in μg

ΔW_1 = weight gain after oxidation to U₃O₈ (μg)

$\frac{\Delta W_2}{S} = \frac{\Delta W_1}{S} \times \frac{3}{4}$ = weight gain per unit area when all the uranium is converted to UO₂ (μg/cm²)

$\frac{\Delta W + \Delta W_2}{S}$ = total weight gain per unit area after reaction with magnesium and oxidation of uranium to UO₂ (μg/cm²)

$\frac{\Delta W_3}{S} = \frac{\Delta W_1}{S} \times \frac{2M_{Mg}}{8/3 M_O}$ = weight of Mg per unit area used up to produce all the uranium metal by reduction from UF₄ (μg/cm²)

$\frac{\Delta W - \Delta W_3}{S}$ = weight of Mg per unit area used up to produce all the UF₃ by reduction from UF₄ (μg/cm²)

M_{Mg} = atomic weight of magnesium

M_O = atomic weight of oxygen

One pellet (run F.36) which had been subjected only to one washing (see Table 3.5) was subsequently oxidised and a substantial weight gain was recorded (see Table 3.6). The total amount of uranium obtained by addition of the amounts determined by the two methods was worked out in Table 3.6 and the corresponding point in the graph of Fig. 3.5 is represented by an open square. The unreliability of the results obtained by chemical analysis was, therefore, due to incomplete dissolution of ~~the~~ uranium.

3.3.3 Kinetics.

The results listed in column b of Table 3.6 were plotted vs. $t^{1/2}$ (fig. 3.5) and are represented by full squares. In the same graph are plotted the results of the final experiments listed in Tables 3.2 and 3.3 which are represented by full circles, with the exception of those experiments where oxidation to UO_2 occurred on cooling (marked with an asterisk in Table 3.2), which are represented by open circles. This type of plot is not expected to be exactly linear but was adopted because it is more convenient for the discussion of the results of the preliminary experiments.

It seems reasonable to assume that the growth of the UF_3 layer follows a parabolic rate law, i.e. the net amount of UF_3 produced at a given moment is a function only of the instantaneous thickness and the fluorine (or uranium) chemical potentials at the interfaces. The square of the weight of Mg per unit area used up to produce

UF₃ (column e in Table 3.6) is plotted versus time in Fig. 3.5a. The accuracy of the results is necessarily low due to the limitations of the experimental method and the plots may be regarded as having only a semi-quantitative value, but at least they do not contradict the hypothesis of a parabolic growth mechanism for the UF₃ layer. The plots pass through the origin, since the mechanism which operates to produce the logarithmic rate law in the initial stages of the overall reaction (section 9.2.6), does not influence the growth of the UF₃ layer.

The parabolic rate constants for the partial reaction yielding UF₃ estimated from Fig. 3.5 are then

$$k_{620^{\circ}\text{C}} = 6.7 \times 10^{-13} \text{ g}^2 \text{ cm}^{-4} \text{ min}^{-1}$$

$$k_{690^{\circ}\text{C}} = 1.1 \times 10^{-10} \text{ g}^2 \text{ cm}^{-4} \text{ min}^{-1}$$

The rate of production of uranium metal is given by the difference between the overall rate of reaction, i.e. the rate of production of MgF₂, and the rate of production of UF₃. Due to the fact that the parabolic plot for the overall rate of reaction does not pass through the origin, that rate is not given by a simple relationship of the parabolic type and since it has no particular physical meaning the relationship will not be developed here. In fact, however, plots of the weight of Mg per unit area used to produce U, against the square root of time, are approximately linear and

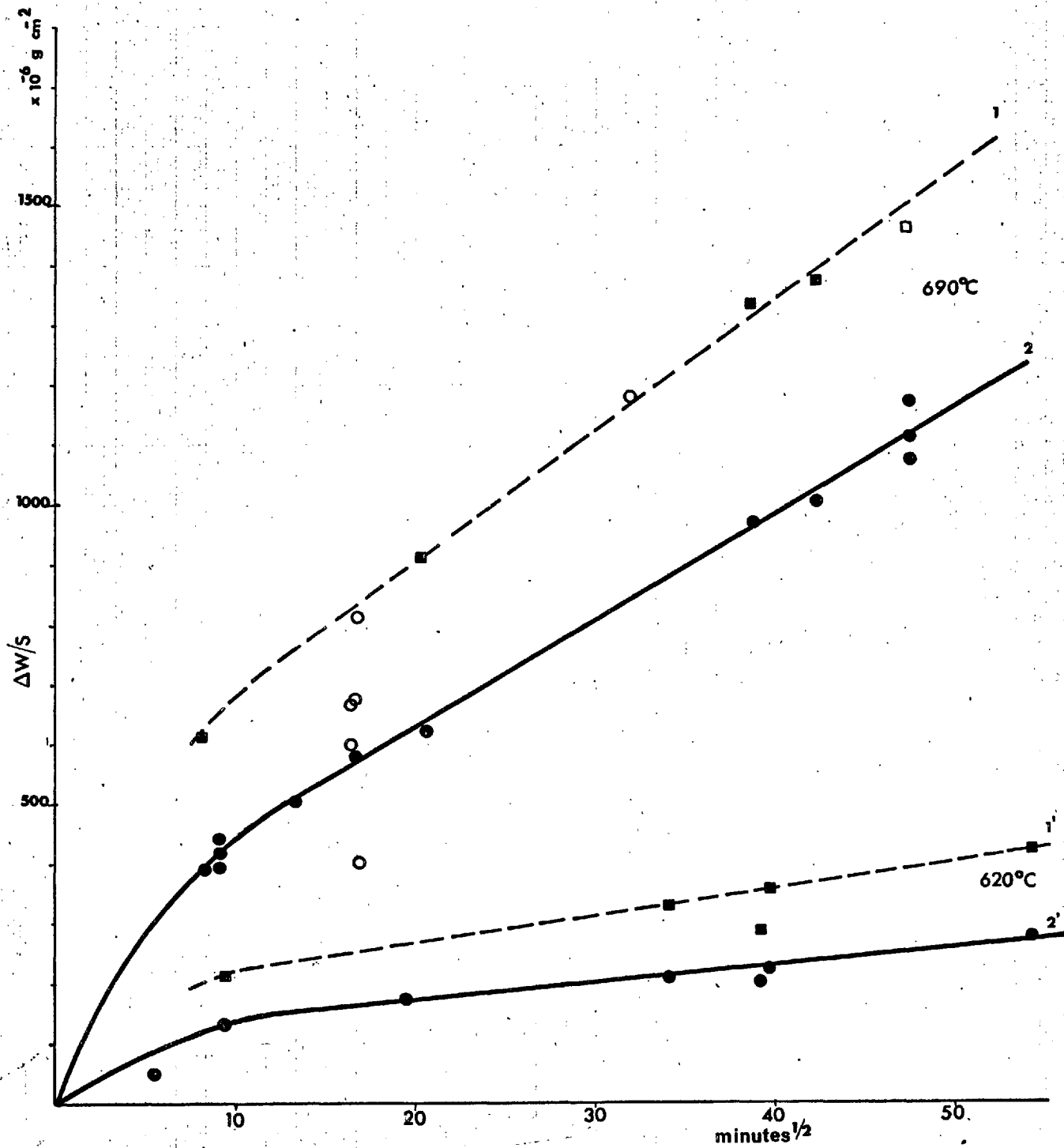


Fig.3.5 - $\Delta W/S$ vs. $t_{1/2}$ from columns a and b in Table 3.6

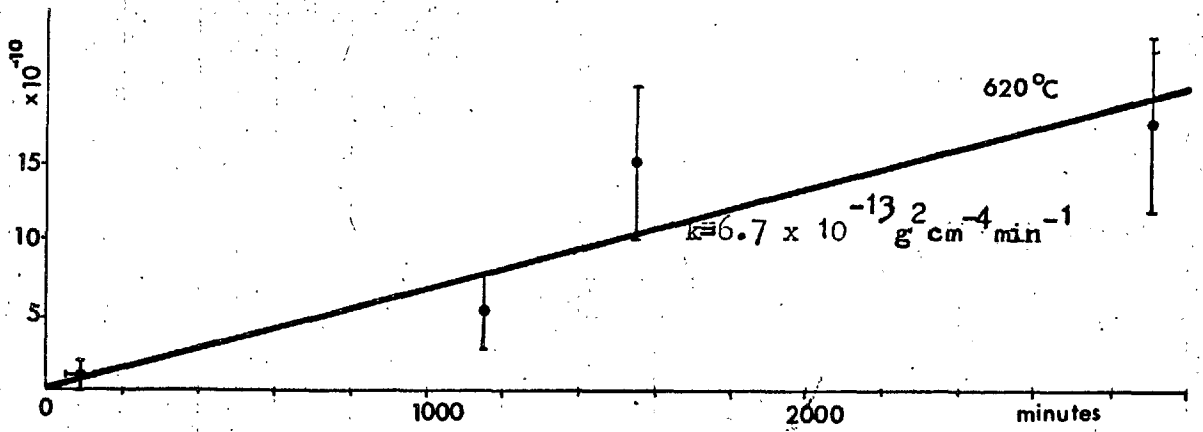
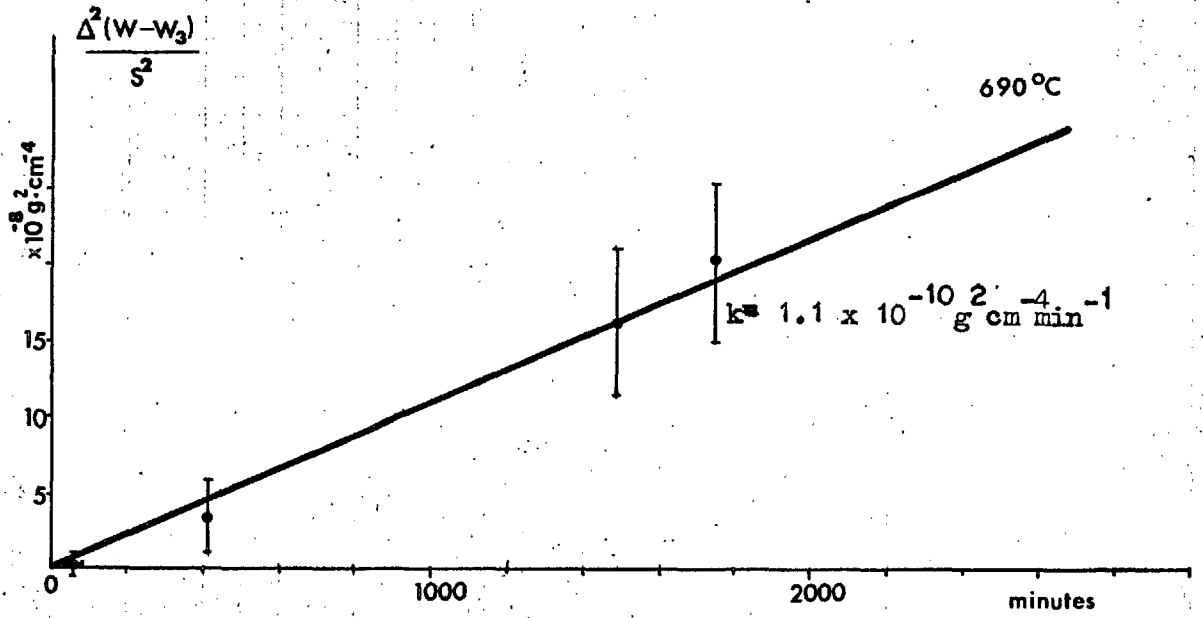


Fig.3.5.a -Kinetics of the Partial Reaction Yielding Uranium Trifluoride

this observation originally led to the assumption that the growth of UF_3 was parabolic.

3.4 X-ray Powder Analysis of the Reaction Products.

X-ray powder patterns were taken of the reaction products for both the preliminary and final experiments.

The powder, scraped from the product layers with a small spatula, was ground in a small agate mortar and loaded into a thin walled Lindemann-glass capillary tube. For the final experiments the whole operation was carried out in a dry box and the capillaries, plugged with a bit of plasticine, were sealed in a small flame immediately afterwards. For the preliminary experiments a 19 cm Debye-Scherrer type X-ray camera was used. An 11.54 cm Phillips camera was utilized for the final experiments.

The X-ray patterns are given in Figs. 3.6 and 3.7 and the interplanar spacings are listed in Table 3.7. Most of the lines in the two cases correspond closely to the lines of UF_3 . For the preliminary experiments, however, 9 extra lines could not be identified since they do not correspond to any of the strongest lines to be found for uranium metal, magnesium fluoride, uranium dioxide, uranyl fluoride or magnesium. For the final experiment the extra lines correspond closely to the

TABLE 3.7 - INTERPLANAR SPACINGS FOR THE REACTION PRODUCTS OF BOTH A PRELIMINARY AND A FINAL EXPERIMENT

Run F.1		Run F.23		UF ₃ see Table 2.1		U Ref.(69)		MgF ₂ Ref.(70)	
d(Å)	I	d(Å)	I	d(Å)	I	d(Å)	I/I ₀	d(Å)	I/I ₀
3.65	VF	3.67	MS	3.67	MS				
3.55	VF	3.58	M	3.57	M				
		3.25	F					3.265	100
3.21	VS	3.21	VS	3.21	VS				
2.60	F	2.56	F	2.56	F	2.563	70		
		2.49	VF			2.521	100		
2.44?	VF								
		2.44	VF			2.473	49		
		2.34?	VF						
		2.27	VF			2.274	58		
		2.22	VF					2.231	96
2.07	S	2.068	S	2.069	S			2.067	34
2.02	VS	2.020	VS	2.022	VS				
1.95?	VF								
1.88?	VF								
1.83	VF	1.832	F	1.833	F				
1.803	S	1.805	S	1.806	S				
		1.76	VF			1.778	40		
1.742	S	1.743	MS	1.743	MS				
		1.711	F					1.711	73
1.635	F	1.633	F	1.635	F				
1.616	F	1.610	VF	1.612	VF				
		1.527	VF			1.532	34		
1.448	MS	1.449	M	1.447	MS				
1.428?	F								
1.403?	F								
1.377	M	1.375	M	1.377	MS			1.375	35
1.361	M	1.360	M	1.360	MS				
1.333	M	1.335	M	1.335	S				
		1.284	VF	1.286	VF				
1.272	VF	1.270	VF	1.272	VF				
1.256?	VF								
1.225	VF	1.225	VF	1.225	VF				
1.199	M	1.196	F	1.197	F				
1.188	S	1.187	MS	1.187	S				

I = Intensity
VS = Very Strong

S = Strong
MS = Medium Strong

M = Medium
F = Faint
VF = Very Faint

TABLE 3.7 (cont)

Run F.1		Run F.23		UF ₃	
1.161	F	1.165	VF	1.161	F
1.139	S	1.139	MS	1.139	S
1.094	VF	1.092	VF	1.093	VF
1.057	F	1.053	M	1.055	M
1.037	F	1.035	VF	1.038	VF
1.009	VF	-		1.010	F
1.005	F	1.001	VF	1.004	F
0.9991	MS	0.9992	MS	0.9992	S
0.9885	M	0.9882	M	0.9884	M
0.9632	VF	0.9620	VF	0.9625	VF
0.9249	M	0.9242	M	0.9243	M
				0.9108	VF
0.9085	M	0.9072	VF	0.9076	F
0.9052	F	0.9041	VF	0.9047	F
0.8927	F	0.8930	VF	0.8927	F
0.8770?	F				
0.8665?	F				
0.8577	M	0.8575	M	0.8576	MS
0.8445	F	0.8440	VF	0.8442	F
0.8410	M	0.8404	M	0.8405	MS
0.8316	MS	0.8316	M	0.8316	MS
0.8258	MS	0.8257	M	0.8260	MS
0.8195	MS	0.8196	M	0.8199	MS
				0.8072	VF
0.8047	F	0.8048	F	0.8050	F
0.7971	M	0.7971	M	0.7971	MS
0.7916	M	0.7917	M	0.7919	MS
0.7842	MS	0.7844	MS	0.7843	S
0.7813	M	0.7813	M	0.7815	MS
0.7783?	M				



Fig 3.6 X-Ray Powder Pattern for the Product Layers
from a Preliminary Experiment (run F. 1)

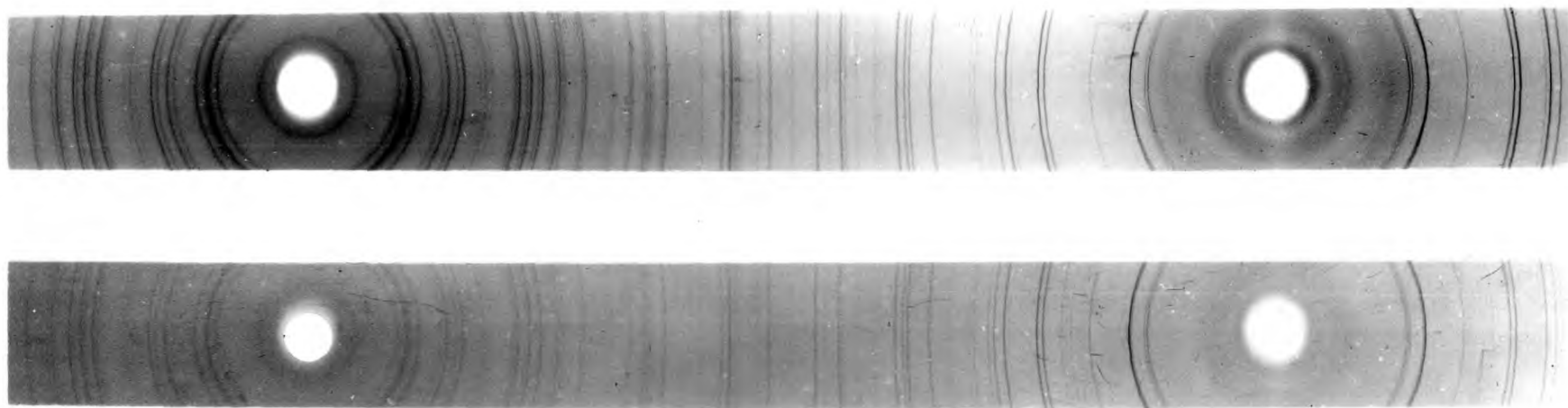


Fig. 3.7 X-Ray Powder Patterns for UF₃ Prepared in this Work (strip above) and for the Products Layers in run F.23 (strip below)

strongest lines (down to 34% of relative intensity) for uranium metal and magnesium fluoride. Only one line ($d = 2.34 \text{ \AA}$) could not be identified.

3.4.1 Errors in X-ray Diffraction Studies

The important sources of systematic errors for the interplanar spacings determined from X-ray powder diffraction lines are: (i) imperfect alignment of the specimen in the camera, (ii) poor collimation of the X-ray beam, (iii) absorption of the beam by the specimen and, (iv) film shrinkage.

Errors from sources (i) and (ii) may be rendered negligible by a careful experimental technique. The film shrinkage does not greatly affect the results when a Phillips camera is used, but may cause detectable errors in the case of the Debye-Scherrer camera. Absorption of X-rays in a powder specimen (source iii) would cause the diffraction peak on the photograph to be moved in the direction of increasing Bragg angle θ . This error increases with elements of higher atomic weight which have higher linear absorption coefficients. In any case errors in θ affect the "d" values increasingly less as θ approaches 90° since the error in d thus becomes vanishingly small.

Apart from the systematic errors just mentioned there are the random errors introduced on measuring the distances between the lines, due to difficulties in correctly locating the peak of the line. This error can be reduced by taking a number of independent measurements, but it is likely to be higher for faint and very faint lines.

The errors in the UF_3 lines ranged from 1% for angles up to about 18° to 0.2% for higher angles. The greatest errors were obtained for faint and very faint lines. For the uranium and magnesium fluoride lines in run F.23, the error in "d" values ranged from 1.2%, for small Bragg angles, down to 0.3% for θ values higher than about 28° .

The errors in these studies may be attributed to the high linear absorption coefficient of uranium and the difficulty in locating exactly the peaks of the faint and very faint lines.

3.5 Microscan X-Ray Analyses

The presence of uranium in the outer product layer was first indicated in the preliminary experiments by the yellow-brownish colour of the layer (Plates 3.1, 3.11 and 3.13) and was confirmed with the Cambridge Microscan X-Ray Analyser. Plates a and b in Fig. 3.8 show the Mg $K\alpha$ and U $L\alpha$ images obtained for equal exposure time at

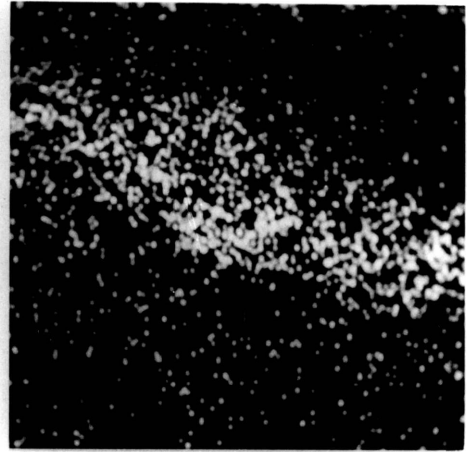
the edge of the cross section of two reacted UF_4 pellets, a preliminary and a final experiment respectively.

Plate a (U X-ray image) shows an apparently regular distribution of uranium in the outer layer (preliminary experiment), while the distribution is more irregular for the second pellet (final experiment). The presence of uranium metal is less well defined in this case due to the lower efficiency of the spectrometer at the time, which is indicated by the lower density of points in the uranium rich inner layer.

The Mg X-ray images show that in both cases the magnesium is confined to the outer layer. These results, however, have only a qualitative value and various attempts were made to determine quantitatively the distribution of uranium and magnesium in the outer layer, by counting the characteristic U and Mg X-ray emission at progressive points along the same line of scan. Unfortunately these two elements are situated at the extreme limits of operability of the apparatus, so that the possibility of obtaining quantitative results was reduced from the start. The high linear absorption coefficient of uranium, the topographic relief of the specimen (due to the difficulty already mentioned in getting well polished sections), the narrowness of the layer (even in most favourable cases the thickness did not exceed



U X-RAY IMAGE

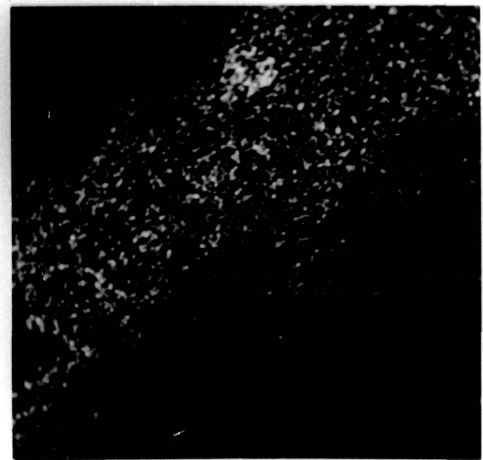


Mg X-RAY IMAGE

a.RUN F.14



U X-RAY IMAGE



Mg X-RAY IMAGE

b.RUN F.34

Fig.3.8 - X-RAY IMAGES AT THE CROSS SECTION EDGE OF TWO REACTED UF₄ PELLETS

10 - 12 μ) and the inefficiency of the spectrometer crystal were other factors that considerably reduced the accuracy of the results which may be regarded as having only a semiquantitative value.

A distribution of uranium across the outer layer for a consecutive time experiment (run F.14) and a typical uranium and magnesium distribution for a final experiment (run F.34) are given in Figs. 3.9 and 3.10 respectively.

The two uranium distribution patterns are essentially different. While, for the consecutive time experiments, a smoothly decreasing concentration gradient is obtained, for the final experiments the distribution is irregular, a uranium rich region being usually followed by a region where the content in uranium is low.

By measuring the area under the uranium distribution curve and taking the average of the counts over the inner layer as corresponding to the stoichiometric percentage in weight of U in UF_3 (80.7%) the average weight percentage of uranium in the outer layer of pellet F.34 is about 27%. This value may be as much as 50% lower than the actual weight percentage due to absorption. In fact, the estimated percentage in weight of uranium in MgF_2 for this pellet taken from the graph of Fig. 3.3 is 52%.

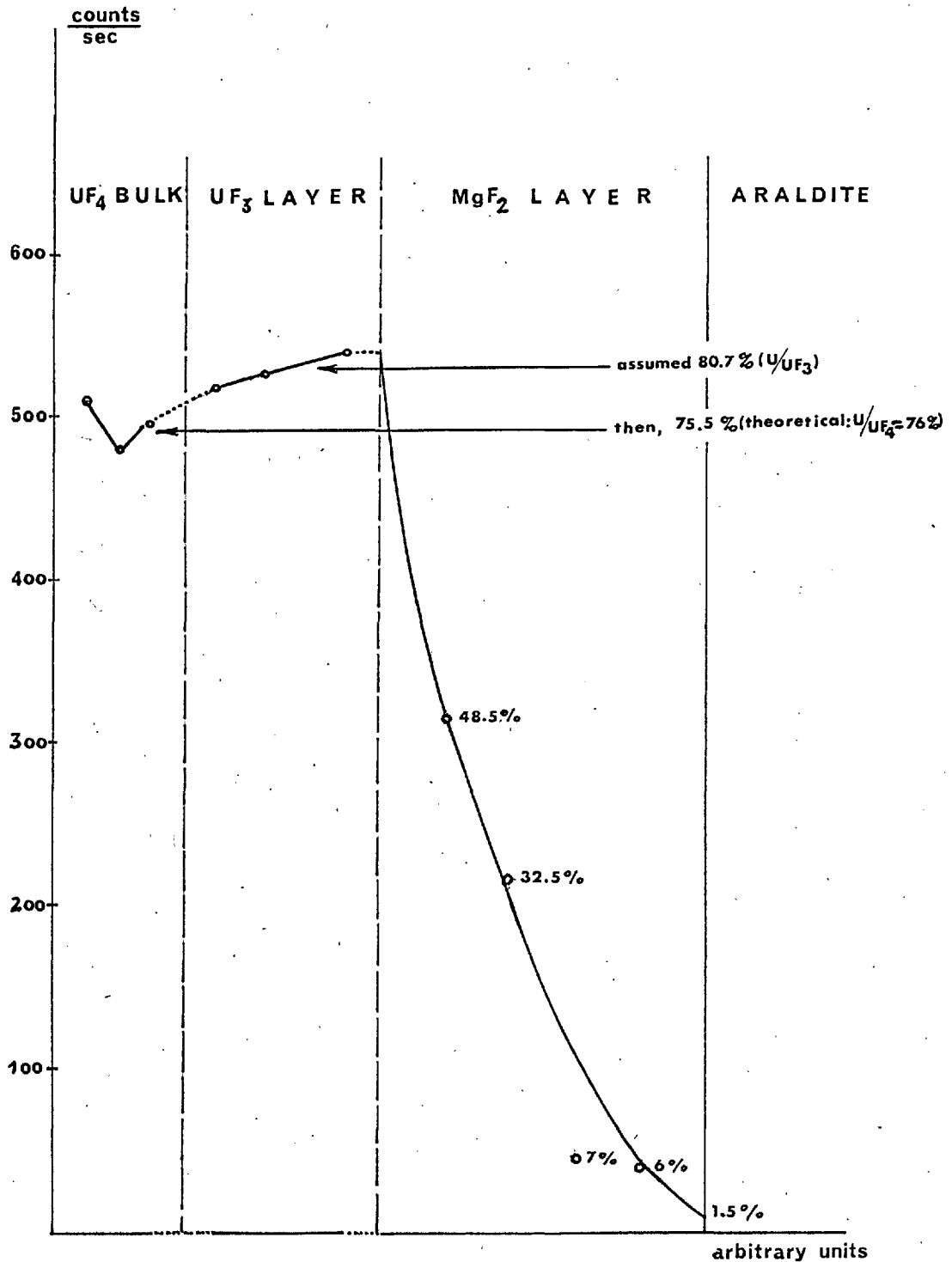


Fig.3.9: Concentration Gradient of U in the MgF_2 Layer for a Preliminary Experiment (Run F.14)

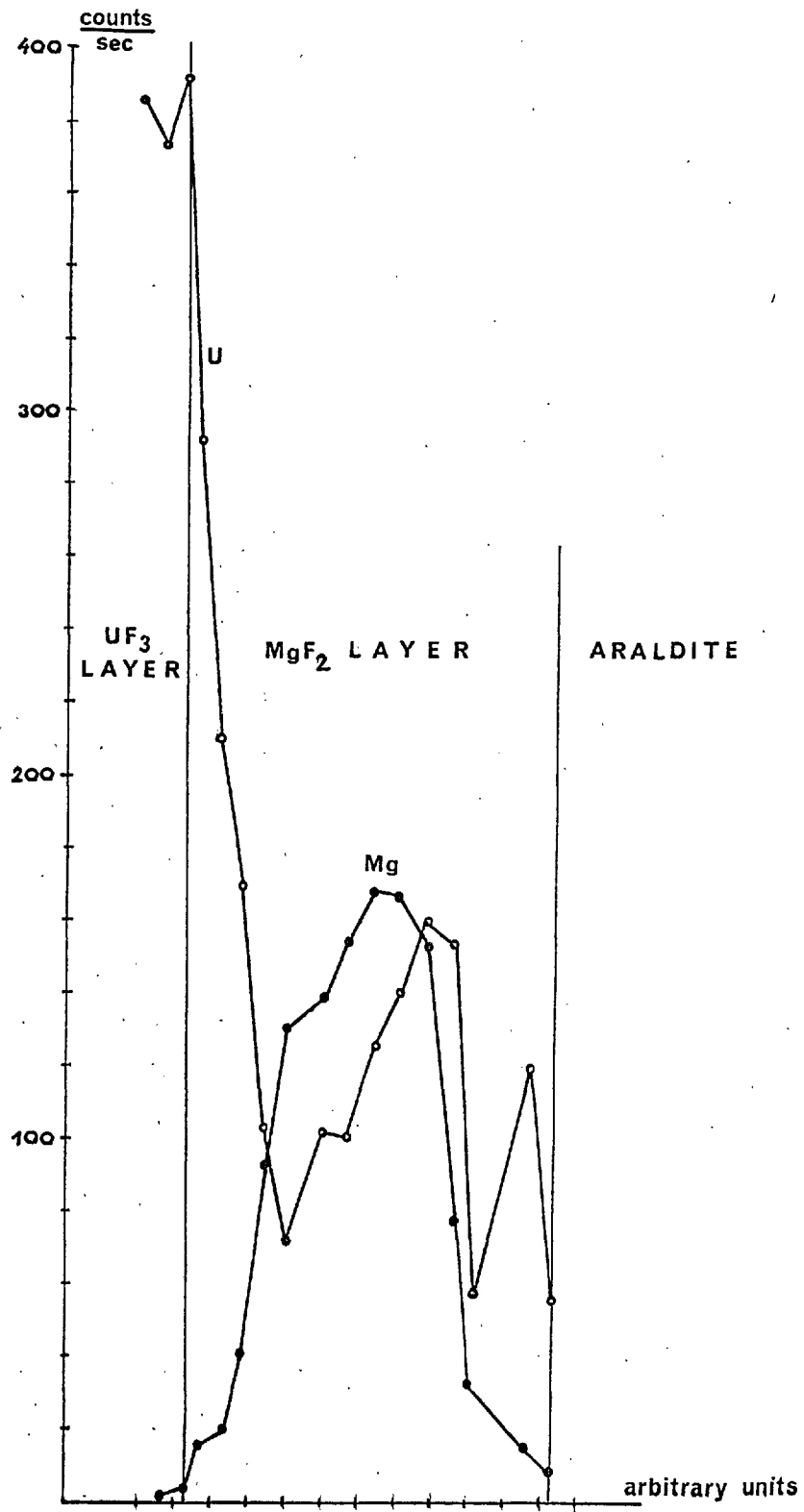


Fig.3.10: Typical Distribution of U and Mg in the MgF₂ Layer for a Final Experiment (Run F.34)

These rough calculations show that at least 50%, and probably much more, of the uranium metal produced in the reaction is disseminated in an irregular way all across the outer layer.

3.6 Identification of the Product Layers

The identification of the layers was made by taking into account the results obtained with the X-ray powder diffraction studies and the microscan X-ray analyses, and by microscopic observation of cross sections of the specimens.

For the final experiments, the X-ray powder diffraction patterns (section 3.3) showed conclusively the characteristic lines of pure UF_3 , MgF_2 and U metal with only one very faint unidentified line that may have been caused by some impurity introduced during the preparation of the specimen. Solid solution of UF_3 in MgF_2 or complex compound formation is, therefore, very unlikely (see also section 4.2.3). The results of the microscan X-ray analyses (section 3.4) showed the MgF_2 to be confined to the outer layer, the inner layer to be formed of UF_3 only, and most of the uranium metal to be interspersed in the MgF_2 ^{with} possibly a relatively small amount concentrated at the UF_3/MgF_2 interface. The microscopic observation of cross sections of unoxidised pellets (Plates 3.4 and 3.5) revealed a violet-red inner layer, which is

characteristic of UF_3 ⁽⁶⁸⁾ and a white, outer layer, as might be expected for the MgF_2 .

For the preliminary experiments, doubts remained as to the nature of the outer layer. The X-ray diffraction patterns showed a series of unidentified lines, apart from the lines for the UF_3 , suggesting a solid solution or a complex compound. Its brown colour is characteristic of UO_2 and the subsequent results (see section 3.1) showed that this compound might have been formed due to oxidation of the uranium metal by traces of oxygen and/or moisture in the argon. Unfortunately, the system UO_2 - MgF_2 is not sufficiently well known to allow any precise conclusion to be drawn.

3.7 Appearance

3.7.1 Final Experiments

In the final experiments the MgF_2 layer appeared flat and whitish to the eye. Under the microscope it looked darker, due to the presence of the UF_3 beneath, but when scratched it detached easily into thin white lamellae. The surface, though generally flat, was dotted with small bumps, 5 to 15 μ across and raised 2 to 5 μ above the flat base. Plate 3.6 was taken focusing the top of these bumps. They also appear as diffuse patches in plates 3.15 and 3.16.

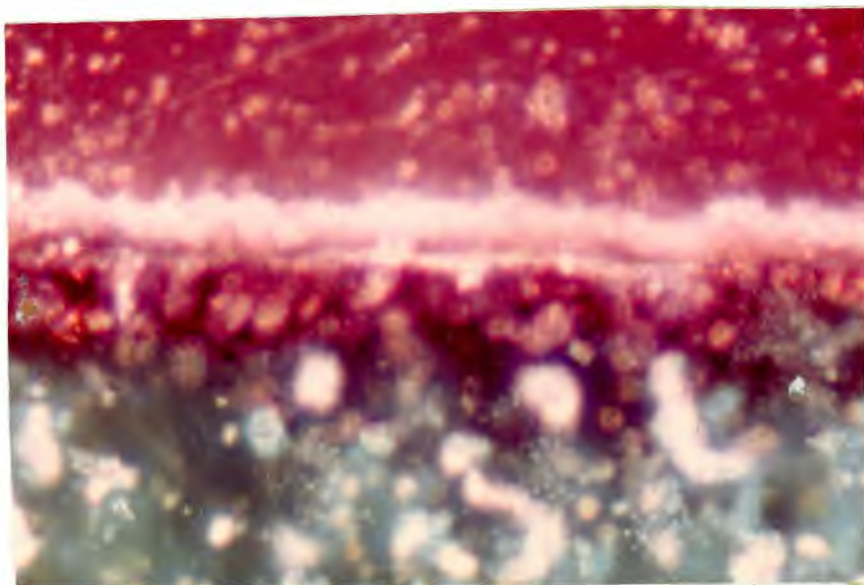
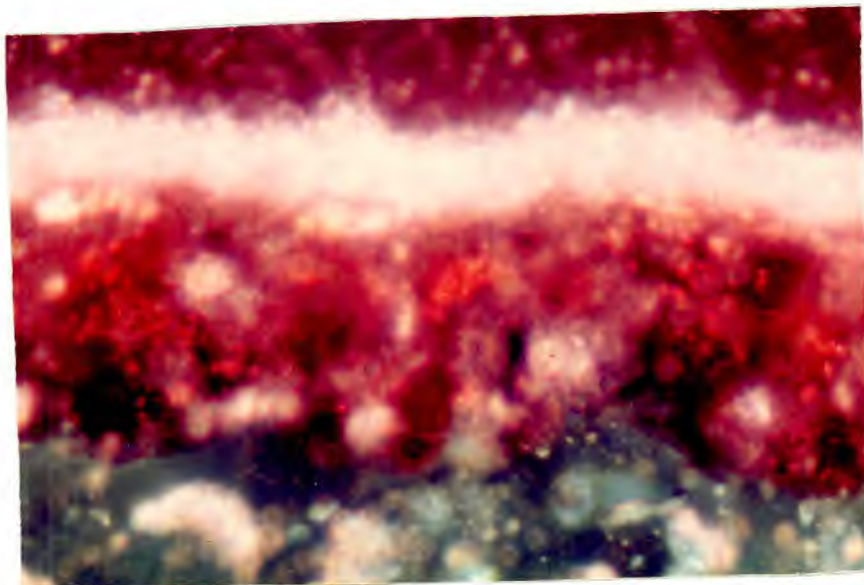


Plate 3.4 (above) - GENERAL VIEW OF THE PRODUCT LAYERS IN AN UNOXIDISED PELLETT (run F.34)
Note the thick, white regular layer of MgF_2 and the more irregular UF_3 layer beneath.
(1000x)

Plate 3.5 (below) - PRODUCT LAYERS IN A SHORT TIME FINAL EXPERIMENT (run F.20) Unoxidised pellet
Note the split of the MgF_2 layer due to the infiltration of Araldite through cracks produced in the outer layer when mounting the pellet (see text)

The MgF_2 layer had a polycrystalline structure with grains much smaller (1 - 2 μ at most) than those of UF_3 and UF_4 .

The UF_3 layer appeared violet to dark red in colour, usually thicker than the MgF_2 layer and unevenly differentiated from the UF_4 , probably due to the irregularity of the grain boundaries. On mounting the pellet in araldite, it was difficult to avoid breaking the MgF_2 layer with the tweezers. As a result the MgF_2 became detached from the UF_3 and in some cases the araldite infiltrated between the two layers. This happened only for the final experiments where it was found that the MgF_2 was much more easily exfoliated from the UF_3 than in the preliminary experiments. Plates 3.5 and 3.7 are examples where this phenomenon occurred.

When the MgF_2 was removed, the surface of the UF_3 was revealed, pock marked and partly covered with a variable amount of a brownish product, certainly UO_2 , resulting from air oxidation of the reactive uranium metal trapped at the UF_3/MgF_2 interface. (Plates 3.8 and 3.9). The amount of brownish product was particularly significant for the UF_3 pellets (Plate 3.9). It is worth mentioning that in this case the marks on the UF_3 surface seem to follow a regular pattern, indicating preferential directions

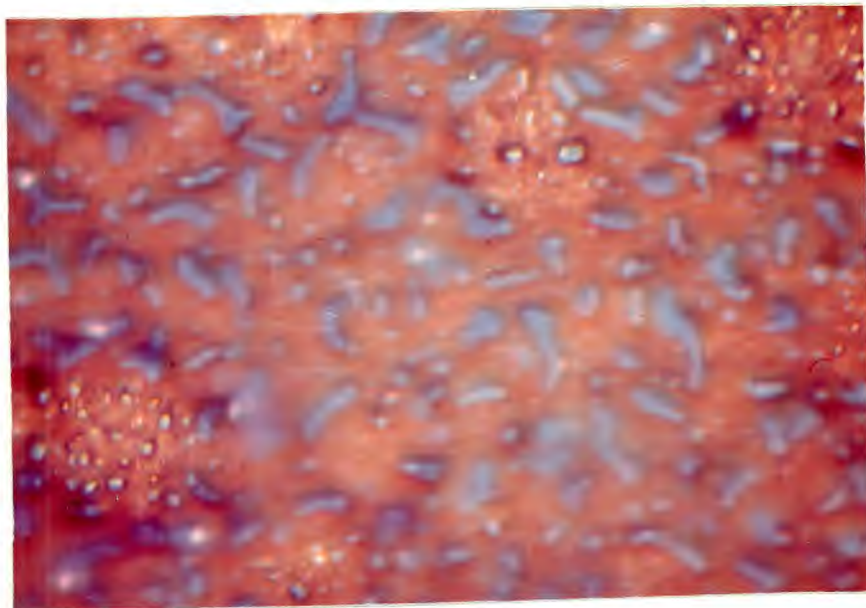


Plate 3.6 - BUMPS ON THE SURFACE OF THE MgF_2 LAYER

View looking down onto the pellet and focused on the top of the bumps. The specimen is a UF_3 reacted pellet (Run F.52). The blue areas are uranium, slightly oxidised at room temperature, after the pellet had been kept for some weeks in a desiccator.

(1600x)

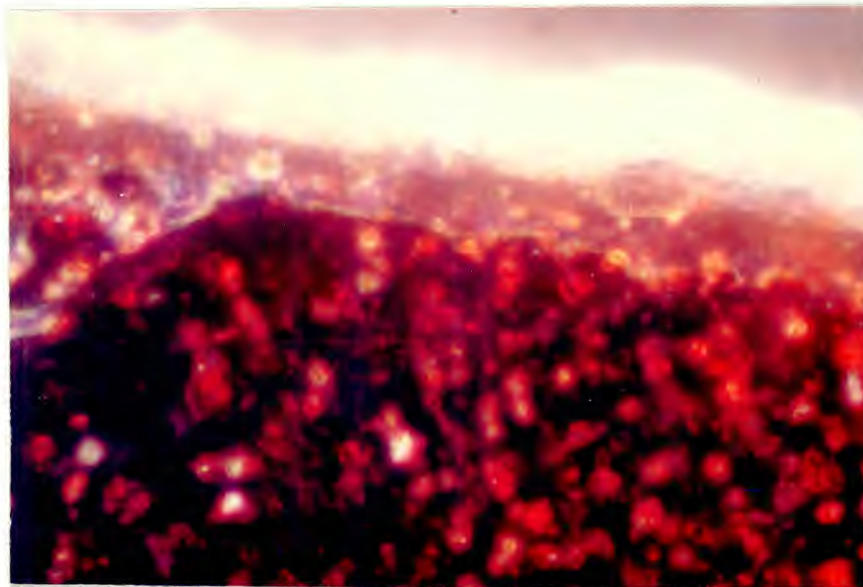


Plate 3.7 - MgF_2 LAYER ON A UF_3 PELLETT (run F.52)

Note the araldite layer at the UF_3/MgF_2 interface. This pellet is the same as in Plates 3.6 and 3.16, but no traces are found of the oxidised uranium particles shown in those photographs. This indicates that oxidation was superficial and the uranium embedded in the layer has not been affected.

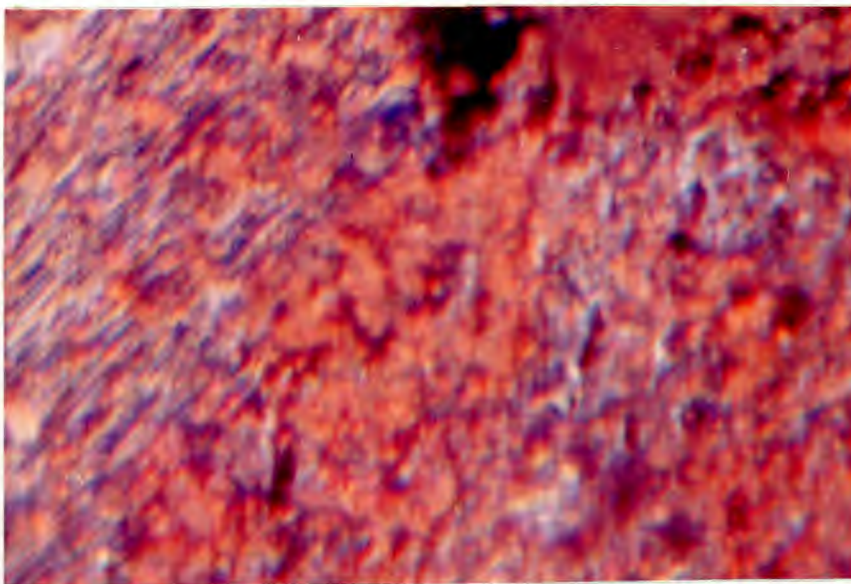
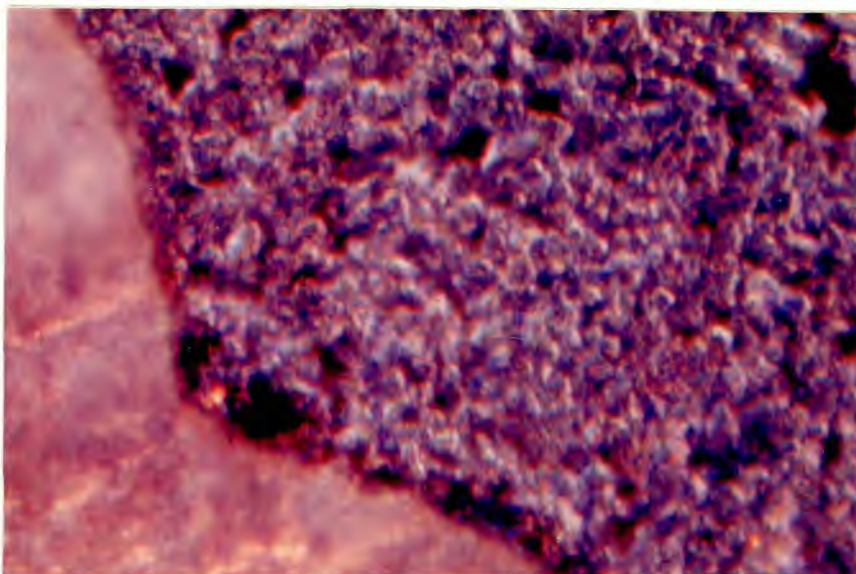
(2400x)

of reaction depending on the crystallographic orientation of the UF_3 grains. This phenomenon was observed only for the UF_3 pellets.

3.7.2 Preliminary Experiments

In the preliminary experiments two layers were also observed on microscopic observation of cross sections. The appearance of the UF_3 layer was much the same as that found in the later experiments, except in one case, run F.12. In this run an old UF_4 pellet (previously used in a consecutive time experiment, run F.8) was used after polishing off the product layers, since no freshly made pellet was available at the time. As shown on Plate 3.10, UF_3 grains were found to scatter all over the UF_4 bulk. The overall rate of reaction did not seem to have been greatly affected by this phenomenon, since it compares very well to that of run F.14 which was carried out with a freshly made UF_4 pellet. In any case a freshly made pellet was used for all subsequent runs.

The MgF_2 layer, as was mentioned in Section 3.1, appeared in these preliminary runs either to be smeared with yellow-brownish patches or uniformly brown in the consecutive time experiments. In cross section the layer was convoluted in places, leaving gaps at the UF_3/MgF_2 interface. (Plates 3.1 and 3.11) In two cases, runs F.5 and F.6, the whole surface of the pellet was covered with



SURFACE OF THE UF₃

Plate 3.8 (above) View looking down onto the pellet, on a spot where the MgF₂ layer exfoliated. The specimen is a marker experiment pellet (run F.18) and some gold globules are visible on the surface of the UF₃ (see Section 3.8)
(1600x)

Plate 3.9 (below) View looking down onto the pellet after the MgF₂ layer has been removed. Note the regular pattern of the marks on the left hand side, and the globular nature of the UO₂ resultant from air oxidation of the uranium metal at the interface.
(2400x)

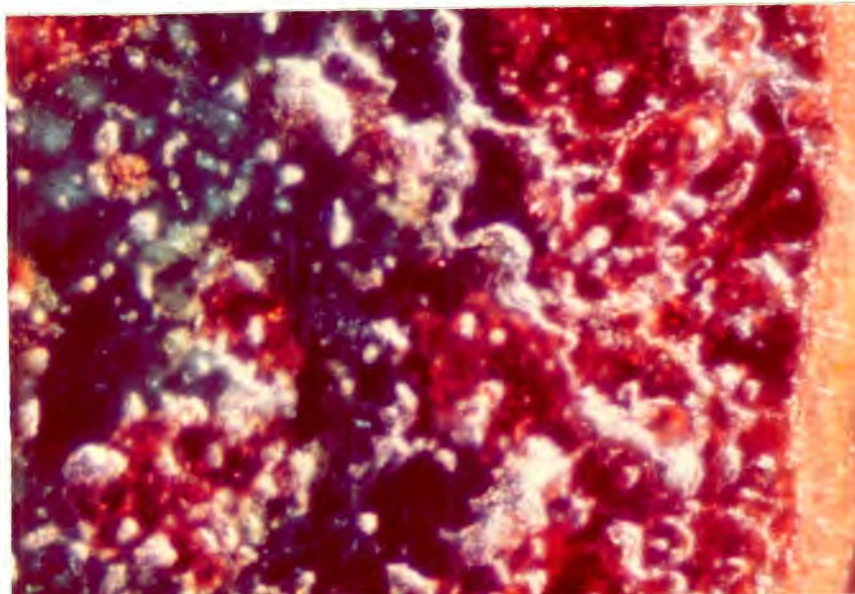


Plate 3.10 - UF_3 FORMED INSIDE THE UF_4 PELLETT (run F.12)
Grains of UF_3 are found embedded in the UF_4
bulk.
(1000x)

mushroom-like balloons (10 - 40 μ across) rising from a relatively flat base to heights comparable to their transverse dimensions (Plate 3.12). In some places the balloons were burst open revealing their hollowed nature and a wall thickness of 1 - 2 μ . By focusing on to the flat base of the layer, the bottom of the burst balloons also came into focus showing that they were actually sitting on the top of the layer. In other preliminary experiments, similar balloons were also observed from time to time, but never in the amounts found for these two runs. A balloon sitting on the top of the MgF₂ layer can actually be seen in Plate 3.11, where the different nature of the balloons and convolutions is well illustrated.

3.8 Marker Experiments

Gold marked UF₄ pellets were reacted at 622°C (run F.19), 630°C (run F.10) and at 690°C (run F.53).

In the first two experiments the UF₄ pellets were marked with gold by condensing, on one face, a strip of gold film about 2mm. wide and about 10⁰ Å thick. After reaction the markers could be seen as small globules, 0.5 - 1.3 μ in diameter, sitting on the top of the MgF₂ layer, which was about 5 μ thick (Plate 3.13). By careful examination it was possible to focus first on to the top of the gold globules and then on to surface of the layer thus proving they were not embedded. On removing the MgF₂ layer

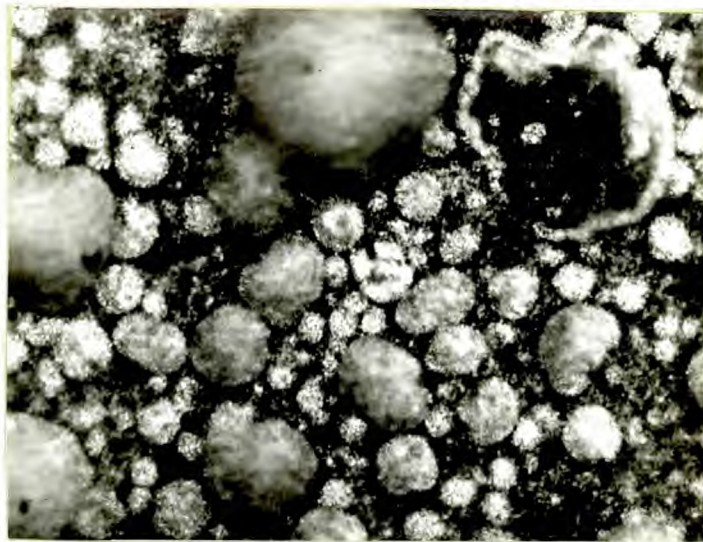
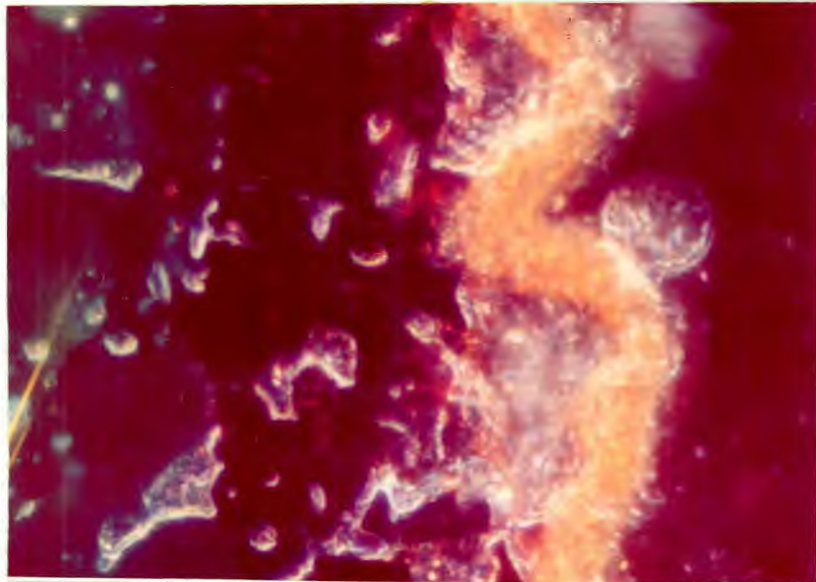


Plate 3.11 (above) - CONVOLUTED NATURE OF THE MgF_2 LAYER FOR A CONSECUTIVE TIME EXPERIMENT (run F.14) Note one balloon of the type mentioned in the text, sitting on the top of the layer. (1600x)

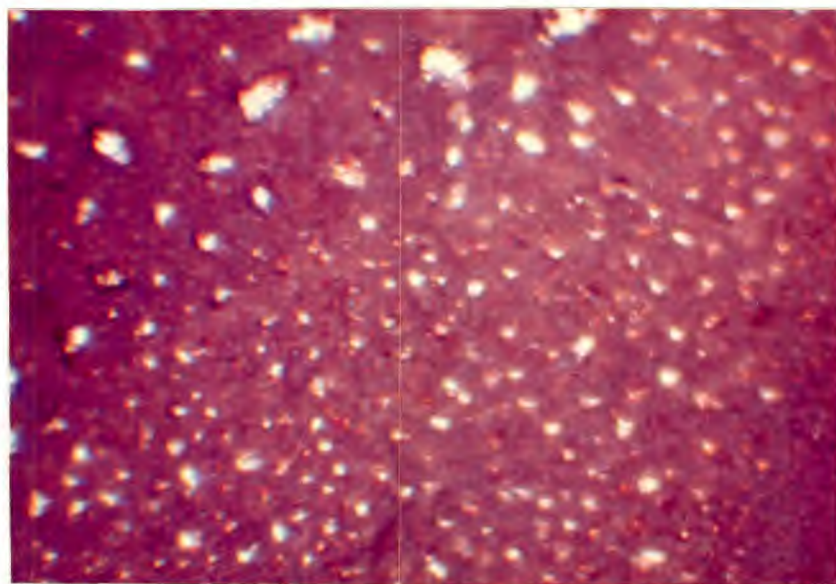
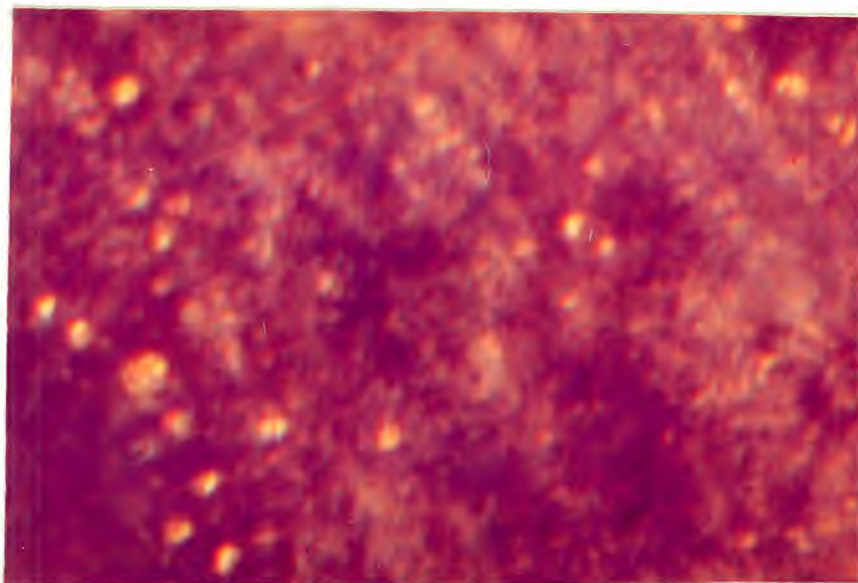
Plate 3.12 (below) - BALLOONS ON THE TOP OF THE MgF_2 LAYER. View looking onto the pellet. Note the burst balloon on the right hand corner.

some odd gold globules were found trapped at the UF_3/MgF_2 interface (Plate 3.8).

In order to avoid the trapping of the markers at the UF_3 interface and to check whether the size of the markers had any effect on their final position, the UF_4 pellet was reacted at 690°C in run F.53, then marked with two intersecting strips of gold and reacted again. Plate 3.14 was taken at the intersection of the two gold films and shows irregularly shaped markers on the upper left hand corner several times the size of the smaller, globular markers in the middle of the field. The smallest markers are less than 1μ in diameter as compared with a MgF_2 layer thickness of about 5μ grown after gold marking. Most of the markers are associated with small uranium globules indicated by their blue colour, certainly due to a surface tension effect.

On examining the edges of the marked areas of the pellets, no change was found in the MgF_2 layer thickness in traversing from over the marked area to over unmarked magnesium fluoride. This was true even for the larger markers in run F.53 and indicates that the presence of the gold does not reduce the rate of the reaction.

It was not possible to locate the markers by examination of cross sections of marked pellets. This



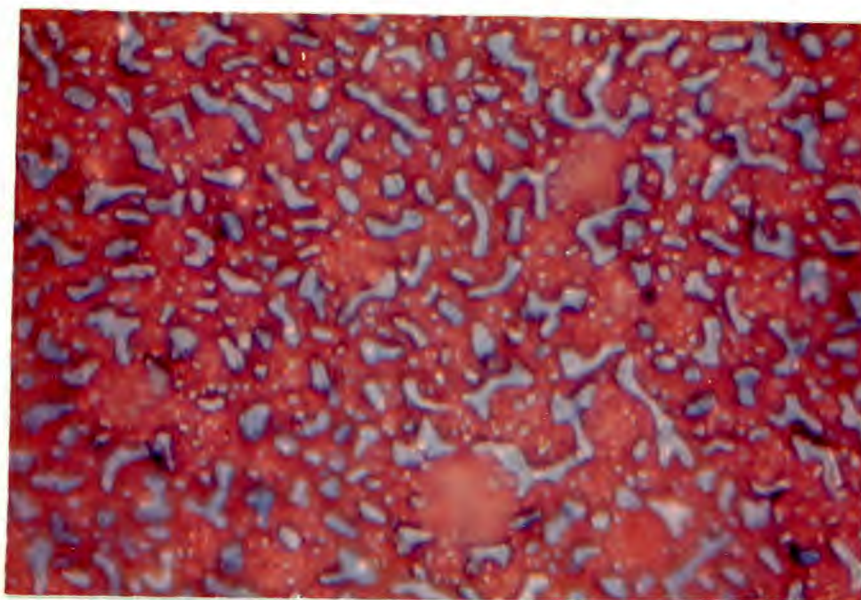
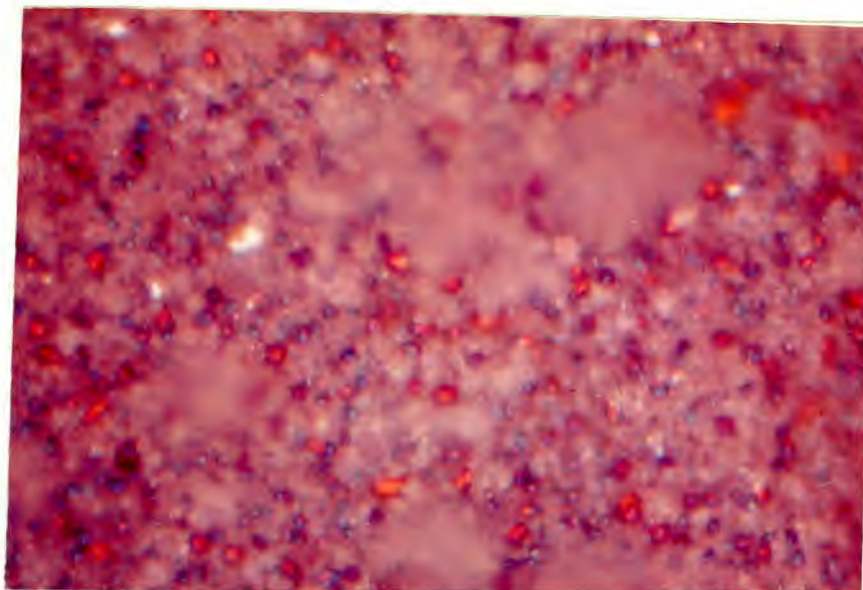
GOLD MARKERS

Plate 3.13 (above) - Gold markers on the top of the MgF_2 layer (run F.19) (2400x)

Plate 3.14 (below) - Gold markers in run F.53. Note the two sizes of markers and the association between most of the markers and the uranium globules which was indicated by their blue colour. (640x)

was probably due to the fact that the araldite/ MgF_2 boundary was always poorly defined in polished cross sections (as result of the difference in hardness) and the thickness of the markers was so small as to become indistinguishable from the dark brown araldite. In any case no markers were observed either at the UF_3/MgF_2 interface or embedded in the MgF_2 layer.

Some other observations were made on unmarked pellets which are equally significant as marker experiments. Observation of the surface of reacted pellets subjected to heating, in air, at $150^\circ C$, showed the presence of greenish black oxidised particles of uranium, on the top of the MgF_2 layer (Plate 3.2). Similar observations were made on pellets which, although not heated to $150^\circ C$, had been exposed to the air for some hours or kept in a desiccator for some weeks. The oxidised uranium particles in this case, instead of the green colour characteristic of U_3O_8 presented a blue or reddish-brown colour. (Plates 3.15 and 3.16). Since the uranium metal could have been produced only at the UF_3/MgF_2 interface and there was no evidence of uranium needles growing into the MgF_2 , its presence on the top of the layer indicates that it was produced in the initial stage of the reaction and pushed away from the interface by the outward growing MgF_2 layer. The occurrence of the balloons, described in section 3.8, is also an indication of outward growth of the MgF_2 layer and will be discussed in section 4.2.



OXIDISED URANIUM ON THE TOP OF THE MgF_2 LAYER

Plate 3.15 - View looking down onto the surface of a reacted UF_4 pellet, showing uranium globules oxidised at room temperature
(run F.35)
(x1600)

Plate 3.16 - The same, but for reacted UF_3 pellet
(run F.52)
(x1000)

CHAPTER 4

DISCUSSION

4.1 Kinetics

4.1.1 The parabolic Rate Period

The relatively flat MgF_2 layer (Plates 3.15 and 3.16) and the more irregular inner UF_3 layer grow according to a parabolic rate law after an initially accelerated weight increase (see Fig. 3.2, 3.3 and 3.4). The reaction must, therefore, proceed by diffusion of one or more of the reactants across the layers, accompanied by the migration of electrons or positive holes. One of these transport processes may thus be assumed to be the rate controlling step.

The experiments carried out on UF_3 pellets at $690^\circ C$ gave a parabolic rate constant which agrees within experimental error with the overall rate of reaction found at the same temperature for the UF_4 pellets (see section 3.2.1). Transfer through the MgF_2 layer is, therefore, the rate controlling step of the overall reaction. A direct semi-quantitative proof of this is given on Plate 4.1 which shows the cross section of a UF_4 pellet used in a single time preliminary experiment.¹ In this plate the MgF_2 has a relatively uniform thickness, while the UF_3 layer is particularly irregular and varies in thickness. The MgF_2 is nonuniformly tinted with yellow

¹ The MgF_2 layer in this long duration single time run exfoliated before it could be weighed and the experiment is, therefore, not listed in Table 3.1.

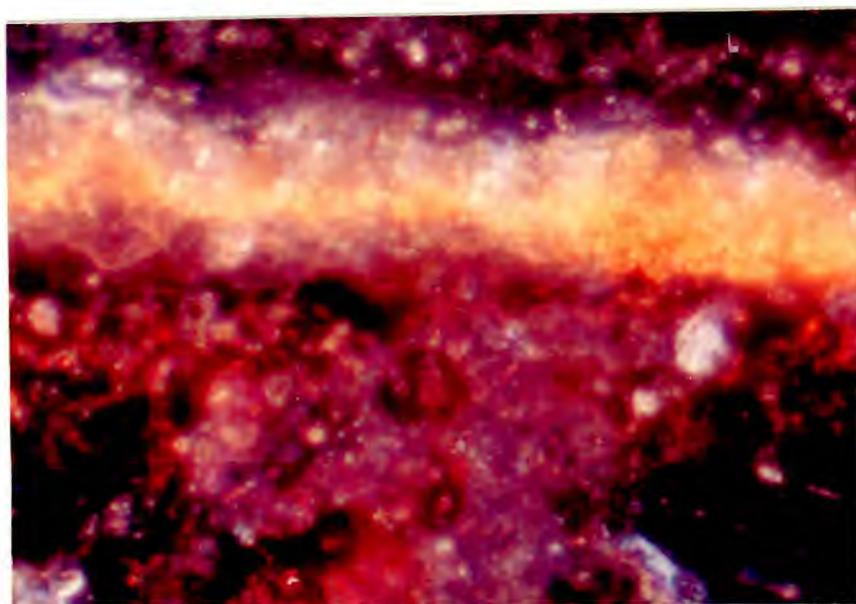


Plate 4.1 THE MgF_2 LAYER THICKNESS CONTROLS
THE OVERALL RATE OF REACTION

Note that a lower than average local thickness of the UF_3 layer corresponds to a greater amount of U metal produced (indicated by the deeper yellow colour), whereas the thickness of the MgF_2 layer is not affected.

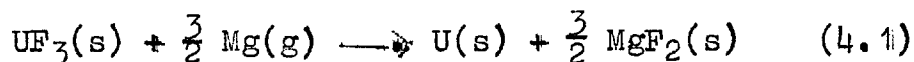
(x2400)

due to the oxidation of U to UO_2 , the deeper colour being found in the region where the UF_3 is thinner. Hence, the thickness of the UF_3 layer did not affect the total amount of MgF_2 produced, i.e. the overall rate of the reaction. Due to either a faster rate of reduction to U metal or a slower rate of reduction to UF_3 , there was a lower than average local yield of UF_3 and the production of a higher amount of uranium metal (indicated by the deeper yellow colour) so that the total amount of magnesium used up by the two reactions remained constant.

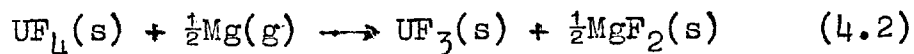
The partial reaction yielding U metal was also found to follow a parabolic rate law (see section 3.3.3); thus, the partial reaction yielding UF_3 must follow a similar rate law, as is seen to be the case from the plots in Fig. 3.5.a The rate controlling step for the production of UF_3 may thus be assumed to be a transport process across the UF_3 layer.

A rough check on the compatibility of the kinetic results can be made by measuring the average thickness of the layers. Taking for instance the pellet in run F.34 (Plate 3.4) the average thicknesses of the MgF_2 and UF_3 layers as measured under the microscope are roughly 12 and 28 μ respectively. The weight gain of the pellet in this run (see Table 3.2) was 1160 $\mu g cm^{-2}$ which

corresponds to $2970 \mu\text{g cm}^{-2}$ of MgF_2 . Taking an average value of 3.0 g cm^{-3} for the density of MgF_2 the corresponding thickness is 10μ . To this value the contribution of the uranium metal interspersed in the layer has to be added. In this particular case the uranium was not determined by oxidation, since the pellet was to be examined with the electron probe analyser, but an estimate can be made from Fig. 3.3 by interpolation. This gives a value of around $2980 \mu\text{g cm}^{-2}$ of U, which, with a density of 19.0 g/cm^3 , contributes 1.6μ to the thickness. Thus the total thickness of the outer layer should be $10 + 1.6 = 11.6 \mu$.¹ The difference between the total weight gain of the pellet, $1160 \mu\text{g cm}^{-2}$, and the amount of Mg used to produce U metal according to the equation



$460 \mu\text{g cm}^{-2}$, is equal to the amount of Mg used to produce UF_3 , $700 \mu\text{g cm}^{-2}$. The amount of UF_3 produced in the reaction:



is then $17000 \mu\text{g cm}^{-2}$.

1 These figures indicate that about 14% of the outer layer thickness is contributed by the uranium metal. It is, therefore, rather surprising that the uranium could not be detected by microscopic observation of cross sections in unoxidised pellets. A possible explanation is that the uranium is present as very fine globules and thin lamellae as the comparison of Plates 3.7 and 3.16 seems to suggest.

In selecting a value for the density of the UF_3 in the layer it has to be taken into account that this grows into the UF_4 and each mole of UF_3 takes the volume previously occupied by one mole of UF_4 if there is no shrinkage. The density of the UF_4 pellets is around 6.0 g cm^{-3} , which corresponds to a molar volume of $52.5 \text{ cm}^3 \text{ mole}^{-1}$. The density of the UF_3 would in that case be 5.6 g cm^{-3} , with a corresponding layer thickness of 30μ . If a density similar to that of the UF_3 pellets (i.e. 7.2 g cm^{-3}) is assumed for the layer, the corresponding thickness is 24μ . The measurement of the UF_3 layer thickness is necessarily inaccurate due to its irregularity, but the results seem to indicate that no considerable shrinkage of the UF_3 occurs.

4.1.2 The Initial Period of Reaction

In Figs. 3.2, 3.3 and 3.4 smoothed curves were drawn to represent the kinetics of the reaction in the initial stages.

The non-parabolic shape of reaction "isotherms" in the early stages has been frequently observed in the oxidation of metals and may be due to two causes. If the heat produced in the reaction is not lost sufficiently rapidly an increase in the temperature of the specimen takes place and the observed rate of reaction does not correspond to isothermal conditions. The other cause

for deviations from parabolic behaviour is a reaction mechanism different from the parabolic in the early stage of the reaction. For the oxidation of metals, this is the period where logarithmic and inverse logarithmic relationships predominate.

In the present case the initial period is extended over such a considerable length of time that the possibility of non-isothermal conditions is very unlikely. Points were taken from the smoothed curves and tested for a cubic and a logarithmic plot. Straight lines were obtained for the logarithmic plot and are shown in Fig. 4.1. The points selected for these plots are given in Table 4.1 and allow a more detailed analysis for the possibility of self-heating of the pellet.

As stated before, self heating occurs when the heat generated by the reaction is not lost (by radiation, conduction or convection) rapidly enough. As a first approximation and in order to consider the more unfavourable case it will be assumed that the heat losses are mainly due to radiation. In the temperature range $600^{\circ} - 690^{\circ}\text{C}$ the heat of reaction¹ is approximately -1.7 kcal/g of Mg.

¹ Reaction represented by equation (4.1) which is predominant in the initial period. If the contribution of reaction (4.2) were also considered, the total heat of reaction would be slightly higher.

TABLE 4.1 - VALUES FROM THE SMOOTHED INITIAL PERIOD CURVES

a. At 690°C

Time t min	$(\frac{\Delta W}{S})^2 \times 10^8$ g ² cm ⁻⁴	log t	$(\frac{\Delta W}{S})^2 \times 10^4$ g cm ⁻²	$\frac{\Delta m}{\Delta t} \times 10^6$ [‡] g cm ⁻² min ⁻¹
20	7.0	1.30	2.65	13.3
50	12.0	1.70	3.46	2.7
100	18.0	2.00	4.24	1.6
150	23.0	2.17	4.80	1.1
200	26.5	2.30	5.15	0.70
250	29.5	2.40	5.43	0.56
280	31.5	2.45	5.61	0.6

b. At 620°C

20	0.50	1.30	0.7	3.5
50	1.15	1.70	1.07	1.2
100	1.65	2.00	1.28	0.3
150	2.05	2.17	1.43	0.18
200	2.30	2.30	1.52	0.16
250	2.55	2.40	1.60	0.08
300	2.70	2.48	1.64	0.08
350	2.83	2.54	1.68	0.08
380	2.90	2.58	1.70	0.04

‡ Average rate of weight gain in the respective time interval.

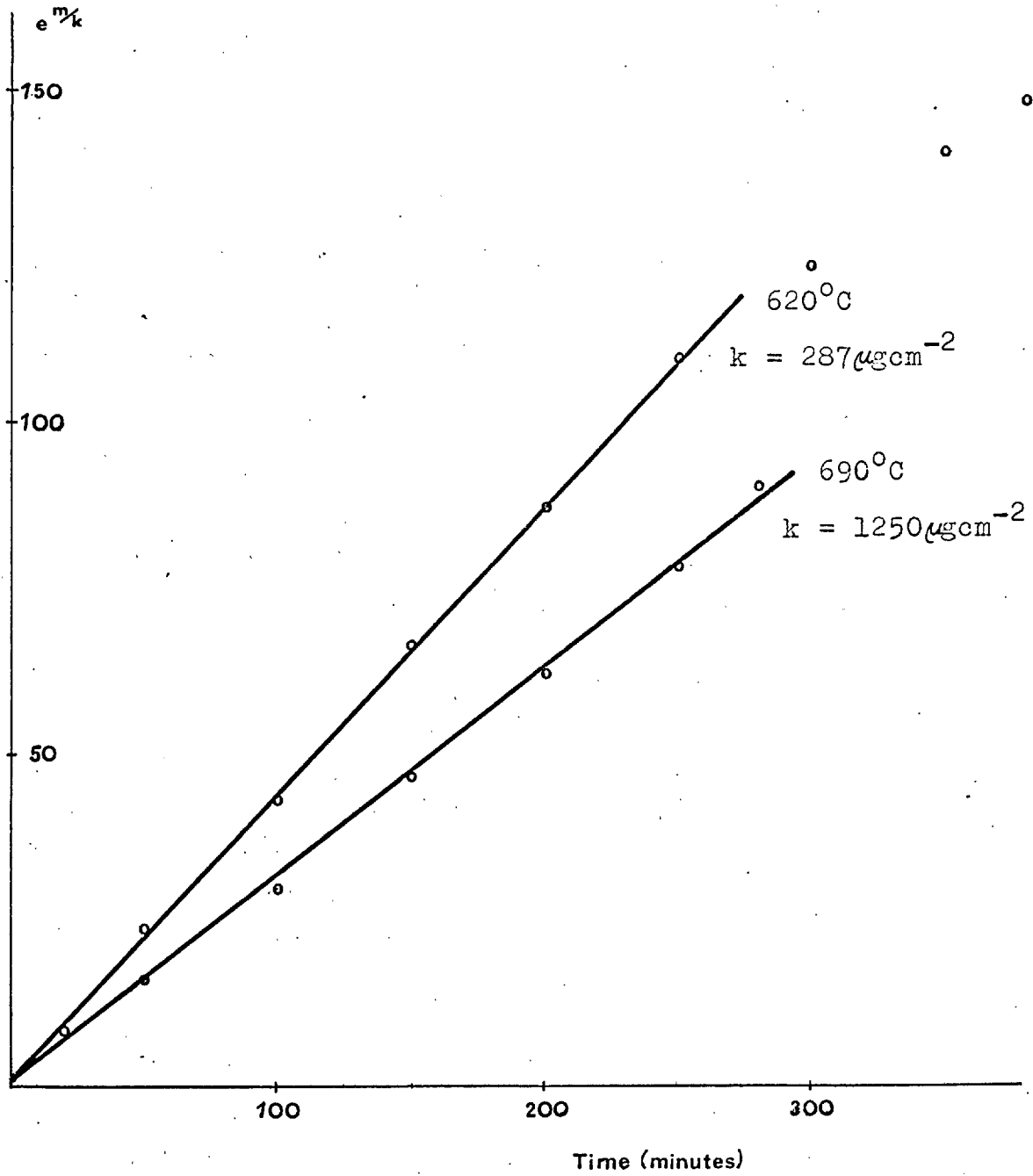


Fig.4.1: Check for Direct Logarithmic Relationship during the Initial Period

Hence, from the last column of Table 4.1, we may compute the rate of heat generation for the consecutive time intervals of the initial period. In the first 20 minutes of reaction the rate is 0.023 and 0.006 cal min^{-1} for 690°C and 620°C respectively.

The rate of energy emission of a grey body at temperature T_p surrounded by a medium at temperature T_s is given by the generalized Stefan-Boltzmann relationship:

$$\phi = \sigma \epsilon A (T_p^4 - T_s^4)$$

where ϕ = radiant flux defined as time rate of radiated energy (cal sec^{-1})

σ = Stefan-Boltzmann natural constant = 1.35×10^{-12}
 $\text{cal cm}^{-2} \text{ deg}^{-4} \text{ sec}^{-1}$

ϵ = emissivity, which can be taken in first approximation as equal to 0.8

A = surface area of the radiating body (cm^2)

For an average pellet of 0.8 cm^2 surface area we may thus write for the first 20 minutes of reaction at 690°C:

$$0.023 = 60 \times 1.35 \times 10^{-12} \times 0.8 \times 0.8 (T_p^4 - T_s^4)$$

or

$$T_p^4 - T_s^4 = 4.5 \times 10^8$$

The temperature T_s of the surroundings may be assumed constant and equal to 963°k. Thus $T_p = 963.2^\circ\text{k}$.

Self heating of the pellet may, therefore, be completely

ruled out. It is thus suggested that in the early stage of the reaction a mechanism different from the parabolic predominates. The weight gain vs. time curves obtained from the smoothed initial period curves suggest that a simple logarithmic relationship can probably describe the thickening of the layer in this initial period. (see discussion of mechanism in section 4.2.6).

4.2 Mechanism of the Reaction

4.2.1 Marker Experiments

The results of the marker experiments show that at 620° and 690°C the MgF₂ layer grows outwards whilst the UF₃ layer grows inwards. In fact, for the two first marker experiments where the gold film was condensed on the surface of the UF₄ pellet, the majority of the gold globules were found on the top of the MgF₂, though some globules could also be seen at the MgF₂/UF₃ interface, thus indicating that the UF₃ layer grows inwards. The outward movement of the markers must represent the true movement of the lattice, since they are too small to interfere with the diffusion and their movement cannot be explained by any mechanical effect. The last marker experiment has in fact shown that for markers several times larger there was no interference with the normal diffusion process when the markers were condensed on the MgF₂ layer. The gold globules found at the UF₃/MgF₂

interface must have been held by a surface tension effect or as a result of their being associated with the uranium formed in the initial period of the reaction.

As was mentioned in section 3.8, the presence of uranium particles on the top of the MgF_2 layer serves also as a marker experiment if it is assumed that the uranium metal is produced at the MgF_2/UF_3 interface. This seems reasonable since, as will be discussed in section 4.2.3, MgF_2 and UF_3 are not likely to form solid solutions.

Whatever the mechanism proposed for the formation of the balloons found in some preliminary experiments (see section 3.7), they must be formed in the initial stage of the reaction and the fact that they are found on the top of the layer is also a confirmation of the marker experiments.

Predominantly inward migration of the Mg^{2+} ions through the MgF_2 layer must, therefore, be assumed as the mechanism of growth of the layer. If outward migration of fluorine ions was assumed, the layer would lie above the markers and the uranium metal produced would be confined to the UF_3/MgF_2 interface unless it grew in filaments fed from the base, which is not the case (see section 4.2.3).

4.2.2 Mechanism of Migration through the MgF_2 Layer

From the above discussion, it is apparent that all the evidence strongly supports a predominant inward diffusion of Mg^{2+} ions through the MgF_2 layer. Moreover, the migration process through this layer is the rate controlling step for the overall reaction.

For a migration process to take place, there must be a chemical potential gradient. In the present case, the magnesium to fluorine ratio at the MgF_2 surface must be greater than at the UF_3/MgF_2 interface. Hence, there are necessarily deviations from the ideal integral stoichiometric composition of the fluoride and accordingly deviations from the strict order of the ideal lattice. The greater ratio of magnesium to fluorine at the surface does not necessarily mean that an excess of metal is present. A deficit of metal is also possible, as has been observed in the case of some oxide layers (e.g. wustite) growing on the respective metals. In these cases, the metal deficit at the metal/oxide interface is somewhat smaller than at the outer surface. The corresponding type of lattice defect is different for the two cases and was discussed in the Introduction (see section 1.4.3).

To date, no work has been reported in the literature on the type of lattice disorder in pure MgF_2 . It will be suggested here, taking into account the results of

the present work and partial evidence scattered in the literature, that the Frenkel type of disorder with an equivalent number of interstitial magnesium ions and vacancies is the most likely type of lattice disorder to be found in stoichiometric MgF_2 crystals and that an excess of metal is present in interstitial positions when the fluoride is exposed to magnesium vapour.

a. Lattice Disorder in the Alkali and Alkaline-earth Halides

Most of the experimental evidence, such as transport number, electrical conductivity and self-diffusion measurements, indicates that alkali halides favour predominantly a Schottky type of lattice disorder. Jost⁽⁷¹⁾ was the first to point out that, on theoretical grounds, for the formation of a Schottky defect the lattice energy is required in first place, but that part of this energy is regained owing to the relaxation and polarization around the vacant lattice site. Schottky⁽⁷²⁾ extended Jost's arguments and compared the heats of formation of Schottky and Frenkel defects, in particular of the alkali and silver halides. Since an interstitial ion is generally much closer to its neighbours than a normal ion the repulsive forces will favour Schottky as opposed to Frenkel disorder in the alkali halides, with the exception perhaps, of extreme cases like LiI , where the cation is

very small. For silver halides crystallizing in the alkali halide type of lattice the result, however, may be different. Here cationic Frenkel disorder is favoured not only due to the small radius of the Ag^+ , but also due to the large Van der Waals energies. The large contribution of the Van der Waals forces to the cohesive energy is demonstrated by the low solubility of these salts in water. The energy gained by the polarization of the water is not sufficient, in this case, to overcome the combined electrostatic and Van der Waals attractions in the solid.

The alkaline-earth halides, such as CaF_2 and SrF_2 , are also highly insoluble in water and this, together with a loose arrangement of the ions in the lattice, is an indication that a Frenkel type of disorder is to be expected. Ketelaar and Williams⁽⁷³⁾ and Zintl and Udgarð⁽⁷⁴⁾ have shown that fluorine ions occupy interstitial positions in SrF_2 and CaF_2 crystals when the fluoride of a higher valent metal is added in solid solution. Electrical conductivity and transference number measurements on pure and doped crystals have also shown that the predominant defect in CaF_2 ⁽⁷⁵⁾ and SrF_2 ⁽⁷⁶⁾ crystals is the anti-Frenkel disorder type involving equal concentrations of negative ion vacancies and negative ions interstitials.

As a first approximation, we may, therefore, conclude that the high insolubility of the MgF_2 and the small ionic radius of the Mg^{2+} ion is a fairly good evidence pointing to the presence of either of the two Frenkel types of disorder in the crystal lattice.

b. Structural Considerations

The crystal structure of the MgF_2 is usually described in terms of an ionic model of the rutile type. This structure may be described as formed of MgF_6 octahedra joined by edges and corners in such a way that each ion is shared by three neighbouring octahedra. The dimensions a and c and parameter x of the tetragonal unit cell were determined by Bauer⁽⁷⁷⁾ from X-ray data and are in close agreement with those determined by Duncanson and Stevenson⁽⁷⁸⁾ and Krishna Rao et al⁽⁷⁹⁾.

$$a = 4.625 \pm 0.002 \text{ \AA}$$

$$c = 3.052 \pm 0.003 \text{ \AA}$$

$$x = 0.303 \pm 0.001$$

The MgF_6 octahedra are not exactly regular and are characterized by:

4	Mg - F	distances of	1.997	$\overset{\circ}{\text{A}}$
2	Mg - F	" "	1.981	$\overset{\circ}{\text{A}}$
8	F - F	" "	2.814	$\overset{\circ}{\text{A}}$
2	F - F	" "	3.052	$\overset{\circ}{\text{A}}$
2	F - F	" "	2.576	$\overset{\circ}{\text{A}}$

As pointed out by Hurlen⁽⁸⁰⁾, in this type of structure the coupling of the octahedra results in parallel chains in which neighbouring octahedra have an edge in common. Two adjacent chains are joined to each other in such a way that the side corners in one chain become the top corners in the other chain. The direction of the chains coincides with the c-axis. This sort of arrangement defines open channels parallel to the c-axis containing a row of identical octahedral interstitial positions for the magnesium ions.

Along the channels every second octahedral hole is turned 90° around the c-axis and overlaps the previous hole. The dimensions of these interstitial F_6 octahedra are such that the formation of magnesium interstitials might cause an expansion of the lattice of only 13.2% along the c axis. The volume of a MgF_6 octahedron is about 10.37 \AA^3 , whereas the volume of an "interstitial" F_6 octahedron is about 11.66 \AA^3 . These considerations show, therefore, that the rutile structure contains favourable octahedral interstitial positions for the magnesium and on this basis it seems likely that the lattice disorder in MgF_2 crystals should be of the Frenkel type with equal concentrations of cation vacancies and cation interstitials.

c. Compounds with similar crystalline structure

The rutile type of structure is also formed by several of the transition metal dioxides and divalent metal fluorides. The most extensively studied compound of this group is TiO_2 , but the literature is particularly rich in contradictory experimental evidence. Hauffe⁽⁸¹⁾ reviewed the literature up to 1954 and concluded that the non-stoichiometry presented by this oxide which may vary between relatively wide limits (TiO_x with possibly $1.9 < x < 2.0$), is due to random removal of some of the oxygen atoms. Hurlen⁽⁸⁰⁾ took the opposite view and suggested that substantially better agreement with physical and crystallographic properties could be reached, if it is assumed that the defect structure is a combination of a non-stoichiometric and a stoichiometric one, both involving titanium interstitial ions. Wadseley⁽⁸²⁾ examined this problem taking into account more recent investigations, and advanced arguments in support of Hurlen's views, i.e. that interstitial octahedral holes are occupied by titanium ions.

d. Non-stoichiometry of MgF_2 in Presence of Mg Vapour

It is a well known fact that most of the alkali halides, when exposed to the respective metal vapour, become strongly visually coloured (darkening) due to the formation of the so called "F centers". It is well

established at the present time that the colouration obtained under these conditions is associated with the presence of an excess of metal ions in the lattice. Vacancies are then simultaneously introduced at the sites ordinarily reserved for the anions or interstitial positions become occupied. When these vacancies or other defects, as the case may be, trap electrons (or electron holes), F centers are produced.

In the case of alkaline earth halides this phenomenon is not well studied, but it was recently reported by Litcher and Bredig⁽⁸³⁾ that an excess of metal varying from 0.42 to 1.70 mole % at 1060° and 1265°C respectively, is present in Ca F₂ when it is exposed to Ca vapour. It is, therefore, reasonable to assume that an excess of metal is also present in the MgF₂ lattice when exposed to Mg vapour though to a lesser extent, as is suggested by the comparison of the systems Ca + CaCl₂ and Mg + MgCl₂ studied by Staffansson⁽⁸⁴⁾ and Rogers⁽⁸⁵⁾ respectively. From the discussion given in the previous sections, it is very likely that these excess metal ions occupy interstitial positions rather than create fluorine vacancies.

e. Proposed Migration Mechanism

All the evidence given seems to indicate that in the stoichiometric MgF₂ lattice an equivalent number of metal ion vacancies and interstitials coexist in equilibrium

and that, when exposed to magnesium vapour, a metal excess is present in the form of cations in interstitial positions and free electrons. This picture is in accord with the higher mobility of the Mg^{2+} ions suggested by the results of the present work. The most likely mechanism of migration through the MgF_2 layer is, therefore, one in which Mg^{2+} ions and free electrons move in to the UF_3/MgF_2 interface. The Mg^{2+} ions move either by an interstitial or a vacancy mechanism or both, depending on their relative mobilities.

4.2.3 Migration Mechanism Through the UF_3 Layer

Only indirect evidence is available as to the nature of the migrating species in the UF_3 layer.

The studies of D'Eye and Martin⁽⁸⁶⁾ on the system $UF_3 + BaF_2$ using differential thermal analysis, X-ray diffraction and density measurements, have shown that BaF_2 dissolves in solid UF_3 to the extent of about 20 mole %: The uranium and barium ions are randomly distributed over the normal cation sites while the anion lattice is incomplete. Further evidence for this vacancy mechanism is given, according to D'Eye and Martin, by considering the interatomic distances which show that the lattice is unlikely to accommodate interstitial cations. In the hexagonal unit cell of the uranium trifluoride there are two sets of anion lattice sites

which are not structurally equivalent. Thus, it is possible that the anion vacancies are not statistically distributed over all anion sites but are concentrated in either of the two positions.

If fluorine vacancies are also present in the lattice of pure UF_3 fluorine ions are likely to have a higher mobility than the uranium ions. There is at least one case (UO_2), where the mobility of the uranium ion was found to be very small as compared with that of the non-metal ion. Recent determinations in this laboratory⁽⁸⁷⁾ of the self diffusion coefficient of U in UO_2 gave a value of $10^{-15} \text{ cm}^2 \text{ sec}^{-1}$ at 1600°C . The self diffusion coefficient of oxygen in stoichiometric UO_2 has also been measured⁽⁹⁰⁾, but at lower temperatures, and for 780°C (maximum temperature of measurement) is $3.1 \times 10^{-12} \text{ cm}^2 \text{ sec}^{-1}$.

Some evidence is also obtained from the results of the present work pointing to a low mobility of the uranium ions in the UF_3 . Everywhere at the UF_3/MgF_2 interface, Mg^{2+} ions react with UF_3 to form MgF_2 and excess U^{3+} ions. If these U^{3+} ions were the predominant mobile species, they would tend to be captured by the already formed metallic nucleus at the interface which would be pushed outwards growing as a filament. Such a phenomenon has been observed in the case of the reduction

of silver sulphide by hydrogen⁽⁸⁸⁾ and was shown by Wagner⁽⁸⁹⁾ to be due to the high mobility of the silver ion in Ag_2S . In the present work no evidence was found of U filaments in the MgF_2 layer; on the contrary, all the observations indicate that uranium metal is present as small globules or thin lamellae (see for instance Plates 3.6, 3.9 and 3.15 and footnote on page 151). It is, therefore, suggested that fluorine ions migrate, possibly by a vacancy mechanism, and accompanied by electron holes, outwards through the UF_3 layer to combine with Mg^{2+} ions and electrons respectively, at the UF_3/MgF_2 interface.

4.2.4 Mechanism of Formation of Uranium Metal

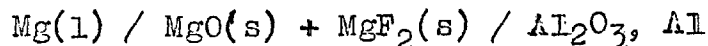
Uranium metal is most probably produced at the UF_3/MgF_2 interface. Observation of the surface of the UF_3 after the outer layer had been removed showed the presence of a brown powder, certainly UO_2 , resulting from the oxidation of the uranium when exposed to the atmosphere (see Plate 3.9). The formation of uranium everywhere in the MgF_2 layer would require the formation of a $\text{UF}_3 + \text{MgF}_2$ solid solution. Alkaline earth fluorides, such as CaF_2 , BaF_2 and SrF_2 , were found to take UF_4 and UF_3 into solid solution^(86, 91, 92) with the excess fluorine ions being accommodated interstitially. The $\text{MgF}_2 + \text{UF}_4$ system, however, did not show any solid solution on either side

of the diagram⁽⁹³⁾ and it is reasonable to assume that the same applies to the $MgF_2 + UF_3$ system. In a recent paper Thoma⁽⁹⁴⁾ reviewed the data available on binary alkali metal fluoride (MF) - metal fluoride ($M^{\text{II}}F$, $M^{\text{II}}F_2$, $M^{\text{II}}F_3$, $M^{\text{II}}F_4$) systems and showed that the number of complex compounds and the occurrence of solid solutions in these systems can be related to the value of the ratio of cation sizes $M^+/M^{\text{III}+}$. For binary mixtures of the alkali halides with the trifluorides of the rare earths and actinide elements, it is shown that simple eutectic systems without intermediate compounds, single intermediate compounds $MF.MF_3$ and congruent melting compounds $3MF.MF_3$ are formed when the cation radius ratio M^+/M^{3+} lies: below 0.67, between 0.77 and 1.40 and above 1.43 respectively. Limited data are available for the tetravalent rare earth and actinide metal fluoride systems, but for those already investigated a similar trend is observed. It is reasonable to assume that a similar rule applies for the alkaline earth metal fluoride (MF_2) - metal fluoride (MF_3 , MF_4) systems. The small ionic radius of Mg (0.65 Å) as compared with those of Ca (0.99), Sr (1.13) and Ba (1.35) would then account for the observed absence of solid solutions in the $MgF_2 - UF_4$ system and would support the hypothesis that no solid solutions also occur in the $MgF_2 - UF_3$ system. The X-ray powder patterns of the product layers in the present work (see Section 3.4) seem

also to confirm this hypothesis, since no systematic deviation of the lines was detected. Also, solid solution of UF_3 in MgF_2 would probably be accompanied by a coloration of the MgF_2 layer and no such coloration was observed for unoxidised pellets (see Plates 3.4 and 3.5). It is, therefore, suggested that everywhere at the UF_3/MgF_2 interface metallic uranium nuclei are formed which, due to the reduced mobility of the uranium ions, do not grow beyond a critical size. These metallic particles prevent the continuation of the reaction on the spot where they are formed and are eventually forced outwards by the MgF_2 growing beneath by lateral diffusion.

4.2.5 Wagner's Theory

No studies have been reported in the literature on the electrical conductivity of either UF_3 or MgF_2 . There is, however, some evidence that magnesium fluoride of stoichiometric composition is mainly an ionic conductor. Treadwell et al.⁽⁹⁵⁾ have determined the free energy of formation of solid MgO by setting up a cell of the type:



The values obtained in this way, between 637° and 727° , are in good agreement with, although slightly lower than, those calculated from thermodynamic data thus indicating that the electronic contribution to the current across

the solid electrolyte $\text{MgF}_2 + \text{MgO}$ is negligible. Since according to Treadwell et al., no solid solution occurs between MgO and MgF_2 at these temperatures and according to Schmalzried⁽⁹⁶⁾ MgO is mainly an ionic conductor, it is reasonable to infer that conduction through MgF_2 is also mainly ionic. In the actual conditions of growth of the MgF_2 layer, however, the electronic contribution may not be negligible and, if the electronic transport number approaches unity, the rate of the overall reaction will be determined by diffusion of Mg^{2+} ions across the layer. If the electronic transport number in these conditions is still very small (say, $< 10^{-4}$) the migration of electrons across the layer will be the rate determining step. For values between 10^{-4} and 1, both migration of Mg ions and electrons will determine the rate of growth.

According to Wagner (see Introduction) the rational rate constant k_r expressed in g. equivalents $\text{cm}^{-2} \text{sec}^{-1}$ is given by:

$$k_r = \frac{300}{96500eN} \int_{\mu_x}^{\mu_x''} (t_1 + t_2)t_3 \sigma \frac{d\mu_x}{|z_2|} \quad (4.3)$$

where the symbols have the meaning already given.

The constant k_r is defined by the equation:

$$\frac{dn}{dt} = k_r \frac{S}{x} \quad (4.4)$$

where n = number of g. equivalents of MgF_2 formed per sec.

t = time in seconds

S = surface area in cm^2

x = instantaneous thickness of the layer in cm.

The parabolic constant k_p in this work is defined by the equation

$$\frac{dm}{dt} = \frac{k_p}{2} \frac{1}{m} \quad (4.5)$$

where m -- grams of Mg reacted per cm^2

t = time in minutes

k_p = parabolic constant in $\text{g}^2 \text{cm}^4 \text{min}^{-1}$

Working out the two equations (4.4) and (4.5) one gets the following relationship between k_r and k_p :

$$k_r = \frac{k_p}{60p M_{\text{Mg}}}$$

where p = density of MgF_2 in $\text{g. cm}^{-3} = 3.0 \text{ g cm}^{-3}$

M_{Mg} = atomic weight of Mg.

The values for k_r are then:

$$k_{r620^\circ} = 4.1 \times 10^{-15} \text{ g. equiv. cm}^{-1} \text{ sec}^{-1}$$

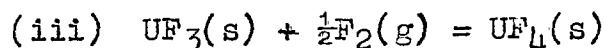
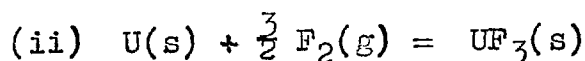
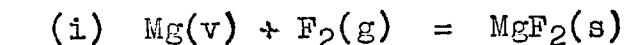
$$k_{r690^\circ} = 1.1 \times 10^{-13} \text{ g. equiv. cm}^{-1} \text{ sec}^{-1}$$

To apply equation 4.3 one must know the dependence of the electrical values under the integral on the metal to non-metal ratio and thus on the chemical potential of the non-metal. As a first approximation, however, one may take average values and equation (4.3) becomes:

$$k_r = \frac{300}{96500 \text{ Ne } |z_2|} (t_1 + t_2)t_3 \sigma \left(\frac{dX}{dt} - \frac{dX'}{dt} \right) \quad (4.6)$$

The electrical conductivity, σ , of MgF_2 has not been measured but a rough estimate can be made. Vorob'ev and Nakhodnova⁽⁹⁷⁾ have measured the electrical conductivities of polycrystalline pellets of oxides of Mg, Ca, Sr and Ba and chlorides and fluorides of Ca, Sr and Ba. According to Vorob'ev and Zavadovskaya⁽⁹⁸⁾ the physical properties (including electrical conductivity and its energy of activation) of these polycrystalline compacts are determined by the lattice energy of the crystal. Thus, it was found that, while the intrinsic electrical conductivity decreases, the activation energy of the current carriers increases with increasing lattice energy. Comparing their values for the different compounds and taking into account the different crystalline structure of MgF_2 , it was estimated that at 620°C the specific conductivity of polycrystalline MgF_2 is of the order of $10^{-7} \text{ ohm}^{-1} \text{ cm}^{-1}$ and at 690°C it is probably 3 times higher.

The activity of the fluorine at the layer interfaces is constant and determined by the equilibria:



at the MgF_2 surface, UF_3/MgF_2 and UF_4/UF_3 interfaces.

respectively. The respective fluorine activities calculated from the data assessed by Kubaschewski and Evans⁽⁹⁹⁾, and Rand and Kubaschewski⁽¹⁰⁰⁾ are listed in Table 4.2.

TABLE 4.2 - FLUORINE ACTIVITIES AT THE INTERFACES

Temp. °C	UF ₄ /UF ₃	UF ₃ /MgF ₂	MgF ₂ surface
620	10 ^{-45.3}	10 ^{-48.3}	10 ^{-56.6}
690	10 ^{-41.5}	10 ^{-44.3}	10 ^{-51.9}

Substituting values in equation (4.6) one gets:

TABLE 4.3 - VALUES OF $(t_1 + t_2)t_3$ from Equation 4.6

$\sigma_{620} \approx$ ohm ⁻¹ cm ⁻¹	$(t_1 + t_2)t_3$	
	620°C	690°C
10 ⁻⁶	5.4 x 10 ⁻⁴	5 x 10 ⁻³
10 ⁻⁷	5.4 x 10 ⁻³	5 x 10 ⁻²
10 ⁻⁸	5.4 x 10 ⁻²	5 x 10 ⁻¹

$\approx \sigma_{690}$ is assumed to be equal to 3 x σ_{620}

It is thus seen that at 690°C, at least, the electronic transport number t_3 may be substantial and that the temperature region studied is probably the one in which diffusion of Mg overtakes the electronic migration as the rate determining step.

Assuming that at these temperatures the transport number of electrons is already nearly unity, the self diffusion coefficient $D_1^{\#}$ of Mg may be computed from the equation (see Introduction):

$$k_r = c_{\text{eq}} \int_{a_x'}^{a_x''} \left(\frac{z_1}{|z_2|} D_1^{\#} \right) d \ln a_x \quad (4.7)$$

The values of $D_1^{\#}$ at the two temperatures are then:

$$D_1^{\#}{}_{620^{\circ}\text{C}} = 2.6 \times 10^{-15} \text{ cm}^2 \text{ sec}^{-1}$$

$$D_1^{\#}{}_{690^{\circ}\text{C}} = 7.5 \times 10^{-14} \text{ cm}^2 \text{ sec}^{-1}$$

which is the order of magnitude one should expect for the diffusion of the cation in ionic salts. For comparison the self diffusion coefficient of the cations, for the identical ratio melting point/temperature, in PbF_2 (fluorite structure), PbI_2 (CdI_2 structure), PbS (rock salt structure) and AgBr (rock salt structure) are of the order of magnitude of 10^{-15} , 10^{-14} and 10^{-11} and $10^{-9} \text{ cm}^2 \text{ sec}^{-1}$. More research would be needed to decide whether migration of ions or electrons or both are the rate determining step.

4.2.6 Mechanism of the Reaction in the Initial Period

As discussed in section 4.1.2, the shape of the smoothed curves for the initial reaction period can only be due to a mechanism of growth different from parabolic and it may probably be described by a direct logarithmic

relationship. Evans⁽³⁷⁾ has recently reviewed the main types of film growth laws and suggested the theoretical foundations of the various laws. There are at least three theoretical interpretations for the direct logarithmic law:

- (i) The reaction rate is controlled by electron transport instead of material transport. This is the case of very thin layers with thickness below 1000 Å.
- (ii) The migration occurs not through the lattice of the film substance but by pores which are mutually blocking.
- (iii) The effective area varies with the time either because at the base of the film cavities accumulate or perhaps due to the formation of particles of a different compound at the interface (a different oxide in the case of oxidation of alloys as is probably the case for the oxidation of iron-aluminium alloys⁽¹⁰¹⁾).

The thickness of the layers at the end of the initial period are far too large (around 4 μ and 1 μ at 690° and 620°C respectively) for its growth to be due to mechanism (i). Formation of cavities at the UF₃/MgF₂ interface is also unlikely since, if a vacancy mechanism is in fact

responsible for the migration of Mg^{2+} ions and F^- ions in the MgF_2 and UF_3 layers respectively, the vacancies would originate at the interface. Pore formation cannot be completely ruled out but the most likely explanation is the reduction of the effective area by the formation of thin uranium lamellae or globules at the UF_3/MgF_2 interface. In fact examination of Figs. 3.5a & 3.2 shows that in the initial period of the reaction a large amount (between 80 and 90%) of the Mg which reacts with the pellet is used to produce uranium. This is also supported by the presence of the relatively large uranium globules and lamellae on the top of the MgF_2 layer (see Plates 3.15 and 3.16). A switch over to the parabolic rate law would occur when a relative larger amount of Mg starts to be used to produce UF_3 and/or when the strain resultant from the outward growth of the MgF_2 layer is sufficient to detach the uranium particles from the UF_3 . A proof that the uranium particles formed initially do not become immediately detached from the interface and are in fact covered by a very thin layer of MgF_2 is given in Plate 4.2. The uranium particles on the top of the layer show different stages of oxidation, the more oxidised ones being nearer to the place where the layer was cracked, thus ceasing to protect the uranium from the attack of the atmosphere.

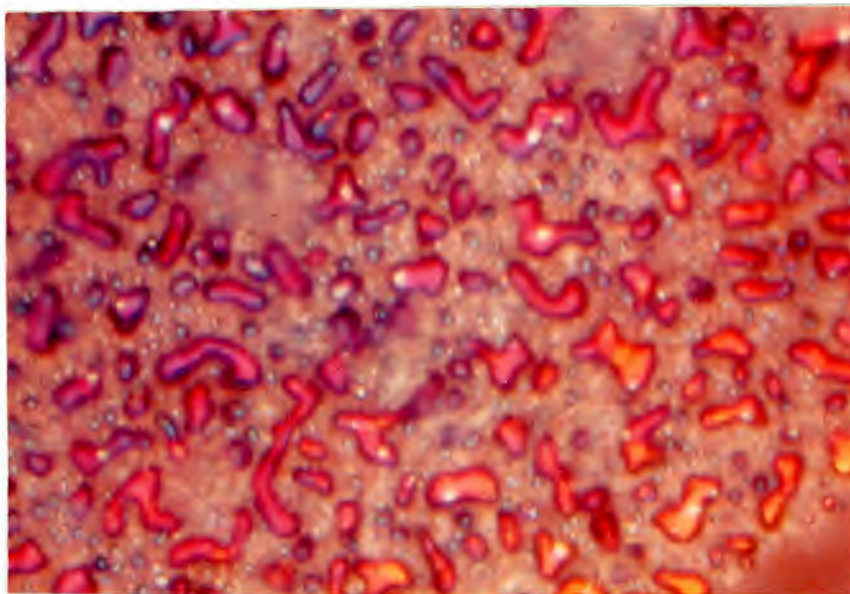


PLATE 4.2 THE MgF_2 LAYER PROTECTS THE U
PARTICLES ON THE TOP OF THE LAYER
 UF_3 pellet exposed to the atmosphere
for some hours after a crack (bottom
right hand corner) has been produced on
the MgF_2 layer. Note that the uranium
particles nearer the crack are more
oxidised than the others.
(1600x)

4.2.7 Activation Energy

The values of the activation energy taken from the measurements at two temperatures are necessarily very inaccurate since they would not take into account any change in slope of the plot $\log k$ vs. $1/T$. The activation energy for the overall reaction and for the partial reaction yielding UF_3 were computed and are 80 kcal and 123 kcal, respectively. These values are rather higher than those usually found for gas-solid reactions, such as oxidation of metals, though not unique. The parabolic rate constants for the oxidation of Cr and Co, for instance, have an activation energy of 79.0 and 65.5 kcal, respectively⁽³⁶⁾.

The activation energy for k_p is a very complex term with contributions from various sources and, since so little is known about the properties of the materials concerned, no attempt will be made towards its theoretical interpretation. It is perhaps worth mentioning that the unusual high value of 120 kcal found for the reaction producing UF_3 gives weight to the hypothesis of D'Eye⁽⁸⁶⁾ (see section 4.2.3) that anion vacancies in the UF_3 lattice are not randomly distributed over all the anion sites but concentrated in one of the two positions available. If in fact the mechanism of migration through the UF_3 is a vacancy mechanism, a very high activation

energy should be expected since only $\frac{1}{3}$, or $\frac{2}{3}$, as the case may be, of the anion sites would contribute to the migration of vacancies. The layer structure of the UF_3 would then permit only the migration of vacancies in planes parallel to the layers thus restricting their freedom of movement.

4.3 Preliminary Experiments

4.3.1 Single Time Experiments

In section 3.1 the scatter of the results in the preliminary experiments was discussed in some detail and was shown to have two possible causes (apart from condensation of magnesium which was prevented from run F.7 onwards):

(i) Initial hydrolysis of the UF_4 pellets by traces of moisture (demonstrated by the result of run F.17) and the consequent formation of a barrier of UO_2 between the UF_4 and the Mg vapour, would prevent or delay the initial period of accelerated weight gain found in the final experiments (see Figs. 3.2 and 3.3). The results would, therefore, be lower and scattered, depending on the extent of the hydrolysis, which in itself would produce a weight loss. Such a phenomenon is well illustrated by the result for the first reaction period of run F.8. The pellet was placed in the reaction chamber after three consecutive reaction periods had been carried out

for run F.7. The efficiency of the uranium getter was, therefore, considerably reduced and the weight increase of the pellet after 430 minutes of reaction was lower than that obtained for the first reaction period of run F.7 which lasted only 70 minutes.

(ii) A scatter would also be produced by partial or total oxidation to UO_2 of the U produced in the reaction, either on cooling (runs F.24 to F.28 and F.33) and/or during the reaction. The weight gains in this case would tend to be high. UO_2 formation is indicated by the yellow-brownish colour of the MgF_2 layer for the single time preliminary experiments.

A test for the plausibility of this interpretation is provided by a comparison between the results of experiments where oxidation occurred and those where it did not. The weight gains per unit area versus $\text{time}^{\frac{1}{2}}$ are shown in Fig. 3.5, for the final experiments (curves 2 and 2' for 690°C and 620°C , respectively). The dashed lines (curves 1 and 1') correspond to the total weight gains of the pellets when the uranium metal had been fully oxidised to UO_2 (see Table 3.6). The results for the F.24 to F.28 and F.33 runs where oxidation of uranium occurred on cooling are represented by open circles and lie between the curves 1 and 2, or very near them, except for one case (Run F.25) which lies below

curve 2. It is interesting to note that for run F.33 where full oxidation to UO_2 is likely to have occurred on cooling (see p.102), the point lies very near the curve 1, which is in good agreement with the final experiments. The curves 1' and 2' for the final experiments at $620^{\circ}C$ are also shown in Fig. 3.1 to allow comparison with the preliminary experiments. The results of the single time experiments¹ are randomly distributed either between curves 1' and 2' or below curve 2', but none are above 1', as would be expected from the interpretation given for the scatter of the results².

4.3.2 Consecutive Time Experiments

The non-reproducibility of the results for the consecutive time experiments is to be expected from the scatter in the weight gains for the first reaction periods as discussed in the previous section. There are, however, some other characteristics of these runs

1. The first reaction period of the consecutive time experiments may also be considered as a single time experiment.
2. One might expect some of the points for runs carried out at $630^{\circ}C$ and particularly for runs up to F.6 (where condensation of Mg occurred) to lie above curve b'. In fact this did not happen either to hydrolysis or to only partial oxidation of the uranium.

which merit some attention:

- (i) The overall rates of reaction are higher, even if allowance is made for the fact that in these experiments the uranium was probably fully oxidised to dioxide. This is seen by comparing the slopes of curves 3 and 4 with curve 1^p in Fig. 3.1.
- (ii) Discontinuities of slope occur in the parabolic curves (curves 3 and 4 in Fig. 3.1).
- (iii) Break away from parabolic behaviour takes place.
- (iv) The MgF_2 layer is convoluted.

As was suggested in section 3.1, the most likely explanation for characteristics (i) and (ii) is the breaking of the MgF_2 layer on heating and/or porosity of the layer during oxidation of the uranium metal which certainly produces strain and deformation in the MgF_2 (see below). Higher reaction rates and discontinuity of slope of the parabolic plots, though with a different origin, have been observed for the oxidation of metals, such as Cu⁽¹⁰²⁾ and Al⁽¹⁰³⁾ in the temperature range where the oxide scale is brittle and breaks periodically. Hence, the reaction which had become comparatively slow, becomes suddenly rapid at each break and the apparent rate of reaction is higher. If the weight gains are

very small and determined in a discontinuous way as in the present work, the parabolic plot will appear as a line with sudden changes of slope due to a variation of the average depth of the breaks in the outer layer.

There are at least two possible causes for the break away from parabolic behaviour, found in the consecutive time experiments, after a few reaction periods. In the first place, it may be due to deeper cracks produced in the outer layer on heating, when the thickness reached a critical value or its mechanical strength had been seriously affected by the presence of UO_2 in considerable amounts. On the other hand, the green to black crystalline powder found in runs F.7 and F.8 (see section 3.1) strongly suggests that U_3O_8 was formed as a result of serious deterioration of the purity of the argon after some consecutive reaction periods. It is difficult to ascertain whether the higher weight gain associated with the formation of U_3O_8 could alone explain the deviation from parabolic behaviour. The fact that the greatest amount of U_3O_8 was found near the edges of the pellet, where the strain in the layer, and, therefore, its tendency to crack, is likely to be higher, suggests that formation of U_3O_8 and breaking of the layer are actually associated.

The convolutions in the MgF_2 layer were found mainly in the consecutive time experiments and are illustrated in Plates 3.1 and 3.11. They bear a striking resemblance, though to a lesser extent, to the wrinkles produced in the MgF_2 by the oxidation of the U metal to U_3O_8 at 180°C , in the final experiments (see Plate 3.3). The gradual oxidation of the uranium to dioxide during the consecutive time experiments and the increase in volume which follows the oxidation, may thus have a similar effect, though to a smaller extent, creating strain in the MgF_2 layer which eventually is released by the formation of convolutions. Another possible cause of the convolutions would be the formation of blisters in the layer on cooling after each reaction period. Such blisters would reduce the effective area in the subsequent runs and a thinner MgF_2 layer should be expected in the region where they are formed. Observation of Plates 3.1 and 3.11, however, does not show any thinning of the layer and such a mechanism is, therefore, improbable.

4.3.3 Balloon Formation

The occurrence of balloons, mentioned in section 3.7.2, was observed only in the preliminary experiments and particularly in runs F.5 and F.6. This indicates that their formation is related to the deficient purification of the argon which was a common characteristic of these

runs. A possible mechanism for their occurrence is that, in the initial period of the reaction and when the MgF_2 layer was still insufficiently thick to protect the UF_3 underneath, hydrolysis of the trifluorides occurred with liberation of HF which blew up the balloons. The high plasticity required from the MgF_2 for such balloon formation could be obtained by a local increase in temperature resulting from the concomitant, highly exothermic oxidation of the uranium metal produced at the interface.

An alternative suggestion is that, on heating, some particles of Mg are condensed on the pellet and as a result of the reaction which follows become overheated and vaporised suddenly, thus blowing the balloons.

4.4 Powder Experiments

The experiments of Paine, Reuhle and Lewis⁽²⁰⁾ on the reduction of UF_4 powder by Mg vapour have already been mentioned in the Introduction. A detailed analysis of the experimental technique and results can now be given here.

A weighed amount (0.5 - 1.5 g.) of UF_4 powder was spread evenly over the bottom of a stainless steel boat which was fastened alongside a similar boat containing granular Mg. Both boats were covered with a stainless

steel cover, bent up at the centre, to give clearance for the Mg vapour to pass. The boats were placed in a flanged stainless steel furnace tube and heated to the reaction temperature under a helium atmosphere. The temperature differential between the ends of the boats varied from 25° at 580°C to 35° at 820°C. The amount of uranium produced in the reaction was determined at the end of each run, by forming uranium hydride, decomposing the hydride by heating, passing the liberated H₂ over hot copper oxide and collecting the water formed in a Nesbitt absorption bulb containing magnesium perchlorate. The amount of magnesium in the reacted sample was also determined by chemical analysis. In the majority of the runs there was no UF₄ left unreacted and the amount of magnesium which had not been required to produce the uranium found was equal to that required to reduce the remainder of the sample from the tetrafluoride. Only two or three runs were carried out, at each temperature, for different times. The % conversion to uranium metal, at each temperature, was assumed to be proportional to the reaction time. The rate of reaction expressed in percentage of U converted per hour was found to fit roughly the equation: $\log \text{rate} = \frac{3}{2} \log P + C$ where P = vapour pressure of Mg at the given temperature (in mm Hg)

C = constant

No theoretical interpretation was given for this equation.

Taking into account the results of the present work, some serious objections may be raised as to the quantitative value of these experiments:

- (i) The assumption of linear rate of reaction at each temperature is a very gross approximation not justified by the results of the present work.
- (ii) No attempt was made to determine the specific area of the powder which is an essential variable in determining the rate of reaction.
- (iii) The large temperature differential in the furnace would introduce a considerable error in the reaction temperature. Due to the high activation energy of the overall rate of reaction, this error is likely to affect considerably the determined rates of reaction.
- (iv) The results were rather scattered which may have been due either to any of the previous causes, or to the effect of the bed depth, as shown by the following results obtained at 705°C.

Duration	Determined	Calculated*	Sample Size
Hrs.	% U	% U	g
1.0	15.7	16	1.50
1.0	34.2	35	0.47
1.0	32.3	37	0.51
2.0	33.0	33	1.44
4.0	54.2	54	0.52

* From the analysis for Mg

Under these conditions the results have only qualitative value and the proposed relationship between the rate of reaction and the vapour pressures of Mg lacks any theoretical or experimental foundation.

4.5 Discussion of the Technological Process

The general aspects of the technological process for the production of uranium by magnesium reduction of uranium tetrafluoride were reviewed in the introduction. The main factors influencing the yield and the quality of uranium metal recovered are the ultimate reaction temperature and the viscosity of the slag. On this basis it is easy to understand the observed effects of such variables, as surface to volume ratio of the reactor, density of the charge, liner thickness and heating rate, since these all affect the ultimate temperature of the reaction in an obvious way. On the other hand, the effect

of impurities, such as UO_2F_2 , UO_2 and UO_3 , which were found to reduce the yield of uranium metal when present in relatively large amounts, may be explained in part by their occurrence in the products as unreduced compounds, but also by their effect on the viscosity of the slag. As pointed out by Bell⁽²¹⁾ the solubility of UO_2 in liquid MgF_2 is very small and any amount taken into solution at higher temperatures will precipitate on cooling and undoubtedly will increase the viscosity of the slag, which is most unfavourable for a good slag-metal separation. Even if the impurities are completely reduced to uranium metal, at the end of the process, a corresponding amount of MgO will be produced. Small additions of MgO to the molten slag may be advantageous since it may lower the melting point of the MgF_2 by as much as 40°C for the eutetic composition of about 5.5 wt. % of MgO ⁽¹⁰⁴⁾. Beyond this composition, however, complete fusion is not attained even at 1700°C and the presence of solid MgO in the slag will increase its viscosity. Some impurities, such as UO_2F_2 and UO_3 may be advantageous from the point of view of the ultimate temperature of reaction, since their reduction by magnesium is almost twice as exothermic as the reduction of UF_4 . The addition of UO_2F_2 and UO_3 , however, should not be overdone, since too much heat can lead to blow outs and also, because of the deleterious effect on the viscosity already mentioned.

The effect of an excess of Mg on the yield may probably be explained on the grounds that up to a certain extent it increases the availability of magnesium vapour at high pressure all over the charge, thus possibly increasing the rate of reaction of the UF_4 and the % conversion of the impurities to uranium metal. Above a certain limit, these advantages are lost due to the adsorption of the considerable amount of heat required to vaporize the Mg, thus lowering the ultimate temperature of the reaction.

Evidence has been given by several authors that, as a result of secondary reactions, the following products are produced during the pre-ignition period:

- (i) H_2 and MgO , as a result of the oxidation of magnesium by moisture probably at temperatures below $500^\circ C$.
- (ii) HF and UO_2 , either due to a cyclic process of the type discussed in the introduction or to the hydrolysis of UF_4 .

1. In the preliminary experiments, it was found that the reaction between Mg and water vapour in the argon was extremely slow at temperatures up to $600^\circ C$ and it is therefore considered more likely that the hydrogen is produced by the series of reactions discussed on page 14.

(iii) MgF_2 films on the Mg, due to the reaction with HF liberated by other secondary reactions.

(iv) UF_3 and MgF_2 , due to the reaction of Mg vapour with UF_4 .

The effect of the formation of UO_2 on the efficiency of the process has already been discussed, but it may also have other effects when produced by hydrolysis. The observation by Milosavljevich and Baird⁽¹²⁾ that brown colouration starts to occur in the charge at 350°C , suggests that this is the temperature at which hydrolysis starts. Similar observations were made during the development stage of the present work. Since reduction by magnesium vapour occurs only at higher temperatures, the formation of thin films of UO_2 on the UF_4 particles may delay, though not prevent, the onset of the reduction, as the results of the preliminary experiments in this work demonstrated. The result may be an increase in the ignition time with a consequently greater amount of undesirable UO_2 formation. Harper and Williams⁽¹¹⁾ have, in fact, observed that whenever the charge was held at temperatures between 400°C and the ignition temperature for more than 30 minutes, poor yields were obtained due to the formation of beads of uranium embedded in a matrix of brown slag. The brown colour is certainly due to the presence of UO_2 which increased the viscosity of the

slag on cooling, thus preventing the agglomeration of the uranium globules as was suggested by Harper and Williams. However, other causes could also have contributed to this result. Thus, the fact that the charge is held for long periods in the region of temperature where the reduction of UF_4 by Mg vapour may occur, will certainly result in the formation of UF_3 and uranium globules interspersed in the MgF_2 , as was demonstrated in the present work. The reduction of UF_3 being less exothermic than the direct reduction of UF_4 gives rise to a lower ultimate temperature and consequently poorer slag/metal separation. This is confirmed by the fact that on adding UF_3 to the charge in percentages above 5 wt. %, poor yields were generally obtained. The fine globules of uranium interspersed in the MgF_2 , produced in the pre-ignition period, will not then be able to collect due both to a lower ultimate temperature and the higher viscosity of the slag, due to the UO_2 . The amount of uranium globules trapped in the slag should then increase with longer pre-ignition periods, and this was also observed by Harper and Williams.

It follows from this analysis that for improved recovery and quality of uranium the rate of heating of the reaction vessel between $400^\circ C$ and ignition should be increased to the maximum compatible with a reasonably uniform distribution of temperature within the charge, so that the extent to which the Mg vapour reacts with the

UF₄ and the possibility of the formation of UO₂ by hydrolysis is reduced to a minimum.

As mentioned in the introduction there are still doubts as to whether the ignition is started off by the magnesium vapour - UF₄ solid reaction. A possible way to tackle the problem would be to check whether the kinetics of the reaction alone can account for the sudden ignition of the charge in the bomb reduction.

Considering one particle of UF₄ of mass W and surface area S undergoing reaction with Mg vapour, the differential equation governing the temperature as a function of time can be written in first approximation as follows:

$$C_p W \frac{dT}{dt} = - X S (T - T_0) + Q S \frac{dm}{dt}$$

where C_p = heat capacity of UF₄

W = mass of the particle of UF₄

X = heat transfer coefficient

S = surface area of the particle

T₀ = temperature of the surroundings

Q = heat of the reaction expressed as a function of the weight of Mg which reacted with the particle

m = weight of Mg reacted with the pellet per unit area.

Since the temperature of the surroundings for a particle of UF₄ inside the bomb is not very different from that

of the particle itself the equation may be written:

$$C_p W \frac{dT}{dt} = Q S \frac{dm}{dt}$$

In the small bombs, the ignition usually takes place in about 30 minutes and therefore the kinetic law which applies is that of the initial period:

$$m = k \ln at$$

By substituting in the equation above and taking into account that $k = k_0 e^{-\frac{E}{RT}}$, the following differential equation is obtained:

$$e^{-\frac{E}{RT}} dT = \frac{Q S k_0}{C_p W} \frac{dt}{t}$$

The solution of this equation requires numerical methods, and no attempt for its integration will be made here.

It will only be mentioned that for the conditions of auto-ignition to occur the second derivation $\frac{d^2T}{dt^2}$ should be positive. Calculations have shown that such a condition is met at 580°C when the specific area of the particle is higher than $30 \text{ cm}^2 \text{ g}^{-1}$, which is a condition very likely to be observed in practice. As a term of comparison, the specific area of a spherical UF_4 particle of 0.1 mm diameter is around $100 \text{ cm}^2 \text{ g}^{-1}$.

An analysis on the lines suggested above, or in the more refined way recently reported by Jacobs and Kureisky (105), could be useful for clarifying this question, though more experimental data would be needed.

4.5 Summary

The reduction of uranium tetrafluoride by magnesium vapour at 620°C and 690°C proceeds through the formation of the trifluoride which concomitantly is reduced to uranium metal. Two coherent product layers are formed on the surface of the UF_4 . Marker experiments and other evidence shows that the outer layer (MgF_2) grows outwards by the inward migration of Mg^{2+} ions while the inner layer (UF_3) grows inwards into the UF_4 , probably by outward migration of fluorine ions. Uranium metal is at the same time produced at the UF_3/MgF_2 interface as very fine globules or thin lamellae. The rate determining step of the overall reaction is the migration through the MgF_2 layer. Both layers grow according to a parabolic rate law after an initial period of reaction which varies between 280 min and 380 min at 690°C and 620°C respectively, where a different rate law is observed.

The parabolic constants for the overall reaction are 1.8×10^{-11} and $4.75 \times 10^{-10} \text{ g}^2 \text{ of Mg cm}^{-4} \text{ min}^{-1}$ at 620° and 690°C respectively. The parabolic constants for the partial reaction yielding UF_3 are 6.7×10^{-13} and $1.1 \times 10^{-10} \text{ g}^2 \text{ cm}^{-4} \text{ min}^{-1}$. The accuracy of the results in the initial period does not allow one to ascertain the type of rate laws followed but the smooth curves fit a direct logarithmic relationship very well. Such a rate law would be accounted for by the decrease in the effective area which results

from the formation of uranium at the interface.

From the evidence obtained in this work and in the literature it was suggested that the more likely type of lattice disorder to be found in the rutile structure of the MgF_2 is the cationic Frenkel disorder with an equal concentration of cation interstitials and vacancies. From Wagner's equation for the parabolic growth of a coherent layer an estimation was made for the transport number of the electrons across the MgF_2 layer. It was found that at 690°C at least, it is very likely that the transport number of the electrons is sufficiently high for the migration of the electrons to cease to be the rate determining step.

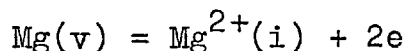
4.6 Suggestions for Further Work

From the results obtained in the present work it is suggested that any further research on the kinetics of the reduction of UF_4 by Mg vapour should be carried out along the following lines:

- (i) The kinetic studies should be extended to higher temperatures in order to determine whether the same rate laws still apply and to determine with higher accuracy the values for the activation energies.
- (ii) Further studies should be made on the mechanism of migration through the UF_3 and MgF_2 layers under

the actual conditions of the reaction.

- (iii) The influence of the vapour pressure of magnesium on the rate of reaction should be determined. If the proposed mechanism of excess magnesium being introduced in the MgF_2 lattice in interstitial sites is valid, the following equilibrium should take place:



If other disorder equilibria are negligible, then the concentration of electrons is twice that of the $\text{Mg}^{2+}(i)$ interstitials: $C_e = 2 C_{\text{Mg}^{2+}(i)}$, and using the ideal mass action law one obtains:

$$C_e^2 \cdot C_{\text{Mg}^{2+}(i)} / P_{\text{Mg}} = \text{const.}$$

Hence,

$$C_e = 2 C_{\text{Mg}^{2+}(i)} = \text{const.} P_{\text{Mg}}^{1/3}$$

i.e., the rate of the reaction should be proportional to the cube root of the magnesium pressure.

APPENDIX I

CONTRIBUTION TO THE STUDY OF THE REDUCTION
OF URANIUM HEXAFLUORIDE BY SODIUM

I.1. Introduction

The successful development of atomic energy, during the last war, led to the establishment of vast industrial complexes to produce plutonium and uranium - 235. The operations included in these industrial complexes are:

- (i) Exploration, mining and milling operations, which produce the raw materials.
- (ii) Feed materials operations, which lead to the production of uranium metal and uranium hexafluoride by reduction and fluorination of the uranium tetrafluoride, respectively,
- (iii) Nuclear reactor and isotope-separation operations, in which plutonium is produced from the U metal and U_{235} from the UF_6 , respectively.

From this simplified scheme, it is apparent that practically all isotopically enriched uranium is initially in the form of UF_6 which must be chemically converted to UO_2 or to uranium metal.

The production of enriched compounds does not differ chemically from that of normal assay uranium. The most widely used procedure consists of continuously reducing the UF_6 to UF_4 with hydrogen, and converting, in a batch operation, the UF_4 to uranium.

The development of a continuous process for direct reduction to uranium could, therefore, bring significant economic advantages. Other possible uses would be the recovery of uranium from tails of the gaseous diffusion isotope separation and from the product of the volatility fuel process scheme[⊠], which is UF₆. The choice of sodium metal as a reducing agent seems to be, potentially, the best. It would be economical and easy to handle from the engineering standpoint because of its low transformation temperatures, low melting slag (NaF) and high slag solubility in water.

I.2. Thermodynamic Considerations

I.2.1. Thermochemical Data

In the following Tables I.1, I.2 and I.3, the more reliable thermochemical data reported in the literature, up to 1960, are listed for the compounds and elements of interest in this work.

[⊠] Fuel elements in a reactor, require metallurgical reprocessing after only part of the fuel material has been consumed. The reasons for this reprocessing include change in thermal properties, lowered reactivity of the reactor due to depletion of the fuel element and poisoning, damage to the fuel element by corrosion, by dimensional changes or by mechanical failure, etc.

The following symbols are used:

C_p	molar heat capacity
G	free energy
ΔG	free energy of reaction
H	heat content
H	heat of reaction
L_e, f, s, t	molar latent heat of evaporation, fusion, sublimation or transformation
S	entropy
ΔS	entropy of reaction
σ_e	molar entropy of evaporation
T	absolute temperature
(sol)	solid state
(liq)	liquid state
(g)	gaseous state

Values enclosed in parentheses are estimated and were taken from Glassner.⁽¹⁰⁶⁾ After this work had been carried out, Rand and Kubaschewski⁽¹⁰⁰⁾ published an assessment of the thermochemical data of uranium compounds; therefore no discussion will be given here of the values encountered in the literature. The values selected in this work do not differ greatly from those proposed by Kubaschewski and Rand, and in their majority are well within the limits of error indicated by these authors. In Table I.1 the limits of uncertainty given

were estimated either to include the majority of the experimental data available in each case, or to represent the upper limit of error to be reasonably expected from the particular method of obtaining the data.

TABLE I.1 HEATS OF FORMATION, STANDARD ENTROPIES AND STANDARD FREE ENERGIES OF FORMATION

Substances	H_{298}° Kcal	S_{298}° e.u.	$-\Delta G_{298}^{\circ}$ Kcal
$F_2(g)$	0	48.5 ± 0.1	0
Na(sol)	0	12.2 ± 0.1	0
NaF(sol)	136.0 ± 0.5	13.1 ± 0.6	129.0 ± 0.7
U(α)	0	12.0 ± 0.1	0
$UF_3(sol)$	340 ± 10	(26 ± 4)	322 ± 12
$UF_4(sol)$	443 ± 5	36.5 ± 0.5	421 ± 6
$UF_5(sol)$	488 ± 8	(48 ± 8)	462 ± 10
$UF_6(g)$	504 ± 6	90.3 ± 0.2	484 ± 6

TABLE I.2 DATA ON TRANSFORMATION, FUSION AND
EVAPORATION

Substance	M.p.	L_f Kcal/mole	B.p. $^{\circ}k$	e Kcal/mole	Remarks
Na(sol)	371	0.62	1187	19.7	
NaF(sol)	1269	7.8	1977	24.3	
U(α)	936 [⊗]	0.69 [⊗]	-	-	⊗ U(α) \rightarrow U(β)
U(β)	1043 [⊗]	1.15 [⊗]	-	-	⊗ U(β) \rightarrow U(δ)
U(δ)	1403	(4.7)	4200	24.0	
UF ₃	(1700)	(8.5)	(2550)	(24)	
UF ₄	1309	(14)	1690	30.7	
UF ₅	(560)	(7)	(800)	(22.5)	
UF ₆	337.2	4.57	330 [⊗]	34.9	⊗ sublimation

TABLE I.3 HEAT CAPACITIES

$$C_p = a + bT + cT^{-2} + dT^2 \text{ cal mole}^{-1} \text{ deg}^{-1}$$

Substance	C_p at 298°K cal. deg. ⁻¹ mole ⁻¹	a	b x 10 ³	c x 10 ⁻⁵	d x 10 ⁶	Temp. range °K
F ₂ (g)	8.33	8.29	0.44	-0.80	-	298-2000
Na (sol)	6.806	9.936	-28.05	-	57.88	298-371
Na (liq)	-	8.958	-4.579	-	2.541	371-1187
Na (g)	-	4.968	-	-	-	1187-
NaF(sol)	11.00	9.66	4.50	-	-	298-1268
NaF(liq)	-	16.0	-	-	-	1268-1977
NaF(g)	-	(8.9)	-	-	-	1977-
U (α)	6.7	3.15	8.44	0.80	-	298-936
U (β)	-	10.38	-	-	-	936-1043
U (γ)	-	9.10	-	-	-	1043-1403
U (liq)	-	(8.99)	-	-	-	1403-
UF ₃ (sol)	(22.2)	(20.1)	(7.1)	-	-	298-1700
UF ₃ (liq)	-	(34.0)	-	-	-	1700-2550
UF ₄ (sol)	27.7	25.3	7.98	-	-	298-1309
UF ₄ (liq)	-	(41)	-	-	-	1309-1690
UF ₅ (sol)	(34.6)	(31.9)	(9.0)	-	-	298-560
UF ₅ (liq)	-	(43.97)	-	-	-	560-800
UF ₅ (gas)	-	(19.9)	(10.0)	-	-	800-
UF ₆ (sol)	39.9	20.082	161.2	10.47	-	298-330
UF ₆ (g)	31.2	32.43	7.936	-3.207	-	298-1000

I.2.2 Standard Free Energies of Formation

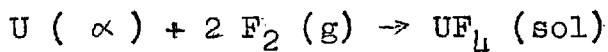
From the data listed in Tables I.1, I.2 and I.3, the Standard Energies of Formation of the different compounds were calculated as a function of temperature, using the well known equations:

$$H_T^{\circ} = H_{298}^{\circ} + \int_{298}^T C_p \, dT$$

$$S_T^{\circ} = S_{298}^{\circ} + \int_{298}^T \frac{C_p}{T} \, dT$$

$$G_T^{\circ} = H_T^{\circ} - T S_T^{\circ}$$

For a reaction of formation like:



the corresponding values for the heat, entropy and free energy of reaction, denoted by ΔH , ΔS and ΔG , may be obtained by taking the difference:

$$\Delta H = \sum H (\text{products}) - \sum H (\text{reactants}) \quad (I.1)$$

and

$$\Delta H_T^{\circ} = \Delta H_{298}^{\circ} + \int_{298}^T \Delta C_p \, dT$$

$$\Delta S_T^{\circ} = \Delta S_{298}^{\circ} + \int_{298}^T \frac{\Delta C_p}{T} \, dT$$

$$\Delta G_T^{\circ} = \Delta H_T^{\circ} - T \Delta S_T^{\circ}$$

where ΔC_p is the change in molar heat capacity for the reaction and is obtained by an equation similar to (I.1).

TABLE I.4. - FREE ENERGY EXPRESSIONS

$$\Delta G^{\circ} = A + BT \ln T + (C \times 10^{-3})T^2 + (D \times 10^{-6})T^3 + (E \times 10^5)T^{-1} + FT \text{ Cal/mole}$$

Reaction	A	B	C	D	E	F	Temp. Range °K
$U(\alpha) + 3F_2(g) \rightarrow UF_6(g)$	-505800	-4.41	0.91	-	0.805	97.14	298-936
$U(\beta) + 3F_2(g) \rightarrow UF_6(g)$	-501700	2.82	-3.308	-	0.403	47.30	936-1043
$U(\gamma) + 3F_2(g) \rightarrow UF_6(g)$	-503000	1.54	-3.308	-	0.403	57.42	1043-1403
$U(liq) + 3F_2 \rightarrow UF_6(g)$	-503200	1.43	-3.308	-	0.403	58.44	1403-
$U(\alpha) + 2F_2(g) \rightarrow UF_4(sol)$	-444300	-5.57	0.67	-	-0.40	108.4	298-936
$U(\beta) + 2F_2(g) \rightarrow UF_4(sol)$	-441900	+1.60	-3.55	-	-0.80	59.5	936-1043
$U(\gamma) + 2F_2(g) \rightarrow UF_4(sol)$	-444300	+0.38	-3.55	-	-0.80	70.36	1043-1309
$U(\gamma) + 2F_2(g) \rightarrow UF_4(liq)$	-444200	-15.3	0.44	-	-0.80	178.2	1309-1403
$U(liq) + 2F_2(g) \rightarrow UF_4(liq)$	-449100	-15.4	0.44	-	-0.80	182.3	1403-1690
$U(liq) + 2F_2(g) \rightarrow UF_4(g)$	-396480	-18.4	0.44	-	-0.80	173.5	1690-
$Na(s) + \frac{1}{2}F_2(g) \rightarrow NaF(sol)$	-135500	4.415	-16.16	9.64	-0.20	0.71	298-371
$Na(liq) + \frac{1}{2}F_2(g) \rightarrow NaF(sol)$	-135800	3.438	-4.429	0.423	0.423	3.93	371-1187
$Na(g) + \frac{1}{2}F_2(g) \rightarrow NaF(sol)$	-162100	-0.552	-2.14	-	-0.20	51.35	1187-1268
$Na(g) + \frac{1}{2}F_2(g) \rightarrow NaF(liq)$	-158740	-6.90	0.11	-	-0.20	91.51	1268-1977

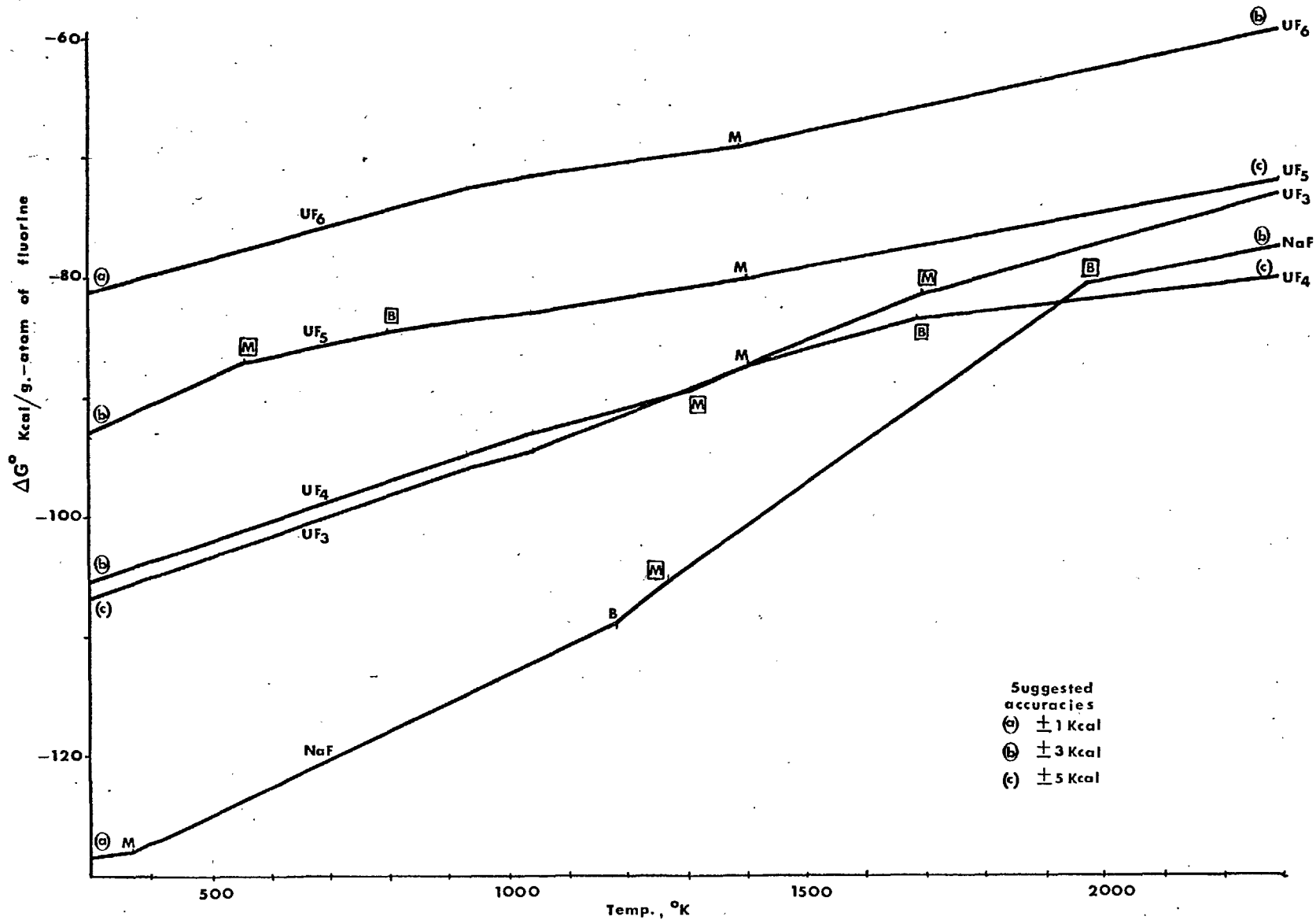


Fig. I.1 - Standard Free Energy of Formation of Fluorides vs. Temperature

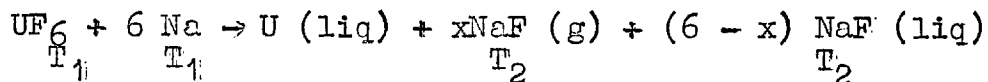
In Table I.4, the results of these calculations have been summarized. Since for the compounds UF_3 and UF_5 , most of the data are estimated, their accuracy does not warrant fresh calculations. The equations proposed by Glassner⁽¹⁰⁶⁾ were used and are not listed here. Values of the Free Energies of Formation in Kilocalories per gram atom of fluorine as a function of temperature have been plotted in Fig. I.1. The advantages of this type of plot have been discussed by Kellogg⁽¹⁰⁷⁾. In this graph the symbols M for melting point and B for boiling point of the elements were used. The same symbols enclosed in a square were employed for the compounds.

I.2.3 Heat of Reaction and Adiabatic Reaction Temperature

The temperature of the reaction products immediately after reaction is, in practice, a function of the proportion of the reactants, the initial temperature of the reactants and the energy exchanges with the surroundings, during reaction. In the ideal case of an energetically isolated (adiabatic) system, the temperature attained by the reaction products is called the "adiabatic reaction temperature".

For the reduction of UF_6 with a stoichiometric amount of sodium, the adiabatic reaction temperature was

calculated to be 1977°K (b.p. of NaF), even for an initial reactants temperature of 298°K, so that if we consider the reaction:



where: T_1 - reactants temperature in °K

$T_2 = 1977^\circ\text{K}$ - products temperature

x - moles of NaF vapour formed per mole of uranium produced

the percentage of NaF vapour in the products can be calculated as a function of the reactants temperature, using the data given in Section I.2. The results of these calculations are given in Table I.5 together with the heat of reaction at the different temperatures.

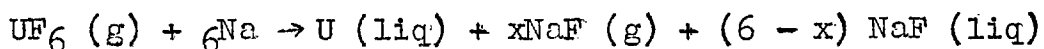
In Fig. I.2, the percentage of vaporized NaF in the products is plotted versus the reactants temperature. Discontinuities in the graph correspond to the transformation points of the different substances involved. These substances and their physical state are also indicated in the graph.

I.2.4 Intermediate Condensed Phases

Assuming that the overall reaction $\text{UF}_6 + 6\text{Na} \rightarrow \text{U} + 6\text{NaF}$ may be represented as composed of successive reduction steps through the intermediate fluorides down to uranium metal, it is of interest to know the nature of the

TABLE I.5 HEAT OF REACTION AND ADIABATIC REACTION

TEMPERATURE FOR THE REACTION:



Temp. of reactants, T_1 °K	Heat of reaction H_{T_1} kcal	x	Adiabatic React. Temp. T_2 °K
298	-312.0	1.87	1977
371 Na (sol)	-312.1	1.98	1977
371 Na (liq)	-315.9	2.04	1977
500	-315.8	2.23	1977
936 U (α)	-312.9	2.89	1977
936 U (β)	-313.8	2.91	1977
1000	-313.0	3.01	1977
1043 U (β)	-312.5	3.06	1977
1043 U (γ)	-311.3	3.07	1977
1187 Na (liq)	-310.5	3.31	1977
1187 Na (g)	-450.9	5.95	1977
1200	-450.3	5.96	1977
1268 NaF (sol)	-448.4	6.00	2022
1268 NaF (liq)	-401.6	6.00	2022
1403 U (γ)	-397.2	6.00	2179
1403 U (liq)	-392.4	6.00	2179

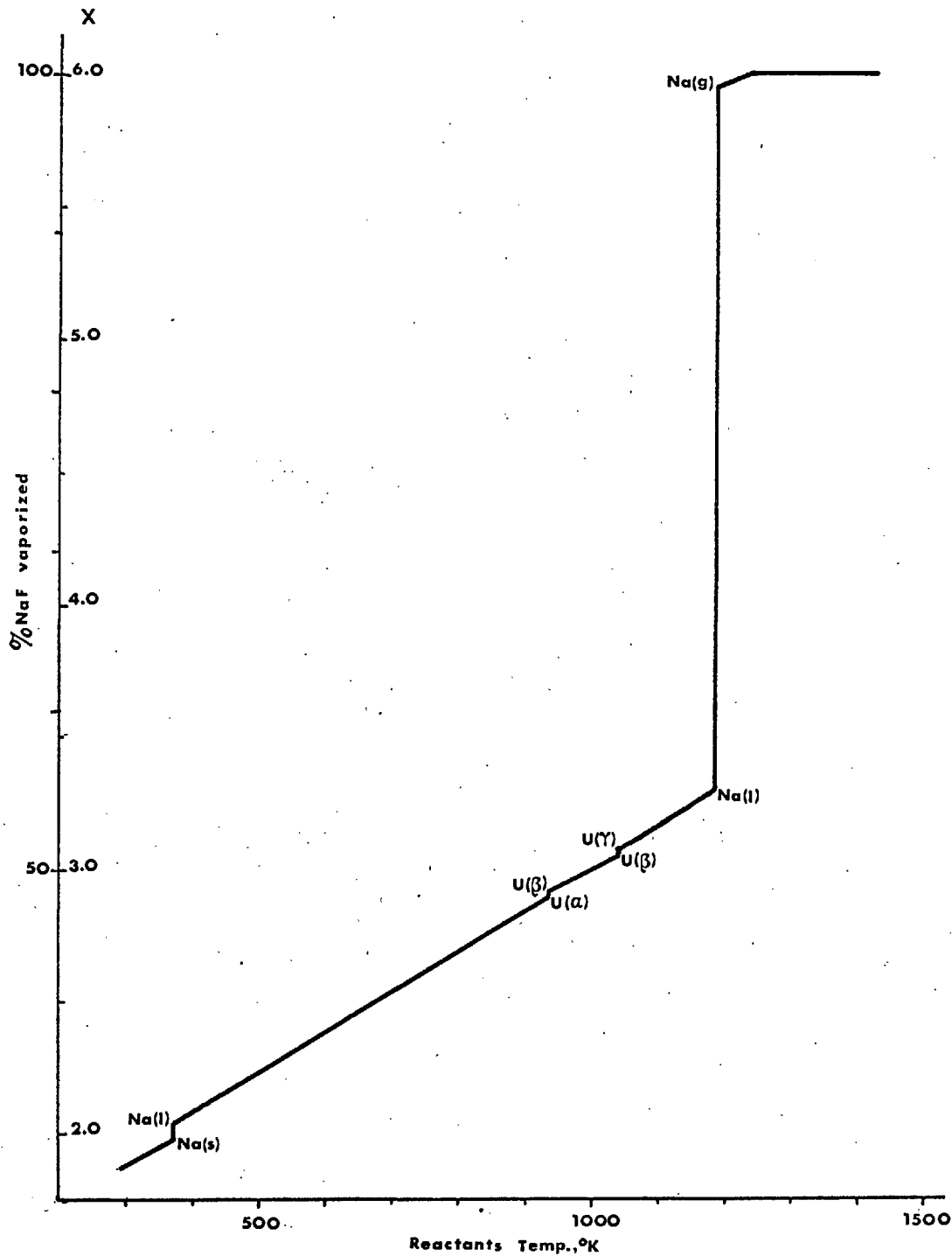
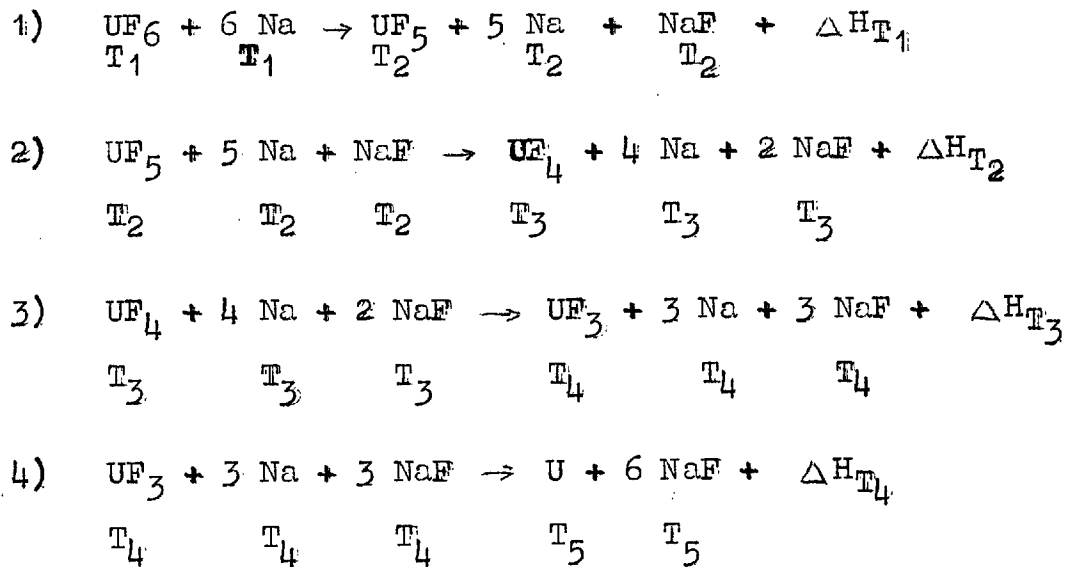


Fig. I.2 - Percentage of NaF vaporized in the products vs. reactants temperature, for the reaction: $UF_6(g) + 6Na \rightarrow xNaF(g) + (6-x)NaF(liq) + U(liq)$

different phases encountered by the reaction on its way to completion. Calculations were made for two reactant temperatures (500°K and 1000°K), assuming that in each step the reaction goes to completion and the heat evolved is used up to heat the products, which then react to give the next fluoride and more heat, and so on, until complete conversion to uranium. The results are given in Table I.6. This stepwise mechanism is illustrated by the following equations:

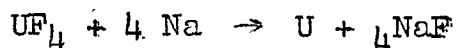


I.2.5 CONCLUSIONS AND PREVIOUS EXPERIMENTAL WORK

From the plot of the standard free energy of formation of the fluorides, in Fig. I.1, it is apparent that sodium reduces all the fluorides over a wide range of temperatures. Only at 1930°K does the NaF line cross the UF₄ line indicating a positive standard free energy change for the reaction.

TABLE I.6. THE NATURE AND COMPOSITION (moles) OF THE PHASES IN THE STEPWISE MECHANISM

Step i	Reactants temp. in each step T_i , °K	Uranium fluorides		Sodium		NaF			Heat of reaction in each step ΔH_{T_i} , Kcal	
			liq	g	liq	g	sol	liq		g
1	500	UF ₆	-	1	6	-	-	-	-	- 120
2	1187	UF ₅	-	1	3.4	1.6	1	-	-	- 138
3	1514	UF ₄	1	-	-	4	-	2	-	- 59
4	1977	UF ₃	1	-	-	3	-	2.7	0.3	- 112
5	1977	U	1	-	-	-	-	3.0	2.4	-
1	1000	UF ₆	-	1	6	-	-	-	-	- 93
2	1187	UF ₅	-	1	3.3	1.7	1	-	-	- 138
3	1690	UF ₄	0.59	0.41	-	4	-	2	-	- 93
4	1977	UF ₃	1	-	-	3	-	1.9	1.1	- 112
5	1977	U	1	-	-	-	-	2.8	3.2	-



The temperature of the reaction should therefore be kept below this temperature, say at 1500°K,¹ if the formation of UF₄ is to be avoided.

The heat of reaction is extremely large at all temperatures and assuming adiabatic conditions and no excess of sodium, it will be sufficient to vaporize part of the slag as it is shown in Fig. I.2. The stabilizing effect of the slag on the reaction temperature is exerted over a wide range of reactants temperatures, up to the boiling point of the sodium (ca. 1200°K). The heat of reaction is probably sufficient to maintain the reaction zone temperature at any predetermined value by controlling either the temperature of the reactants entering the reactor or the excess of sodium used.

From the results presented in Table I.6 it is apparent that, if a stepwise mechanism of reduction is actually occurring, the uranium trifluoride and at least part of the tetrafluoride are likely to be found in the liquid state. This may have an adverse effect on the kinetics of the reduction and, if the residence time of

1 Taking into account the limits of accuracy suggested for the free energy curves in Fig. 2.1.

the reactants is too short, some uranium may be lost in the off-gas line as unreduced fluoride.

At the time the present work was started the only reference found in the literature to a UF_6/Na reduction process was a series of progress reports on engineering development work, carried out at the Oak Ridge National Laboratory[‡], up to December 1959. In this work, the chemical feasibility of the process was fully established and in one case a yield of 93.5% of consolidated uranium was obtained. Fully operability of the process cannot be achieved, however, without additional engineering development, mainly on materials resistant to the highly corrosive reactants and slag and on a more suitable design for the reactor. A final report was published in 1961⁽¹⁰⁸⁾, in which the experimental work is summarized and similar conclusions are drawn.

‡ Operated by Union Carbide Corporation, Tennessee, U.S.A.

APPENDIX II

ANALYSIS FOR URANIUM AND FLUORINE
IN AQUEOUS SOLUTION

Experimental Procedure

The following procedure was adopted for the determination, by chemical analysis, of the amount of uranium metal present in the reacted UF_4 pellets:

- (i) The reacted UF_4 pellet was carefully placed in a 10 ml sintered glass funnel connected to a suction pump through a 25 ml filter-flask.
- (ii) 3 ml of 0.1N hydrochloric acid solution were added to the pellet. Bubbling would start after some seconds and would continue for 8 - 10 minutes.
- (iii) After bubbling had subsided the solution was sucked into the filter-flask and the pellet washed three times with 2 ml of redistilled water.
- (iv) The pH of the solution was adjusted to 3.1 using a pH meter, the solution was transferred into a 25 ml volumetric flask and the volume made up to the mark with HCl (pH=3.1) solution.
- (v) Two samples of 10 ml of the solution thus prepared were analysed for uranium and fluorine, respectively.

Analysis for fluorine

- (vi) The sample of 10 ml was pipetted into a 50 ml beaker and 3 ml of Ferrisal solution added.
- (vii) The solution was stirred for 2 minutes and the percentage transmission of the coloured solution

was immediately measured at 530 m μ using 4 cm cells on a Unicam SP 600 spectrophotometer.

The following reagents were prepared:

Salicylic acid solution: 685.0 mg of analar salicylic acid were dissolved in water and diluted to 1 litre.

Ferric chloride solution (300 mg Fe/ml): 1450.0 mg of analar FeCl₃ · 6H₂O were dissolved in water; 1 ml of hydrochloric acid was added to prevent hydrolysis and the volume made to 1 litre with water.

Ferrisal solution: 10 ml of ferric chloride solution were added to 20 ml of salicylic acid solution; the pH was adjusted to 3.1 using a pH meter and the volume made up to 250 ml with HCl (pH = 3.1) solution. The solution which had a deep violet colour was stored in an amber bottle and remained unaltered for weeks.

Hydrochloric acid solution, pH = 3.1: 7 ml of 0.1N HCl were diluted to 1 litre with water and the pH adjusted to 3.1 using a pH meter.

Standard solution of fluorine: analar hydrogen fluoride was diluted to approximately 0.1N and its content determined by titration with standardized 0.1N sodium hydroxide. The HF solution was stored in polythene bottles and titrations carried out in polythene beakers. The calibration curve

was determined by following procedure (vi) and (vii) with solutions obtained by dilution of the standard and with a content of 1.02, 2.55, 5.10, 7.14, 10.2 and 12.24 μ /ml F. Beer's law is not obeyed; this is not surprising, since the method is based on the discoloration of the ferric-salicylic complex rather than on the colour intensity of a complex of the fluorine ion.

Analysis for uranium

- (viii) The sample of 10 ml was pipetted into a 50 ml beaker and 2 ml of colourless analar nitric acid were added.
- (ix) The beaker was kept in a water bath for two hours to convert the uranium ions to valence state (VI) and then allowed to cool down.
- (x) The solution was neutralised with 1:1 ammonia and 2 ml of ammonium thioglycollate solution were added.
- (xi) The pH was adjusted to about 8.5 with 1:1 ammonia using indicator paper.
- (xii) The solution was transferred to a 25 ml volumetric flask and made to volume with water.
- (xiii) The percentage transmission of the colour developed was measured, at 380 $m\mu$ using 4 cm cells, on the spectrophotometer.

The following solutions were used:

Ammonium thioglycollate solution: 10 ml of thioglycollic acid were diluted with approximately 40 ml of water and neutralised with 1:1 ammonia. The volume was then made up to 100 ml.

Standard Uranium solution: a standard solution containing 2 g/l U was prepared by dissolving 12.5932 g of iron-free uranyl nitrate in water and diluting to 1 litre. The concentration of uranium was then checked by gravimetry.

The calibration curve was determined by preparing a standard solution containing 0.1 mg/l uranium and treating 2, 4, 6, 8 and 10 ml portions according to procedures (x) to (xiii). The blank was prepared in a similar way with no uranium present. Beer's law is obeyed within the whole range of concentrations.

The amount of uranium metal in the pellet was estimated by subtracting from the total uranium content found in solution, the stoichiometric amount of uranium corresponding to the fluorine content, assuming that only UF_3 and uranium went into the solution.

REFERENCES

1. Wilkinson, W.D., "Uranium Metallurgy" vol. 1, chap. 2, Interscience Publishers, New York (1962)
2. Goldschmidt, B. and Vertes, P., "Proc. Intern. Conf. Geneve", 8, P/341, 152, United Nations, New York (1955)
3. "Uranium Metallurgy in Belgium", Ibid., 8, P/1104, 156, (1955)
4. Grainger, L., Ibid., 8, P/407, 149, (1955)
5. Wilhelm, H.A., Ibid., 8, P/817, 162, (1955)
6. Harrington, C.D. and Ruehle, A.E., "Uranium Production Technology", chap. 2, 8 and 9, D. Van Nostrand, New York (1959)
7. Beatty, K.O., and Magoteaux, O.R., USAEC Report NLCO - 771 (1959)
8. Baird, J.E., "Nuclear Reactor Experiments" ed. J.B. Hoag, D. Van Nostrand, New York (1958)
9. Weber, L.G., USAEC Report NYO - 1334 (1960)
10. Beatty, K.O., USAEC Report FMPC - 471 (1954)
11. Harper, J. and Williams, A.E., "Extraction and Refining of the Rarer Metals", a symposium, Inst. Min. Metall., London (1957)
12. Milosavljevich, J. and Baird, J.E., "A Contribution to the Study of the Reduction of UF_4 to Uranium Metal", Intern. Inst. Nucl. Scin. Eng., Argonne Ntl. Lab., unpublished report quoted in ref. (1).
13. Magoteaux, O.R. and Smitherman, C.C., USAEC Report NLCO - 794 (1959)
14. Baker, R.D., Hayward, B.R., Hull, C., Raich, H., and Weiss, A.R., USAEC Report LA - 472 (1958)
15. Schwartz, C.M. and Vaughan, D.A., USAEC Report BMI - 266 (1960)
16. Leifield, R.F. and Neumann, N.F., USAEC Report MCW - 1412 (1958)
17. Lloyd, J.E., Private communication (1963)
18. Stenvenson, J.W. and Ruehle, A.E., USAEC Report NYO - 1339 (1960)
19. Leifield, R.F. and Neumann, N.F., USAEC Report MCW - 1410 (1958)
20. Paine, R.M., Ruehle, A.E. and Lewis, G.W., USAEC Report NYO - 1335 (1957)
21. Bell, D.H., Ph.D. Thesis, University of London (1960)

22. Welch, B.J., Private communication quoted in ref. (21)
23. Domange, L. and Wohlhuter, M., Compt. rend., 228, 1591, (1949)
24. Ferris, L.M., J. Am. Chem. Soc., 79, 5419 (1957)
25. Ind. Eng. Chem., 51, 200 (1959)
26. Kuhlman, W.C., USAEC Report MCW - 175 (1949)
27. Wagner, C., Z. Phys. Chem., (B) 21, 25 (1933)
28. Mott, N.F. and Gurney, R.W., "Electronic Processes in ionic Crystals", pp. 227 ff. & 262 ff., Clarendon Press, Oxford (1940)
29. Tammann, G., Z. anorg. Chem., 111, 78 (1920)
30. Evans, V.R., Trans. Am. Electrochem Soc., 46, 247 (1924)
31. Fischbeck, K., Z. Elektrochem., 39, 316 (1933)
32. Jost, W., "Diffusion und Chemische Reaktion in Festen Stoffen", S.31, Dresden und Leipzig (1937)
33. Nöltge, H., Physik. Z. 39, 546 (1938)
34. Mott, N.F., Trans. Faraday Soc. 43, 429 (1947)
J. chim. physique 44, 172 (1947)
Bull. Soc. chim., D84 (1949)
Cabrerera, N. and Mott N.F., Rep. Progress Phys. 12, 163 (1949)
35. Tammann, G. and Koester, W., Z. anorg. Chem. 123, 196 (1922)
36. Kubaschewski, O. and Hopkins, B.E. "Oxidation of Metals and Alloys", Butterworths, London (1962)
37. Evans, V.R., "The Corrosion and Oxidation of Metals", E. Arnold, London (1960)
38. Wagner, C., Z. Phy. Chem., (B) 11, 139 (1930)
39. Wagner, C., "Seminar on Atom Movements", p. 153, Amer. Soc. Metals, Cleveland (1951)
40. Carter, R.E. and Richardson, F.D., AIME, 203, 336 (1955)
41. "Non Stoichiometric Compounds", Ed. Lyon Mandlecorn, Academic Press, New York (1964)
42. Pohl, R.W., Phys. Z., 35, 107 (1934); 39, 36 (1938); Proc. Phys. Soc. 49, 3, (1937) (extra part)
43. Baedeker, K., Ann. Physik (4) 22, 749 (1907)
44. Baedeker, K., Physik. Z., 13, 1080 (1912)
45. Wagner, C., Z. Phys. Chem., (B) 32, 447 (1936)
46. Pfeil, L. B., J. Iron Steel Inst., 119, 501 (1929)
47. Pfeil, L.B., Ibid., 123, 237 (1931)

48. Davies, M.H., Simnad, M.T., and Birchenall, C.E.,
Trans. AIME 191, 889 (1951)
49. Davies, M.H., Simnad, M.T., and Birchenall, C.E.,
Ibid., 197, 1250 (1953)
50. Himmel, L. (1951), Results quoted in ref. 49
51. Hocking, M.G., Ph.D. Thesis, University of London
(1962)
52. Sachs, K., Metallurgia, Manchr. 54, 11 (1956), quoted
in ref. 36, p. 166
53. E. I. du Pont de Nemours & Co. GER 1080991, May 5, 1960
54. British Patent 865. 270, April 12, 1961
55. Spencer-Palmer, H.J., UKAEA Report BR.422 (1944)
56. Chiotti, P. and Raeuchle, R., USAEC Report CC.1525
(1944)
57. Runnalls, O.J.C., Canad. J. Chem. 31, 694 (1953)
58. Gilpatrick, L.O., Russe, B. and Sites, J.R., USAEC
Report ORNL.1376 (1952)
59. Staritzky, E. and Douglass, R.M. Anal. Chem. 28,
1056, (1956)
60. Katz, J.J., and Rabinowitch, E. "The Chemistry of
Uranium" USAEC Report TID.5290, Book 1, Paper 9,
74 (1958)
61. Penrica, T.W., Powder Metallurgy No. 1/2, 79 (1958)
62. Bell, G.D. and Proudfoot, E., UKAEA Report RDB (C)-
TN-23 (1958)
63. Kortüm-Seiler, M. Angew. Chem. A 59, 159 (1947)
64. Davenport Jr., W. H., and Thomason, P.F., Anal.
Chem. 1093 (1949)
65. Hooper, W., Ph.D. Thesis, London University (1959)
66. Teter, E.K., USAEC Report NYO.1321 (1951)
67. Alberman, K.B. and Anderson, J.S., J. Chem. Soc.
S 303 (1949)
68. Katz, J.J. and Rabinowitch, E. "The Chemistry of
Uranium" chap. XXI, p. 352, McGraw-Hill, New York
(1951)
69. Jacob, C.W. and Warren, B.E., J. Am. Chem. Soc. 59,
2588 (1937)
70. NBS Circular 539, vol IV, pp. 33 - 34 (1955)
71. Jost, W., J. Chem. Phys. 1, 466 (1933)
72. Schottky, W., Z. Phys. Chem. (B) 29, 335 (1935)

73. Ketealar, J.A. and Willems, A., *Recc. trav. chim.* 56, 29 (1939)
74. Zintl, E. and Udgård, A., *Z. anorg. chem.* 240, 150 (1940)
75. Ure, R.W., *J. Chem. Phys.* 26, 1363 (1957)
76. Croatto, U. and Bruno, M., *Gazz. chim. ital.*, 78, 95 (1948)
77. Bauer, V.W.H., *Acta cryst.*, 9, 515 (1956)
78. Duncanson, A., and Stevenson, R.W.H., *Proc. Phys. Soc. Lond.* 72, 1001 (1958)
79. Krishna Rao, K.V., Nagender Naidu, S.V. and Setty, P.L.N., *Acta Cryst.* 15, 528 (1962)
80. Hurlen, T., *Acta chem. Scand.* 13, 365 (1959)
81. Hauffe, K., "Reaktionen in und an Festen Stoffen", Springer Verlag, Berlin (1957)
82. Wadseley, A.D., "Non Stoichiometric Compounds" Ed. Lyon Mandelcorn, chap. 3, p. 108, Academic Press (1964)
83. Litcher, B.D. and Bredig, M.A., USAEC Report ORNL, privately communicated (1964)
84. Staffanson, L.I., Ph.D. Thesis, University of London (1960)
85. Rogers, P.S., Ph.D. Thesis, University of London (1957)
86. D'Eye, R.W.M. and Martin, F.S., *J. Chem. Soc.* 1847 (1957)
87. McNamara, P., Ph.D. Thesis, University of London, (1963)
88. Kohlschütter, H.W., *Z. Elektrochem.* 38, 345 (1932)
89. Wagner, C., *J. Chem. Phys.* 21, 1819 (1953)
90. Auskern, A.B. and J. Belle, *J. Nucl. Materials*, 3, No 3, 267 (1961)
91. D'Eye, R.W.M. and Fergusson, I.F., *J. Chem. Soc.* 3401 (1959)
92. Galkin, L.N. and Feofilov, P.P., *Doklady Akad. Nauk. SSSR* 114, 745 (1957)
93. Bell, D.H., Ph.D. Thesis, University of London (1960)
94. Thoma, R.E., *Inorg. Chem.* 1, 220 (1962)
95. Treadwell, E.D., Ammann, A. and Zürcher Th., *Helv. chim. Acta* 19, 1255 (1936)
96. Schmalzried, H., *J. Chem. Physics*, 33, 940 (1960)
97. Vorob'ev A.A. and Nakhodnova, A.P., *Zhur. Tekh. Fiz.* 28, 2192 (1958)

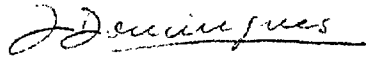
98. Vorob'ev A.A. and Zavadovskaya, E.K., *Isvest. Tonsk. Politekh. Inst.* 83, 3 (1956)
99. Kubaschewski, O. and Evans, E. LL., "Metallurgical Thermochemistry" Pergamon Press (1958)
100. Rand, M.H. and Kubaschewski, O., "The Thermochemical Properties of Uranium Compounds" Oliver & Boyd, London, (1963)
101. Portevin, A.M., Prétet, E. and Jolivet, H., *J. Iron St. Ind.* 130, 219 (1934)
102. Pilling, N.B. and Bedworth, R.E., *J. Inst. Met.* 29, 529 (1923)
103. Vernon, W.H.J., *Trans. Farad. Soc.*, 23, 152 (1927)
104. Penniston, J.T. and Neumann, N.F., USAEC Report MCW-1410 (1958)
105. Jacobs, P.W.M. and Tariq Kureishy, A.R.,
Symp. (intern.) Combust., 9th Cornell Univ., Ithaca, N.Y., 366, (1962), (Publ.1963)
106. Glassner, A., USAEC Report ANL.5750 (1957)
107. Kellog, H.H., *J. Metals*, 188, 862 (1950)
108. Scott, C.C., USAEC Report ORNL.3012 (1961)

ACKNOWLEDGMENTS

The author is indebted to the Junta de Energia Nuclear, Lisbon, to the Comissão Coordenadora da Investigação para a OTAN, Lisbon, and to the United Kingdom Atomic Energy Research and Development Branch, Springfields, for their financial support of this research, to Professor F. D. Richardson for the provision of the research facilities and to Mr. F. M. Videira, (Head of the Department of Chemistry and Metallurgy of J.E.N.) for making his stay in England possible.

The author particularly wishes to express his gratitude to his supervisor, Dr. J. W. Tomlinson, whose constant interest, guidance and encouragement has contributed greatly to the successful completion of this work.

Thanks are also due to Dr. P. S. Rogers for his useful criticism and suggestions in connection with this thesis, to Dr. G. Thomas and Mr. T. K. Kelly for their help in the electron probe studies and to his colleague Miss A. Kubik for checking the manuscript. The author is also grateful to his other colleagues in the Nuffield Research Group for stimulating discussions and to the permanent staff of the laboratory for their cooperation.


J. T. H. Domingues,
Nuffield Research Group,
Royal School of Mines,
London.